10-23-2019

Quartz Crystal Microbalance Based Sensors for Detection and Discrimination of Volatile Organic Compounds Using Ionic Materials

Stephanie R. Vaughan

QUARTZ CRYSTAL MICROBALANCE BASED SENSORS FOR DETECTION AND DISCRIMINATION OF VOLATILE ORGANIC COMPOUNDS USING IONIC MATERIALS

A Dissertation

Submitted to the Graduate Faculty of the
Louisiana State University and
Agricultural and Mechanical College
in partial fulfillment of the
requirements for the degree of
Doctor of Philosophy

in

The Department of Chemistry

by
Stephanie R. Vaughan
B.S., Xavier University of Louisiana, 2013
December 2019

I dedicate this dissertation to my beautiful mother and loving brother. For without them I would not be where or who I am today. I have been blessed with a selfless mother who has sacrificed so much for me and never complained about it. She is the strongest woman I know and I am glad to have her blood running through my veins. And to my brother for teaching me how to read, I am forever indebted to you. Without this life lesson there is no way I could have made it to this level of education and I thank you for that. You both have *kept it real* with me my entire life and that has been essential to my success. I do not have to hope that you both are proud of me because you are not shy to let me know. I love you both!

ACKNOWLEDGEMENTS

It is said that it takes a village to raise a child and the same can be said to produce a PhD chemist. Without my village, my journey towards a PhD would have ended prematurely. For that, I express my sincerest and most deserved appreciation.

To my advisor, Professor Isiah Warner: Thank you for all of your guidance, believing in me, and providing me with an environment to reach my full potential. I faced many struggles while at LSU, but you never gave up on me. In my heart, I know that if I had a different research advisor, I would not be where I am today in my academic career. Lastly, thank you for helping me find the confidence that you knew I had, but that I could not yet see.

To my mentor, Dr. Gloria Thomas: When I walked into your class at Xavier, I would have never guessed that you would be such an influential person in my academic career. You have always provided me with a listening ear and honest advice. Thank you for always being there for me personally and academically.

To my post docs, Rocio Perez and Pratap Chhotaray: Thank you for your helpful discussions in both research and life, and for our friendship.

To my PhD committee: Past and present members, thank you for committing your time to my graduate studies.

To the Warner Research Group: Past and present members thank you for your helpful suggestions and questions during group meetings, as well as when preparing for any presentation. A special thank you to Dr. Nicholas Speller for introducing me to the QCM. The support and friendship I have received from the Warner Group is truly appreciated.

Last, but certainly not least, thank you to my family and friends who have been the heart of my village. I am grateful to LSU for bringing Dr. Milcah Jackson, Ashley Fulton, and the LSU NOBCChE 2018 – 2019 E-board into my life during this hectic journey. Ashley, thank you for being your genuine self and being one of my biggest cheerleaders, you have no idea the impact you have had on my life. Thank you to my Denver friends and family for helping me to remain humble.

TABLE OF CONTENTS

ACKNOWLEDGEMENTS iii

ABSTRACT vii

CHAPTER 1. INTRODUCTION 1
1.1. Volatile Organic Compounds Effects and the Impact of Detection 1
1.2. Electronic Noses 3
1.3. Statistical Techniques 7
1.4. Quartz Crystal Microbalance Based Sensors 9
1.5. Materials for QCM-based Sensors 17
1.6. Scope of Dissertation 19
1.7. References 20

CHAPTER 2. CLASS SPECIFIC DISCRIMINATION OF VOLATILE ORGANIC COMPOUNDS USING A QUARTZ CRYSTAL MICROBALANCE BASED MULTISENSOR ARRAY 31
2.1. Introduction 31
2.2. Materials and Methods 34
2.3. Results and Discussion 38
2.4. Conclusion 45
2.5. References 46

CHAPTER 3. QUARTZ CRYSTAL MICROBALANCE BASED SENSOR ARRAYS FOR DETECTION AND DISCRIMINATION OF VOCS USING PHOSPHONIUM IONIC LIQUID COMPOSITES 50
3.1. Introduction 50
3.2. Materials and Methods 52
3.3. Results and Discussion 55
3.4. Conclusions 71
3.5. References 72

CHAPTER 4. IONIC LIQUID-POLYMER COMPOSITES FOR MIXTURE ANALYSIS 75
4.1. Introduction 75
4.2. Materials and Methods 77
4.3. Results and Discussion 79
4.4. Conclusion 90
4.5. References 90

CHAPTER 5. CONCLUSIONS AND FUTURE WORK 93
5.1. Conclusions 93
5.2. Future Work 94

APPENDIX A. SUPPORTING INFORMATION FOR CHAPTER 2 96

APPENDIX B. SUPPORTING INFORMATION FOR CHAPTER 3 111

APPENDIX C. SUPPORTING INFORMATION FOR CHAPTER 4 120

LIST OF REFERENCES 121

VITA 134

ABSTRACT

Volatile organic compounds (VOCs) are prevalent in everyday life, ranging from household chemicals, naturally occurring scents from common plants and animals, to industrial-scale chemicals. Many of these VOCs are known to cause adverse health and environmental effects and require regulation to prevent pollution. Detecting VOCs plays a critical role in food quality control, environmental quality control, medical diagnostics, and explosives detection. Thus, development of adequate sensing devices for detection and discrimination of VOCs is of great importance. In recent years, use of quartz crystal microbalance (QCM) based sensor arrays for analyses of VOCs has attracted significant interest. Detection of VOCs using QCM-based sensors is dependent upon coating materials; hence, development of suitable coating materials is also of great importance. Over the years, QCM-based sensors have provided great promise for detecting VOCs; however, they have not provided this same potential for discrimination between different VOCs. Thus, this dissertation is focused on development of reusable QCM-based sensor arrays for detection and discrimination of VOCs using ionic liquids (ILs) and a ***g***roup of ***u***niform ***m***aterials ***b***ased on ***o***rganic ***s***alts (GUMBOS) as coating materials. GUMBOS and ILs are similar classes of ionic materials, where GUMBOS represent solid phase organic salts with melting points between 25°C and 250°C, while ILs are organic salts with melting points below 100°C and are typically liquid at room temperature.

Within this dissertation the synthesis and characterization of novel ILs and GUMBOS are discussed. Moreover, composite materials using IL-polymer blends are also presented. Vapor sensing properties of all ILs, GUMBOS, and composites were evaluated for use as coating materials in sensor arrays for detection and discrimination

towards a wide range of VOCs. Two different sensor array schemes, multisensor array (MSA) and virtual sensor array (VSA), are described and examined throughout this dissertation. Finally, statistical techniques, such as principal component analysis (PCA) and discriminant analysis (DA), were used to develop predictive models to quantify the accuracy of MSAs and VSAs.

The first reports of a QCM-based MSA to discriminate VOCs by classes, and a QCM-based VSA for discrimination of closely related chlorinated VOCs are presented within this dissertation. Overall, these studies demonstrate capabilities of QCM-based vapor sensor arrays with ionic coating materials for accurate discrimination and detection of VOCs.

CHAPTER 1. INTRODUCTION

1.1. Volatile Organic Compounds Effects and the Impact of Detection

1.1.1. Volatile Organic Compounds

Volatile organic compounds (VOCs) are a group of carbon-based organic chemicals that evaporate easily at room temperature and atmospheric pressure. In fact, the Environmental Protection Agency (EPA) defines VOCs as any organic compound having an initial boiling point less than or equal to 250° C when measured at a standard atmospheric pressure of 101.3 kPa.[1]

VOCs can be classified into three categories based on their boiling points that indicate their ease of emission. Very volatile organic compounds (VVOCs), volatile organic compounds (VOCs), and semi-volatile organic compounds (SVOCs) have respective boiling points of < 0° to 50-100° C, 50-100° C to 240-260° C, and 240-260° C to 380-400° C.[1] VOCs, in singular form or complex mixtures, are emitted from both natural and artificial sources. Natural sources include, but are not limited to plants, animals, and volcanoes.[2-4] There are various reasons for natural sources to emit VOCs, such as self-defense mechanisms[5-7] or communication.[8-12] Artificial sources are primarily anthropogenic, including industrialization, agricultural activities, solvent use, and motor vehicles.[4, 13-16] Since VOCs are present in everyday life, detecting and analyzing these vapors is of great concern.[17]

1.1.2. Impact of VOC Detection

While some VOCs are harmless, many of them can cause adverse environmental and health effects. For instance, the formation of ozone at surface level as well as smog are often consequences of pollution due to VOCs in the environment.[1, 18-19] Furthermore,

it has been found that indoor air can contain as much as ten times more pollutants than outdoor air due to VOCs emitted from many household products.[19-20] For example, paints, upholstered fabrics, and cleaning products contain VOCs and thus release VOCs while in use.[19, 21] Health effects of VOC exposure are dependent on length of exposure time. Short-term exposure results in acute health effects such as epistaxis, dizziness, headaches, or dermatitis. In contrast, long-term exposure can result in respiratory complications, damage to kidneys, cancer, or reproductive issues.[20, 22] The EPA estimates that Americans spend 90% of their time indoors; therefore, the development of vapor sensing techniques for detection and discrimination of VOCs has become a prevalent target among scientists.[23] Detection of VOCs is not limited to environmental protection; it also includes industry, health and safety applications.[24-27] More specifically, detection of explosives,[28-33] disease conditions,[24, 34-37] and food quality[38-42] can be monitored due to the presence of certain VOCs. In this regard, several methods for VOC detection and analyses have been developed.

1.1.3. Common VOC Detection Techniques

The most traditional technique for VOC detection is gas chromatography coupled to mass spectrometry (GC-MS); however, such instrumentation can be expensive, complex, and require a skilled employee for efficient operation.[43-44] Other common techniques, such as ion mobility spectrometry,[45] photoionization detector,[46] and flame ionization detector,[47] face similar burdens; thus, the need for more cost effective and simplistic techniques has become the focus of recent research. In this respect, electronic noses (e-nose) has gained substantial interest.

1.2. Electronic Noses

The term “e-nose” was coined by Julian Gardner and Philip Bartlett in 1988.[48] E-noses are engineered to simulate the human olfactory system. There are 400 scent receptors in the human nose.[49] When the nose encounters a scent, those receptors will interact with it to detect components of the scent and send a signal to the brain. The brain then processes the signal and, ultimately, identifies the scent. Drawing inspiration from this process, an e-nose typically consists of several chemically distinct sensors that act as cross-reactive elements within an array configuration. This concept is also known as cross-reactive sensor arrays (CRSAs).[50] When sensors are exposed to vapors from VOCs, the sensors will interact with the vapors to generate analyte specific response patterns. Eventually, sensor responses are analyzed using pattern recognition techniques, specifically, statistical techniques, such as artificial neural networks (ANN), linear regression, analysis of variance (ANOVA), principal component analysis (PCA), or discriminate analysis (DA) to discriminate or identify the vapor. A schematic of the operating principle is illustrated in Figure 1.1. E-noses utilize several types of materials for vapor sensing, such as metal-oxides,[51-53] conductive polymers,[54-55] electrochemical,[56] optical,[57] and acoustic wave.[51, 58]

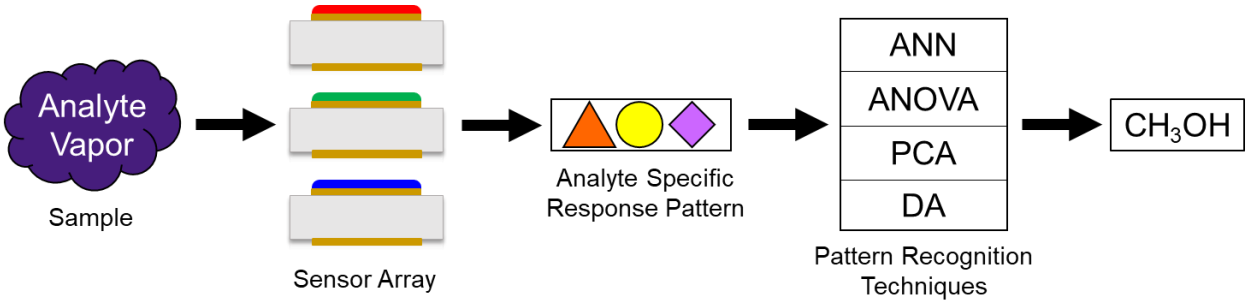

Figure 1.1. Schematic for operating principle of e-noses and CRSA.

Metal-oxides are comprised of a ceramic support tube containing a heater spiral that is typically composed of platinum, and operates based on changes in resistance and conductivity.[48] These sensors are known for detecting oxidizing and reducing compounds and having high sensitivity; however, coating materials are limited and require high operating temperature, which results in increased power consumption.[48] Similar to metal-oxides, conductive polymers have a method of detection that is based on conductivity and resistance change. Conductive polymer gas sensors exhibit high sensitivity to a variety of VOCs, have short response times, and offer a more diverse range of coating materials with respect to metal-oxides.[48] While this class of e-noses has many benefits, there are a few challenges. For example, polymer sensors typically have a higher chance of being overloaded by analytes, ultimately limiting the lifetime, and often times they are not reusable.

Electrochemical sensors allow detection of VOCs based on voltage or current change and are advantageous in their ability to operate at ambient temperature and low power consumption, but are limited to sensing only VOCs of low molecular weight.[48] Unlike electrochemical sensors, optical sensors are sensitive, wide range detectors of VOCs, regardless of molecular weight. Detection principles for optical sensors are typically based on light modulation and optical changes such as absorbance[59-60] or fluorescence.[57, 61] The optics and electrical components required for these sensors are delicate, and thus reduces portability and ultimately constrains them to laboratory testing.

Acoustic wave sensors allow measurement of mass change and are classified as gravimetric transducers. Common types of acoustic wave gas sensors include bulk acoustic wave (BAW),[58, 62] surface acoustic wave (SAW),[58, 62] and thickness shear mode

(TMS).[58, 62-63] SAW devices are based on surface waves that propagate on the surface of the substrate, whereas for BAW devices the wave propagates through the substrate. TMS devices are based on elastic waves propagating through the substrate upon excitation from an appropriate voltage. These devices are inexpensive and typically sensitive to most VOCs.[48] The focus of this dissertation is on use of a TMS device, more specifically a quartz crystal microbalance (QCM). Operation and theory of the QCM will be discussed in section 1.4. In order to understand the process by which the QCM is employed as a gas sensor, CRSA schemes must first be examined.

1.2.1. QCM-based Multisensor Arrays

The most common CRSA scheme is a multisensor array (MSA). This system consists of multiple sensors with chemically distinct coatings that respond to a vast range of chemical vapors. When exposed to analyte vapor, each sensor will generate a single response. Although each sensor will produce one response, responses will vary significantly between sensors. An example of a QCM-based MSA scheme is illustrated in Figure 1.2. Individual responses are collectively compiled to generate analyte specific response patterns. As previously mentioned in section 1.2, patterns are analyzed using pattern recognition techniques. PCA and DA are used for data analysis in this dissertation and will be explained in detail in section 1.3. Although this scheme is simple and reliable, researchers have explored other QCM-based CRSA schemes to address certain limitations of MSAs, such as increased preparation time for sensors. In this regard, virtual sensor arrays have been investigated.

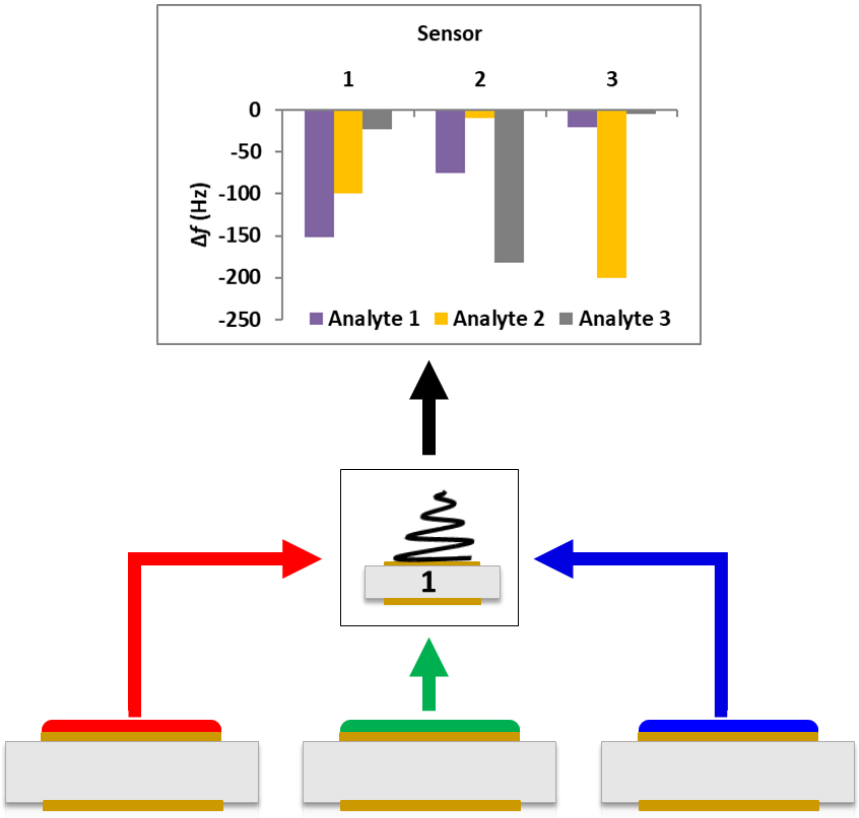

Figure 1.2. Schematic for QCM-based MSA. Red, green, and blue represent chemically distinct coatings corresponding to three different sensors. Each sensor generates a single response, represented by the small sensor labeled one. The graph is a visual representation of the analyte specific responses generated by each sensor.

1.2.2. QCM-based Virtual Sensor Arrays

Virtual sensor arrays (VSAs) consist of a single sensor that produces multiple pseudo-independent responses. Essentially, the VSA represents a large number of sensors; however, there is only one physical sensor and remaining “sensors” are imaginary. An example of a QCM-based VSA is depicted in Figure 1.3. Similar to MSAs, VSA responses will vary among the sensors, resulting in analyte specific response patterns that can be analyzed using statistical analyses. Since VSAs are comprised of one sensor, only one coating material is required to achieve multiple responses, which addresses the limitation of extensive preparation time encountered with MSAs.

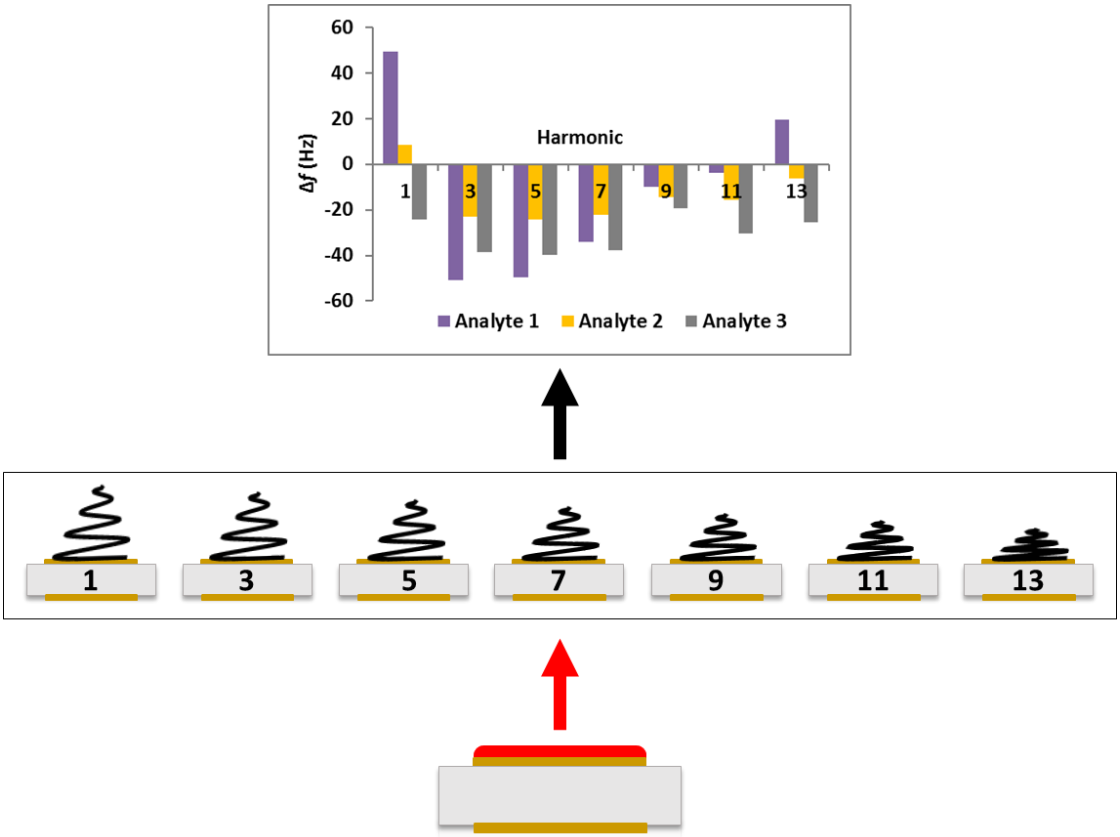

Figure 1.3. Schematic for QCM-based VSA. Red represents one chemically coated sensor that produces multiple responses. Smaller sensors, labeled 1 – 13, represent "imaginary" sensors. The graph is a visual representation of analyte specific responses generated by each sensor.

1.3. Statistical Techniques

The field of statistical techniques is a branch of pattern recognition used by researchers to analyze data and gain more information on the capabilities of each sensing device.[64] Essentially, statistical techniques provide additional interfaces for data presentation as well as further interpretation of aforementioned data. These techniques include methods for prediction, classification, and discrimination of data (ANN, linear regression, ANOVA, PCA, DA, etc.). Within this dissertation PCA and DA are used to develop sensor arrays.

1.3.1. Principal Component Analysis

Principal component analysis (PCA) is a multivariate, unsupervised technique used to reduce dimensionality of a data set.[64-65] This is a mathematically intensive technique; however, with advancement of technology, statistical software such as SAS, MATLAB, and JMP has been developed to reduce labor intensity for analysts. Herein, a non-mathematical description of PCA is presented.

The objective of PCA is to create a smaller number of predictors that are based on the full set of originally measured variables and retain as much of the variability in the original variables as possible. These new variables are linear combinations of original variables and referred to as principal components (PCs).[65] PCs are based on eigenvectors and eigenvalues, which are based on the number of variables in a data set. Briefly, every eigenvector has a corresponding eigenvalue. Here, an eigenvector indicates direction of variance while an eigenvalue provides the amount of variance. Fundamentally, PCs are directions for where the most variance occurs in a data set. In this regard, an eigenvector with the highest eigenvalue is the first PC, indicating the most variance, while an eigenvector with the second highest eigenvalue is the second PC, indicating the second most variance, and so forth until 100% of total variance in the original data set is accounted for. Qualitative information of a data sets variance can be achieved by displaying PCs graphically; however, to obtain quantitative information DA must be implemented. Traditionally, PCs produced from PCA are used as predictor variables for analysis; however, in Chapter 2 of this dissertation the original data set was used as predictor variables in the analysis.

1.3.2. Discriminant Analysis

Discriminant analysis (DA) is a set of supervised techniques used to distinguish and identify patterns within a data set. DA is based on known continuous responses, i.e. supervised. Predictor variables are analyzed to construct a new set of axes, called canonical axes, that best maximize separation of data groups.[65] Without going into mathematical detail, DA is similar to PCA in that eigenvectors are used to determine new variables, in this case, canonical axes. However, unlike PCA, canonical axes indicate directions with the most separation between groups, not variance. Group classification is established by estimating the distance from each point to each group's multivariate mean, or centroid, using Mahalanobis distance.[66] Essentially, Mahalanobis distance is the distance from a point to the mean point of the group. Thus, analytes are classified into the closest group. Cross validation must be performed to quantify the accuracy of DA. The work in this dissertation employs quadratic discriminant analysis (QDA) with cross-validation to quantify accuracy. Typically in QDA, members of the same group are tightly clustered together, while different groups are spatially separated. QDA assumes the covariance matrix is different within each group, which allows for a better fit of data; however, this requires estimation of more parameters. Cross-validation was used to provide the least biased and most accurate assessment of QCM sensors in this dissertation.

1.4. Quartz Crystal Microbalance Based Sensors

The quartz crystal microbalance (QCM) is a simple, sensitive, cost effective instrument with rapid response that is traditionally used as a mass detector. However, within this dissertation the QCM is utilized as a vapor sensor. QCM-based sensors are

composed of a quartz crystal resonator (QCR) with a suitable chemosensitive coating material for detection of VOC vapors. This section of the dissertation will discuss the fundamental details of the QCM.

1.4.1. Piezoelectric Effect

In 1880 the Curie brothers, Pierre and Jacques, discovered the piezoelectric effect when studying structures of crystalline materials.[67] It was found that when crystalline materials with asymmetrical structures, such as quartz and topaz, undergo mechanical deformation an electric voltage is generated.[68] Alternatively, a mechanical deformation is produced when an electric voltage is applied, which is known as the converse, or reverse, piezoelectric effect. Quartz crystal was the piezoelectric material of choice for studies in this dissertation.

1.4.2. Quartz Crystal Resonators

Electrical and physical properties of QCRs are determined by orientation and cut of the quartz. The most common types of cuts are AT- and BT-cut quartz. AT-cut crystals are used for studies conducted within this dissertation, and the cutting scheme is presented in Figure 1.4. QCRs are comprised of an AT-cut quartz crystal sandwiched between two metal electrodes. QCRs in this dissertation are comprised of gold metal electrodes as depicted in Figure 1.5.

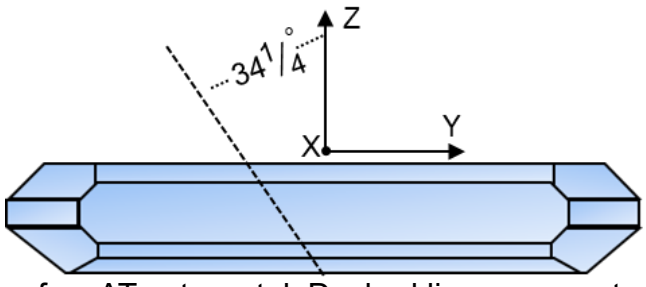

Figure 1.4. Schematic of an AT-cut crystal. Dashed line represents angle of cut.

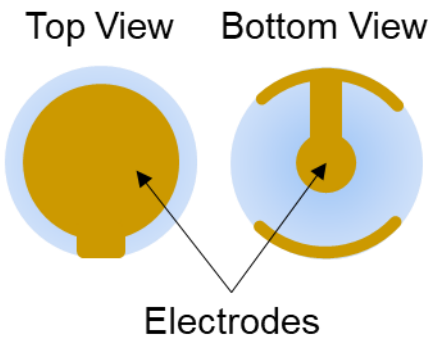

Figure 1.5. Schematic of QCR with gold electrodes.

1.4.3. Acoustic Shear Waves

As previously discussed in section 1.2, the QCM is a TMS device that is based on elastic waves propagating through the substrate upon excitation from an appropriate voltage. In this regard, an AC voltage is applied across gold electrodes on the QCR, causing the crystal to oscillate, which results in an acoustic shear wave. The wavelength of the wave is dependent on the thickness of the crystal due to nodes of the wave being inside the crystal and antinodes being at the surface. This relationship is given by the following equation:

$$f = \frac{c_q}{\lambda} = \frac{c_q}{2(d_q + d_f)} \qquad (1.1)$$

where f is frequency, c_q is speed of sound, λ is wavelength, d_q is thickness of QCR, and d_f is the film thickness.[69] This generated wave is known as resonance frequency and, herein, will be referred to as such. Based on equation 1.1, an increasing thickness of the QCR would result in decreases of resonance frequency. Essentially, addition of materials on the surface of the QCR would ultimately decrease resonance frequency. This relationship led Gunter Sauerbrey to discover that the QCM was useful as a mass detector.[70] The German physicist derived an equation, now known as the Sauerbrey

equation (1.2), relating the change in resonance frequency to change in mass on the surface of the QCR.

$$\Delta f = -\frac{n}{c}\Delta m = -\frac{n}{c}\rho_f t_f \qquad (1.2)$$

Where Δf is change in resonance frequency, η is harmonic number, c is mass sensitivity which is 17.7 ngcm^{-2}Hz^{-1} for a 5 MHz AT-cut crystal as used in this dissertation; ρ_f is density of the film, and t_f is film thickness.[70]

1.4.4. Harmonics

The natural resonance frequency of a QCR is known as the fundamental frequency. It is possible, however, to generate higher resonance frequencies from the fundamental frequency, which are known as harmonics. Harmonics can only be generated in odd multiples of the fundamental frequency due to nodes of the wave residing inside the crystal. Thus, the amount of nodes inside the crystal will dictate the harmonic number. In this respect, a wave with one node inside the crystal represents the fundamental frequency, or 1st harmonic, while a wave with three nodes inside the crystal indicates the 3rd harmonic. Figure 1.6 illustrates this relationship. Since wavelength decreases as the number of nodes increases, harmonics exhibit higher frequencies as compared to the fundamental frequency. Within this dissertation, sensor development employed fundamental frequency alone, as well as with multiple harmonics.

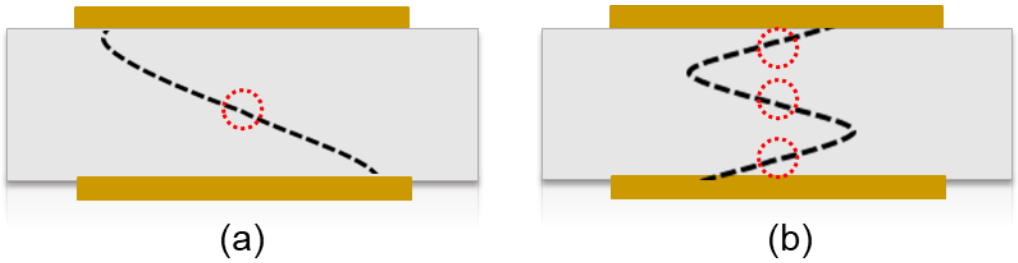

Figure 1.6. Schematic of wave behavior inside a QCR for (a) fundamental frequency, and (b) 3rd harmonic. Dashed line represents acoustic shear wave, while red dotted circles indicate nodes.

In order to generate these multiple harmonic states, voltage was applied to the QCR across a range of frequencies and resultant currents of the system were measured. Frequency with peak current is denoted as the harmonic, as depicted in Figure 1.7.[71] QCRs used in this work are capable of seven harmonics. The first harmonic, denoted as the fundamental frequency, exhibits a frequency at 5 MHz and remaining harmonics are odd multiples of this frequency. Thus, the 3rd harmonic would exhibit a frequency at 15 MHz, 5th harmonic at 25 MHz, 7th harmonic at 35 MHz, 9th harmonic at 45 MHz, 11th harmonic at 55 MHz, and 13th harmonic at 65 MHz. The bandwidth presented in Figure 1.7 is related to energy dissipation, which will be further discussed in section 1.4.5, and is expressed by equation 1.3.[71-72]

$$D = \frac{2\Gamma}{f} \qquad (1.3)$$

Where D is the dissipation factor, Γ is bandwidth, and f is resonance frequency. The dissipation factor is defined as:

$$D = \frac{E_{dissipated}}{2\pi E_{stored}} \qquad (1.4)$$

where $E_{dissipated}$ is energy lost per oscillation cycle and E_{stored} is total energy stored in the oscillation system.[73]

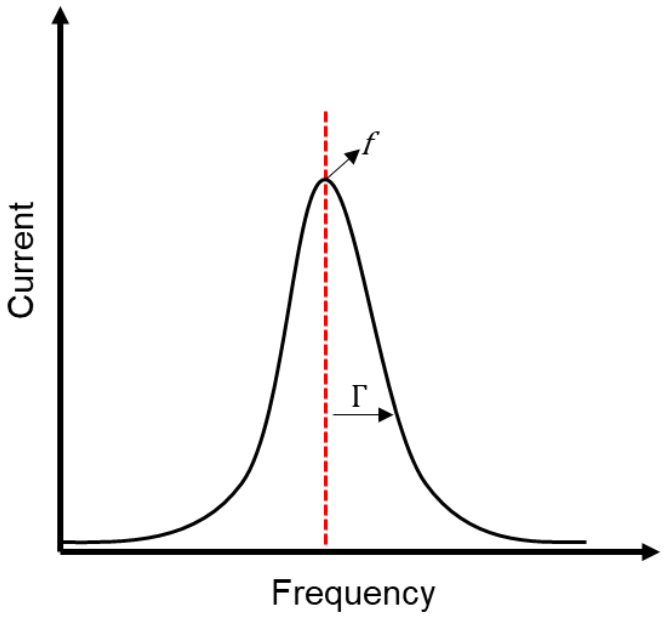

Figure 1.7. Generic plot of frequency versus current.

1.4.5. QCM with Dissipation Monitoring

QCM with dissipation monitoring (QCM-D) is a type of QCM capable of measuring frequency and dissipation at multiple harmonics. The operating principle of the QCM-D is based on a technique described by Kasemo, known as the ring-down-approach.[74] In this approach, voltage is applied to the QCR for a short amount of time, and then, the amplitude of the oscillation decay is measured. Figure 1.8 illustrates a schematic of this decay, while equation 1.5 defines amplitude decay.[73]

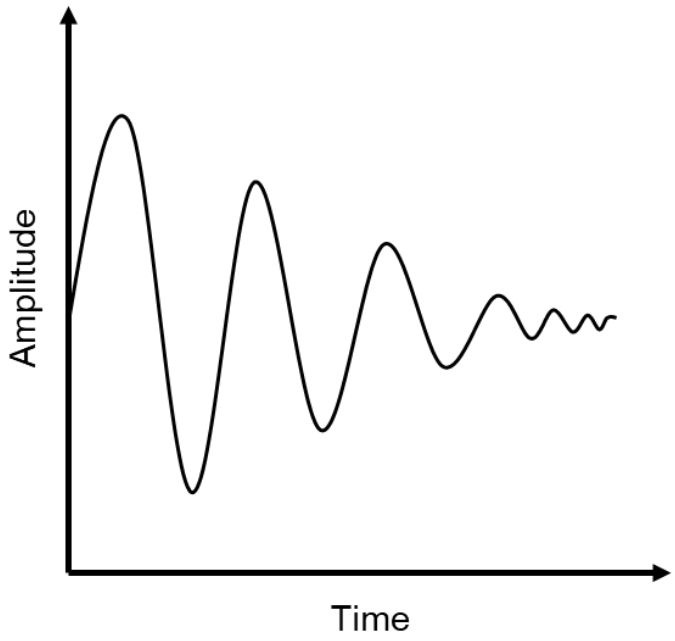

Figure 1.8. Schematic of amplitude decay versus time.

$$A_t = A_o e^{-\frac{t}{\tau}} \sin(\omega t + \varphi) + c, t \geq 0 \qquad (1.5)$$

Where A_t is amplitude at time t, A_o is amplitude $t = 0$, τ is the decay time constant, ω is angular frequency, φ is the phase, and c is the dc offset. Thus, the dissipation factor is calculated as:

$$D = \frac{2}{\omega\tau} \qquad (1.6)$$

where D is dissipation factor, τ is the decay time constant, and ω is angular frequency. The QCM-D is capable of monitoring frequency and dissipation at multiple harmonics due to impulse excitation of the QCR. In this respect, the fundamental frequency is excited and resonance decay is monitored. The 3rd harmonic is then excited and resonance decay is monitored. This process is repeated as fast as 200 times per second until all seven harmonics are excited and resonance decays are monitored.[75]

1.4.6. QCM Gravimetric and Non-gravimetric Sensing

Traditionally, the QCM has been used as a gravimetric sensing technique, which is defined by the Sauerbrey equation (1.2). This equation expresses that change in frequency is directly proportional to change in mass deposited on the QCR surface. Essentially, deposition of mass on the QCR surface should result in a decreased frequency. This is known as ideal Sauerbrey behavior, which only applies to rigid, thin, and uniform films. These materials would exhibit small dissipation values, if any. Films that do not meet these characteristics, such as soft and thick films, deviate from ideal behavior and are said to exhibit non-ideal Sauerbrey behavior with larger dissipation values.[76] Thus, resonance, thickness, and viscoelasticity of each film will affect detection response.[69, 76] Viscoelastic films demonstrate elastic and viscous properties, which result in behavioral changes under resonant conditions as compared to rigid films. Due to these properties, viscoelastic materials are exploited to develop QCM-based sensor arrays.

QCM-based sensor arrays are based on non-gravimetric sensing, where change in frequency is directly proportional to change in mass deposited on the QCR surface; however, rather than calculating change in mass, change in frequency is used to measure vapor detection. Essentially, physical changes of film materials will affect sensor response, as illustrated in Figure 1.9. This plot was adapted from a study investigating effects of viscoelasticity and film thickness on sensor response.[76] It should be noted that these films could exhibit positive frequency responses, a trait that is indicative of non-ideal Sauerbrey behavior. Consequently, the QCM as a transducer is fundamentally non-selective. Thus, chemosensitive materials are necessary for proper function of QCM-based sensor arrays.

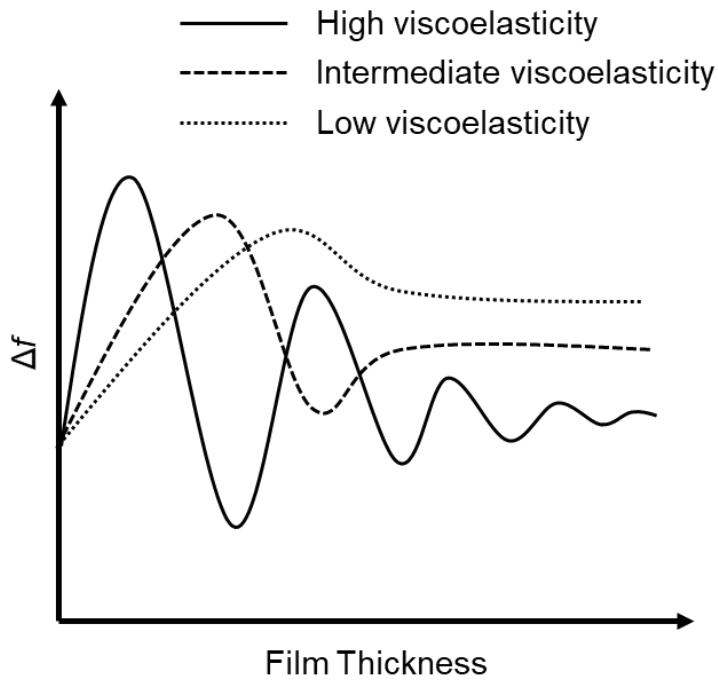

Figure 1.9. Schematic of frequency response based on viscoelasticity and film thickness.

1.5. Materials for QCM-based Sensors

Materials for QCM-based sensors are coated on the QCR surface, which determine selectivity and sensitivity of the sensor. For vapor sensing, these materials also affect sorption-desorption profiles of analytes and, ultimately, sensor performance. Therefore, research has been focused on expansion of novel chemosensitive materials for vapor sensing. These materials should meet certain criteria, such as stability under operating conditions, reversible sorption-desorption, cost efficiency, and partial selectivity to a range of analytes. A broad range of materials have been employed as coating materials for QCM-based sensor arrays including molecularly imprinted polymers,[77-80] calixarenes,[81-83] zeolites,[84] metalloporphyrins,[85-86] and conventional polymers[87-90] among many others. However, there are limitations associated with use of such materials including intricate deposition procedures, slow response times, and high material cost.

Due to these disadvantages, a class of organic salts has been investigated as coating materials for QCM-based sensors.

1.5.1. Ionic Liquids and GUMBOS

Ionic liquids (ILs) and GUMBOS are a class of materials based on organic salts that address limitations associated with materials detailed in section 1.5. ILs are organic salts composed of bulky cations and/or anions with melting points below 100°C.[91] ILs can be further classified into two groups: room temperature ionic liquids (RTILs) and frozen ionic liquids (FILs). RTILs are liquid at room temperature, while FILs are solid at room temperature. ILs exhibit a number of tunable properties such as low vapor pressure, high conductivity, and high thermal stability.[91-92] A large selection of cations and anions can produce 10^{18} possible ternary combinations of ILs.[93] The tunable properties and countless possibilities of ILs has led these materials to be used in a wide range of applications. The acronym GUMBOS was introduced by the Warner Research Group and derived from a ***g***roup of ***u***niform ***m***aterials ***b***ased on ***o***rganic ***s***alts.[94] This class of compounds resembles ILs in the ability to vary a counterion and tune desired properties; however, GUMBOS represent solid phase organic salts with melting points between 25°C and 250°C.[94] Similar to ILs, these materials have been employed for many applications including dye-sensitized solar cells,[95-97] organic light emitting diodes,[98] biomedical imaging,[99] chemotherapeutic agents,[100-103] matrices for MALDI mass spectrometry,[104] sensors,[105-106] and vapor sensing.[107-112]

The first application of ILs as coating materials in QCM-based vapor sensing was explored in 2002 by Liang, et al.[113] In this study, sensing properties of an IL was investigated by detecting a range of VOCs and exploiting the viscosity of the IL. It was

found that exposure to VOC vapors resulted in positive frequency changes, which is characteristic of non-ideal Sauerbrey behavior. This study suggested that ILs exhibit partial selectivity to an assortment of VOCs and that variation of a counterion could further tune that selectivity. The first QCM-based IL sensor array was developed in 2006 by Jin, et al.[114] In this research, seven RTILs were used as coating materials to create a sensor array and detect four VOCs at high temperatures. Using DA, it was found that this sensor array was 100% accurate discriminating between the four VOCs. Following this development in sensor arrays, Xu, et al, designed a QCM-based IL sensor array demonstrating selectivity of imidazolium halides towards alcohols.[115] With advancements in QCM IL based sensor arrays, Toniolo, et al, developed a sensor array capable of real sample analysis in 2013.[39] This study focused on monitoring food quality control by detecting and discriminating between 31 VOCs and two complex mixtures. Although there has been great advancement in QCM-based sensor array developments, limitations remain present with a low range of sensitivity, as well as little to no reversibility and reusability. The work presented in this dissertation is aimed at addressing these limitations.

1.6. Scope of Dissertation

The objective of this dissertation was to develop reusable QCM-based sensor arrays for detection and discrimination of VOCs using GUMBOS and ILs as coating materials. The second chapter of this dissertation is focused on the synthesis of four novel phthalocyanine based GUMBOS for use as recognition elements in a MSA. Gas-sensing properties of GUMBOS was investigated by exposing the MSA to a set of ten VOCs. Statistical analyses were performed to evaluate accuracy of the MSA.

The third chapter is a description of two sensing systems for detection and discrimination of closely related VOCs. Three novel phosphonium ILs were synthesized and their gas-sensing properties were examined and compared to phosphonium IL-polymer composites. Using phosphonium ILs and phosphonium IL-polymer composites, two sensing schemes were developed and compared using statistical analyses.

The fourth chapter of this work is focused on a sensor array development for mixture analysis. IL-polymer composites were prepared and their gas-sensing properties were investigated. Mixture analysis of alcohols was evaluated using various statistical analyses. The fifth chapter concludes this dissertation by summarizing findings and discusses future research aims for the work presented.

1.7. References

1. Indoor Air Quality (IAQ) - Technical Overview of Volatile Organic Compounds. https://www.epa.gov/indoor-air-quality-iaq/technical-overview-volatile-organic-compounds#8.

2. Guenther, A.; Hewitt, C. N.; Erickson, D.; Fall, R.; Geron, C.; Graedel, T.; Harley, P.; Klinger, L.; Lerdau, M.; McKay, W., A global model of natural volatile organic compound emissions. *Journal of Geophysical Research: Atmospheres* **1995,** *100* (D5), 8873-8892.

3. Derwent, R. G., Sources, distributions, and fates of VOCs in the atmosphere. In *Volatile Organic Compounds in the Atmosphere*, Hester, R. E.; Harrison, R. M., Eds. The Royal Society of Chemistry: 1995; Vol. 4, pp 1-16.

4. Kansal, A., Sources and reactivity of NMHCs and VOCs in the atmosphere: A review. *Journal of hazardous materials* **2009,** *166* (1), 17-26.

5. Kessler, A.; Baldwin, I. T., Defensive function of herbivore-induced plant volatile emissions in nature. *Science* **2001,** *291* (5511), 2141-2144.

6. Kesselmeier, J.; Staudt, M., Biogenic volatile organic compounds (VOC): an overview on emission, physiology and ecology. *Journal of atmospheric chemistry* **1999,** *33* (1), 23-88.

7. Baldwin, I. T.; Kessler, A.; Halitschke, R., Volatile signaling in plant–plant–herbivore interactions: what is real? *Current opinion in plant biology* **2002,** *5* (4), 351-354.

8. Weller, A., Human pheromones: Communication through body odour. *Nature* **1998,** *392* (6672), 126.

9. Wyatt, T. D., *Pheromones and animal behaviour: communication by smell and taste*. Cambridge university press: 2003.

10. Blande, J. D.; Holopainen, J. K.; Li, T., Air pollution impedes plant-to-plant communication by volatiles. *Ecology letters* **2010,** *13* (9), 1172-1181.

11. Shorey, H. H., *Animal communication by pheromones*. Academic Press: 2013.

12. Agosta, W. C., *Chemical communication: the language of pheromones*. Henry Holt and Company: 1992.

13. Simon, H.; Reff, A.; Wells, B.; Xing, J.; Frank, N., Ozone trends across the United States over a period of decreasing NOx and VOC emissions. *Environmental science & technology* **2014,** *49* (1), 186-195.

14. Weinhold, B., The future of fracking: new rules target air emissions for cleaner natural gas production. National Institute of Environmental Health Sciences: 2012.

15. Matsumoto, N.; Elder, M.; Ogihara, A., Japan's policy to reduce emissions of volatile organic compounds: factors that facilitate industry participation in voluntary actions. *Journal of Cleaner Production* **2015,** *108*, 931-943.

16. Ambient (outdoor) air quality and health. https://www.who.int/news-room/fact-sheets/detail/ambient-(outdoor)-air-quality-and-health.

17. McConnell, V. D.; Schwab, R. M., The impact of environmental regulation on industry location. *Land Economics* **1990,** *66* (1), 67.

18. Kampa, M.; Castanas, E., Human health effects of air pollution. *Environmental pollution* **2008,** *151* (2), 362-367.

19. Adgate, J. L.; Church, T. R.; Ryan, A. D.; Ramachandran, G.; Fredrickson, A. L.; Stock, T. H.; Morandi, M. T.; Sexton, K., Outdoor, indoor, and personal exposure to VOCs in children. *Environmental health perspectives* **2004,** *112* (14), 1386-1392.

20. Kouch, T. Know the Air You're Breathing: Volatile Organic Compounds. http://www.critical-environment.com/blog/know-the-air-you%E2%80%99re-breathing-volatile-organic-compound-2-of-4/ (accessed January 20).

21. Chao, C. Y.; Chan, G. Y., Quantification of indoor VOCs in twenty mechanically ventilated buildings in Hong Kong. *Atmospheric Environment* **2001,** *35* (34), 5895-5913.

22. Volatile Organic Compounds' Impact on Indoor Air Quality. https://www.epa.gov/indoor-air-quality-iaq/volatile-organic-compounds-impact-indoor-air-quality (accessed February).

23. Report on the Environment - Indoor Air Quality. https://www.epa.gov/report-environment/indoor-air-quality#note1.

24. Di Natale, C.; Macagnano, A.; Martinelli, E.; Paolesse, R.; D'Arcangelo, G.; Roscioni, C.; Finazzi-Agro, A.; D'Amico, A., Lung cancer identification by the analysis of breath by means of an array of non-selective gas sensors. *Biosensors and Bioelectronics* **2003,** *18* (10), 1209-1218.

25. Ayad, M. M.; Torad, N. L., Alcohol vapours sensor based on thin polyaniline salt film and quartz crystal microbalance. *Talanta* **2009,** *78* (4), 1280-1285.

26. Hierlemann, A.; Weimar, U.; Kraus, G.; Schweizer-Berberich, M.; Göpel, W., Polymer-based sensor arrays and multicomponent analysis for the detection of hazardous oragnic vapours in the environment. *Sensors and Actuators B: Chemical* **1995,** *26* (1-3), 126-134.

27. Stetter, J. R.; Jurs, P. C.; Rose, S. L., Detection of Hazardous Gases and Vapors: Pattern Recognition Analysis of Data from an Electrochemical Sensor Array. *Analytical Chemistry* **1986,** *58*, 860-866.

28. Lin, H.; Suslick, K. S., A colorimetric sensor array for detection of triacetone triperoxide vapor. *Journal of the American Chemical Society* **2010,** *132* (44), 15519-15521.

29. Ewing, R. G.; Clowers, B. H.; Atkinson, D. A., Direct real-time detection of vapors from explosive compounds. *Analytical chemistry* **2013,** *85* (22), 10977-10983.

30. Hu, Z.; Pramanik, S.; Tan, K.; Zheng, C.; Liu, W.; Zhang, X.; Chabal, Y. J.; Li, J., Selective, sensitive, and reversible detection of vapor-phase high explosives via two-dimensional mapping: A new strategy for MOF-based sensors. *Crystal Growth & Design* **2013,** *13* (10), 4204-4207.

31. Ewing, R. G.; Atkinson, D. A.; Clowers, B. H., Direct real-time detection of RDX vapors under ambient conditions. *Analytical chemistry* **2012,** *85* (1), 389-397.

32. Staples, E. J.; Viswanathan, S., Ultrahigh-speed chromatography and virtual chemical sensors for detecting explosives and chemical warfare agents. *IEEE Sensors Journal* **2005,** *5* (4), 622-631.

33. Yinon, J., Peer Reviewed: Detection of Explosives by Electronic Noses. *Analytical Chemistry* **2003,** *75* (5), 98 A-105 A.

34. Mazzone, P. J.; Hammel, J.; Dweik, R.; Na, J.; Czich, C.; Laskowski, D.; Mekhail, T., Diagnosis of lung cancer by the analysis of exhaled breath with a colorimetric sensor array. *Thorax* **2007,** *62* (7), 565-568.

35. Machado, R. F.; Laskowski, D.; Deffenderfer, O.; Burch, T.; Zheng, S.; Mazzone, P. J.; Mekhail, T.; Jennings, C.; Stoller, J. K.; Pyle, J., Detection of lung cancer by sensor array analyses of exhaled breath. *American journal of respiratory and critical care medicine* **2005,** *171* (11), 1286-1291.

36. Sankaran, S.; Mishra, A.; Ehsani, R.; Davis, C., A review of advanced techniques for detecting plant diseases. *Computers and Electronics in Agriculture* **2010,** *72* (1), 1-13.

37. Chen, X.; Cao, M.; Li, Y.; Hu, W.; Wang, P.; Ying, K.; Pan, H., A study of an electronic nose for detection of lung cancer based on a virtual SAW gas sensors array and imaging recognition method. *Measurement Science and Technology* **2005,** *16* (8), 1535.

38. Capone, S.; Epifani, M.; Quaranta, F.; Siciliano, P.; Taurino, A.; Vasanelli, L., Monitoring of rancidity of milk by means of an electronic nose and a dynamic PCA analysis. *Sensors and Actuators B: Chemical* **2001,** *78* (1-3), 174-179.

39. Toniolo, R.; Pizzariello, A.; Dossi, N.; Lorenzon, S.; Abollino, O.; Bontempelli, G., Room Temperature Ionic Liquids As Useful Overlayers for Estimating Food Quality from Their Odor Analysis by Quartz Crystal Microbalance Measurements. *Analytical Chemistry* **2013,** *85* (15), 7241-7247.

40. Barié, N.; Bücking, M.; Rapp, M., A novel electronic nose based on miniaturized SAW sensor arrays coupled with SPME enhanced headspace-analysis and its use for rapid determination of volatile organic compounds in food quality monitoring. *Sensors and Actuators B: Chemical* **2006,** *114* (1), 482-488.

41. Schaller, E.; Bosset, J. O.; Escher, F., 'Electronic Noses' and Their Application to Food. *LWT - Food Science and Technology* **1998,** *31* (4), 305-316.

42. O'Connell, M.; Valdora, G.; Peltzer, G.; Negri, R. M., A practical approach for fish freshness determinations using a portable electronic nose. *Sensors and Actuators B: chemical* **2001,** *80* (2), 149-154.

43. Fens, N.; Schee, M.; Brinkman, P.; Sterk, P., Exhaled breath analysis by electronic nose in airways disease. Established issues and key questions. *Clinical & Experimental Allergy* **2013,** *43* (7), 705-715.

44. Delgado-Rodríguez, M.; Ruiz-Montoya, M.; Giraldez, I.; López, R.; Madejón, E.; Díaz, M. J., Use of electronic nose and GC-MS in detection and monitoring some VOC. *Atmospheric Environment* **2012,** *51*, 278-285.

45. Westhoff, M.; Litterst, P.; Freitag, L.; Urfer, W.; Bader, S.; Baumbach, J. I., Ion mobility spectrometry for the detection of volatile organic compounds in exhaled breath of patients with lung cancer: results of a pilot study. *Thorax* **2009,** *64* (9), 744-748.

46. Nyquist, J. E.; Wilson, D. L.; Norman, L. A.; Gammage, R. B., Decreased sensitivity of photoionization detector total organic vapor detectors in the presence of methane. *American Industrial Hygiene Association Journal* **1990,** *51* (6), 326-330.

47. Faiola, C.; Erickson, M.; Fricaud, V.; Jobson, B.; VanReken, T., Quantification of biogenic volatile organic compounds with a flame ionization detector using the effective carbon number concept. *Atmospheric Measurement Techniques (Online)* **2012,** *5* (8).

48. Wilson, A.; Baietto, M., Applications and Advances in Electronic-Nose Technologies. *Sensors* **2009,** *9* (7), 5099.

49. Morrison, J. Human nose can detect 1 trillion odours. https://www.nature.com/news/human-nose-can-detect-1-trillion-odours-1.14904.

50. Albert, K. J.; Lewis, N. S.; Schauer, C. L.; Sotzing, G. A.; Stitzel, S. E.; Vaid, T. P.; Walt, D. R., Cross-reactive chemical sensor arrays. *Chemical reviews* **2000,** *100* (7), 2595-2626.

51. Yamazoe, N.; Shimanoe, K., New perspectives of gas sensor technology. *Sensors and Actuators B: Chemical* **2009,** *138* (1), 100-107.

52. Egashira, M.; Shimizu, Y., Odor sensing by semiconductor metal oxides. *Sensors and Actuators B: Chemical* **1993,** *13* (1-3), 443-446.

53. Shurmer, H.; Gardner, J.; Chan, H., The application of discrimination technique to alcohols and tobaccos using tin-oxide sensors. *Sensors and Actuators* **1989,** *18* (3-4), 361-371.

54. Lonergan, M. C.; Severin, E. J.; Doleman, B. J.; Beaber, S. A.; Grubbs, R. H.; Lewis, N. S., Array-based vapor sensing using chemically sensitive, carbon black−polymer resistors. *Chemistry of Materials* **1996,** *8* (9), 2298-2312.

55. Hatfield, J.; Neaves, P.; Hicks, P.; Persaud, K.; Travers, P., Towards an integrated electronic nose using conducting polymer sensors. *Sensors and Actuators B: Chemical* **1994,** *18* (1-3), 221-228.

56. Gardner, J. W.; Bartlett, P. N., Electronic noses. Principles and applications. IOP Publishing: 2000.

57. Zhu, W.; Li, W.; Yang, H.; Jiang, Y.; Wang, C.; Chen, Y.; Li, G., A Rapid and Efficient Way to Dynamic Creation of Cross-Reactive Sensor Arrays Based on Ionic Liquids. *Chemistry – A European Journal* **2013,** *19* (35), 11603-11612.

58. Fanget, S.; Hentz, S.; Puget, P.; Arcamone, J.; Matheron, M.; Colinet, E.; Andreucci, P.; Duraffourg, L.; Myers, E.; Roukes, M. L., Gas sensors based on gravimetric detection—A review. *Sensors and Actuators B: Chemical* **2011,** *160* (1), 804-821.

59. Suslick, B. A.; Feng, L.; Suslick, K. S., Discrimination of complex mixtures by a colorimetric sensor array: coffee aromas. *Analytical chemistry* **2010,** *82* (5), 2067-2073.

60. Janzen, M. C.; Ponder, J. B.; Bailey, D. P.; Ingison, C. K.; Suslick, K. S., Colorimetric Sensor Arrays for Volatile Organic Compounds. *Analytical Chemistry* **2006,** *78* (11), 3591-3600.

61. Hu, Z.; Deibert, B. J.; Li, J., Luminescent metal–organic frameworks for chemical sensing and explosive detection. *Chemical Society Reviews* **2014,** *43* (16), 5815-5840.

62. Drafts, B., Acoustic wave technology sensors. *IEEE Transactions on microwave theory and techniques* **2001,** *49* (4), 795-802.

63. Bodenhöfer, K.; Hierlemann, A.; Noetzel, G.; Weimar, U.; Göpel, W., Performances of Mass-Sensitive Devices for Gas Sensing: Thickness Shear Mode and Surface Acoustic Wave Transducers. *Analytical Chemistry* **1996,** *68* (13), 2210-2218.

64. Asht, S.; Dass, R., Pattern recognition techniques: A review. *International Journal of Computer Science and Telecommunications* **2012,** *3* (8), 25-29.

65. Abdi, H.; Williams, L. J., Principal component analysis. *Wiley interdisciplinary reviews: computational statistics* **2010,** *2* (4), 433-459.

66. Blackledge, R. D., *Forensic Analysis on the Cutting Edge: New Methods for Trace Evidence Analysis*. Wiley: 2007.

67. Heywang, W.; Lubitz, K.; Wersing, W., *Piezoelectricity: Evolution and Future of a Technology*. Springer Berlin Heidelberg: 2008.

68. Jaffe, H.; Berlincourt, D., Piezoelectric transducer materials. *Proceedings of the IEEE* **1965,** *53* (10), 1372-1386.

69. Johannsmann, D., *The Quartz Crystal Microbalance in Soft Matter Research*. Springer International Publishing Switzerland, 2015.

70. Sauerbrey, G., Use of quartz vibration for weighing thin films on a microbalance. *Z. phys* **1959,** *155*, 206-212.

71. DeNolf, G. C.; Haack, L.; Holubka, J.; Straccia, A.; Blohowiak, K.; Broadbent, C.; Shull, K. R., High Frequency Rheometry of Viscoelastic Coatings with the Quartz Crystal Microbalance. *Langmuir* **2011,** *27* (16), 9873-9879.

72. Johannsmann, D., Viscoelastic, mechanical, and dielectric measurements on complex samples with the quartz crystal microbalance. *Physical Chemistry Chemical Physics* **2008,** *10* (31), 4516-4534.

73. Rodahl, M.; Höök, F.; Krozer, A.; Brzezinski, P.; Kasemo, B., Quartz crystal microbalance setup for frequency and Q-factor measurements in gaseous and liquid environments. *Review of Scientific Instruments* **1995,** *66* (7), 3924-3930.

74. Rodahl, M.; Kasemo, B., A simple setup to simultaneously measure the resonant frequency and the absolute dissipation factor of a quartz crystal microbalance. *Review of Scientific Instruments* **1996,** *67* (9), 3238-3241.

75. QCM-D Measurements. https://www.biolinscientific.com/measurements/qcm-d.

76. McHale, G.; Lücklum, R.; Newton, M. I.; Cowen, J. A., Influence of viscoelasticity and interfacial slip on acoustic wave sensors. *Journal of Applied Physics* **2000,** *88* (12), 7304-7312.

77. Fu, Y.; Finklea, H. O., Quartz Crystal Microbalance Sensor for Organic Vapor Detection Based on Molecularly Imprinted Polymers. *Analytical Chemistry* **2003,** *75* (20), 5387-5393.

78. Matsuguchi, M.; Uno, T., Molecular imprinting strategy for solvent molecules and its application for QCM-based VOC vapor sensing. *Sensors and Actuators B: Chemical* **2006,** *113* (1), 94-99.

79. Bunte, G.; Hürttlen, J.; Pontius, H.; Hartlieb, K.; Krause, H., Gas phase detection of explosives such as 2,4,6-trinitrotoluene by molecularly imprinted polymers. *Analytica Chimica Acta* **2007,** *591* (1), 49-56.

80. Kikuchi, M.; Tsuru, N.; Shiratori, S., Recognition of terpenes using molecular imprinted polymer coated quartz crystal microbalance in air phase. *Science and Technology of Advanced Materials* **2006,** *7* (2), 156-161.

81. Koshets, I. A.; Kazantseva, Z. I.; Shirshov, Y. M.; Cherenok, S. A.; Kalchenko, V. I., Calixarene films as sensitive coatings for QCM-based gas sensors. *Sensors and Actuators B: Chemical* **2005,** *106* (1), 177-181.

82. KALCHENKO, V. I.; KOSHETS, I. A.; MATSAS, E. P.; KOPYLOV, O. N.; SOLOVYOV, A.; KAZANTSEVA, Z. I.; SHIRSHOV, Y. M., Calixarene-based QCM sensors array and its response to volatile organic vapours *Materials Science* **2002,** *20* (3), 73-88.

83. Holloway, A. F.; Nabok, A.; Thompson, M.; Ray, A. K.; Wilkop, T., Impedance analysis of the thickness shear mode resonator for organic vapour sensing. *Sensors and Actuators B: Chemical* **2004,** *99* (2), 355-360.

84. Potyrailo, R. A.; Surman, C.; Nagraj, N.; Burns, A., Materials and Transducers Toward Selective Wireless Gas Sensing. *Chemical Reviews* **2011,** *111* (11), 7315-7354.

85. Montmeat, P.; Madonia, S.; Pasquinet, E.; Hairault, L.; Gros, C. P.; Barbe, J.; Guilard, R., Metalloporphyrins as sensing material for quartz-crystal microbalance nitroaromatics sensors. *IEEE Sensors Journal* **2005,** *5* (4), 610-615.

86. Regmi, B. P.; Galpothdeniya, W. I. S.; Siraj, N.; Webb, M. H.; Speller, N. C.; Warner, I. M., Phthalocyanine-and porphyrin-based GUMBOS for rapid and sensitive detection of organic vapors. *Sensors and Actuators B: Chemical* **2015,** *209*, 172-179.

87. Wang, X.; Ding, B.; Sun, M.; Yu, J.; Sun, G., Nanofibrous polyethyleneimine membranes as sensitive coatings for quartz crystal microbalance-based formaldehyde sensors. *Sensors and Actuators B: Chemical* **2010,** *144* (1), 11-17.

88. Bougharouat, A.; Bellel, A.; Sahli, S.; Ségui, Y.; Raynaud, P., Plasma polymerization of TEOS for QCM-based VOC vapor sensing. *The European Physical Journal - Applied Physics* **2011,** *56* (2), 24017.

89. Voinova, M. V.; Rodahl, M.; Jonson, M.; Kasemo, B., Viscoelastic Acoustic Response of Layered Polymer Films at Fluid-Solid Interfaces: Continuum Mechanics Approach. *Physica Scripta* **1999,** *59* (5), 391-396.

90. Strashilov, V. L.; Alexieva, G. E.; Velichkov, V. N.; Mateva, R. P.; Avramov, I. D., Polymer-Coated Quartz Microbalance Sensors for Volatile Organic Compound Gases. *Sensor Letters* **2009,** *7* (2), 203-211.

91. Brennecke, J. F.; Maginn, E. J., Ionic liquids: Innovative fluids for chemical processing. *AIChE Journal* **2001,** *47* (11), 2384-2389.

92. Kulkarni, P. S.; Branco, L. C.; Crespo, J. G.; Nunes, M. C.; Raymundo, A.; Afonso, C. A. M., Comparison of Physicochemical Properties of New Ionic Liquids Based on Imidazolium, Quaternary Ammonium, and Guanidinium Cations. *Chemistry – A European Journal* **2007,** *13* (30), 8478-8488.

93. Holbrey, J. D.; Seddon, K. R., Ionic Liquids. *Clean Products and Processes* **1999,** *1* (4), 223-236.

94. Warner, I. M.; El-Zahab, B.; Siraj, N., Perspectives on moving ionic liquid chemistry into the solid phase. *Analytical chemistry* **2014,** *86* (15), 7184-7191.

95. Jordan, A. N.; Das, S.; Siraj, N.; de Rooy, S. L.; Li, M.; El-Zahab, B.; Chandler, L.; Baker, G. A.; Warner, I. M., Anion-controlled morphologies and spectral features of cyanine-based nanoGUMBOS – an improved photosensitizer. *Nanoscale* **2012,** *4* (16), 5031-5038.

96. Kolic, P. E.; Siraj, N.; Cong, M.; Regmi, B. P.; Luan, X.; Wang, Y.; Warner, I. M., Improving energy relay dyes for dye-sensitized solar cells by use of a group of uniform materials based on organic salts (GUMBOS). *RSC Advances* **2016,** *6* (97), 95273-95282.

97. Siraj, N.; Kolic, P. E.; Regmi, B. P.; Warner, I. M., Strategy for Tuning the Photophysical Properties of Photosensitizers for Use in Photodynamic Therapy. *Chemistry – A European Journal* **2015,** *21* (41), 14440-14446.

98. Siraj, N.; Hasan, F.; Das, S.; Kiruri, L. W.; Steege Gall, K. E.; Baker, G. A.; Warner, I. M., Carbazole-derived group of uniform materials based on organic salts: solid state fluorescent analogues of ionic liquids for potential applications in organic-based blue light-emitting diodes. *The Journal of Physical Chemistry C* **2014,** *118* (5), 2312-2320.

99. Bwambok, D. K.; El-Zahab, B.; Challa, S. K.; Li, M.; Chandler, L.; Baker, G. A.; Warner, I. M., Near-Infrared Fluorescent NanoGUMBOS for Biomedical Imaging. *ACS Nano* **2009,** *3* (12), 3854-3860.

100. Magut, P. K. S.; Das, S.; Fernand, V. E.; Losso, J.; McDonough, K.; Naylor, B. M.; Aggarwal, S.; Warner, I. M., Tunable Cytotoxicity of Rhodamine 6G via Anion Variations. *Journal of the American Chemical Society* **2013,** *135* (42), 15873-15879.

101. Bhattarai, N.; Mathis, J. M.; Chen, M.; Pérez, R. L.; Siraj, N.; Magut, P. K. S.; McDonough, K.; Sahasrabudhe, G.; Warner, I. M., Endocytic Selective Toxicity of Rhodamine 6G nanoGUMBOS in Breast Cancer Cells. *Molecular Pharmaceutics* **2018,** *15* (9), 3837-3845.

102. Bhattarai, N.; Chen, M.; Pérez, R. L.; Ravula, S.; Chhotaray, P.; Hamdan, S.; McDonough, K.; Tiwari, S.; Warner, I. M., Enhanced chemotherapeutic toxicity of cyclodextrin templated size-tunable rhodamine 6G nanoGUMBOS. *Journal of Materials Chemistry B* **2018,** *6* (34), 5451-5459.

103. Chen, M.; Bhattarai, N.; Cong, M.; Pérez, R. L.; McDonough, K. C.; Warner, I. M., Mitochondria targeting IR780-based nanoGUMBOS for enhanced selective toxicity towards cancer cells. *RSC Advances* **2018,** *8* (55), 31700-31709.

104. Al Ghafly, H.; Siraj, N.; Das, S.; Regmi, B. P.; Magut, P. K. S.; Galpothdeniya, W. I. S.; Murray, K. K.; Warner, I. M., GUMBOS matrices of variable hydrophobicity for matrix-assisted laser desorption/ionization mass spectrometry. *Rapid Communications in Mass Spectrometry* **2014,** *28* (21), 2307-2314.

105. Galpothdeniya, W. I. S.; Fronczek, F. R.; Cong, M.; Bhattarai, N.; Siraj, N.; Warner, I. M., Tunable GUMBOS-based sensor array for label-free detection and discrimination of proteins. *Journal of Materials Chemistry B* **2016,** *4* (8), 1414-1422.

106. Galpothdeniya, W. I. S.; McCarter, K. S.; De Rooy, S. L.; Regmi, B. P.; Das, S.; Hasan, F.; Tagge, A.; Warner, I. M., Ionic liquid-based optoelectronic sensor arrays for chemical detection. *RSC Advances* **2014,** *4* (14), 7225-7234.

107. Regmi, B. P.; Monk, J.; El-Zahab, B.; Das, S.; Hung, F. R.; Hayes, D. J.; Warner, I. M., A novel composite film for detection and molecular weight determination of organic vapors. *Journal of Materials Chemistry* **2012,** *22* (27), 13732-13741.

108. Regmi, B. P.; Speller, N. C.; Anderson, M. J.; Brutus, J. O.; Merid, Y.; Das, S.; El-Zahab, B.; Hayes, D. J.; Murray, K. K.; Warner, I. M., Molecular weight sensing properties of ionic liquid-polymer composite films: theory and experiment. *Journal of Materials Chemistry C* **2014,** *2* (24), 4867-4878.

109. Speller, N. C.; Siraj, N.; McCarter, K. S.; Vaughan, S.; Warner, I. M., QCM VIRTUAL SENSOR ARRAY: VAPOR IDENTIFICATION AND MOLECULAR WEIGHT APPROXIMATION. *Sensors and Actuators B: Chemical* **2017**.

110. Speller, N. C.; Siraj, N.; Regmi, B. P.; Marzoughi, H.; Neal, C.; Warner, I. M., Rational Design of QCM-D Virtual Sensor Arrays Based on Film Thickness, Viscoelasticity, and Harmonics for Vapor Discrimination. *Analytical Chemistry* **2015,** *87* (10), 5156-5166.

111. Speller, N. C.; Siraj, N.; Vaughan, S.; Speller, L. N.; Warner, I. M., Assessment of QCM array schemes for mixture identification: citrus scented odors. *RSC Advances* **2016,** *6* (98), 95378-95386.

112. Speller, N. C.; Siraj, N.; Vaughan, S.; Speller, L. N.; Warner, I. M., QCM virtual multisensor array for fuel discrimination and detection of gasoline adulteration. *Fuel* **2017,** *199*, 38-46.

113. Liang, C.; Yuan, C.-Y.; Warmack, R. J.; Barnes, C. E.; Dai, S., Ionic Liquids: A New Class of Sensing Materials for Detection of Organic Vapors Based on the Use of a Quartz Crystal Microbalance. *Analytical Chemistry* **2002,** *74* (9), 2172-2176.

114. Jin, X.; Yu, L.; Garcia, D.; Ren, R. X.; Zeng, X., Ionic liquid high-temperature gas sensor array. *Analytical chemistry* **2006,** *78* (19), 6980-6989.

115. Xu, X.; Li, C.; Pei, K.; Zhao, K.; Zhao, Z. K.; Li, H., Ionic liquids used as QCM coating materials for the detection of alcohols. *Sensors and Actuators B: Chemical* **2008,** *134* (1), 258-265.

CHAPTER 2. CLASS SPECIFIC DISCRIMINATION OF VOLATILE ORGANIC COMPOUNDS USING A QUARTZ CRYSTAL MICROBALANCE BASED MULTISENSOR ARRAY*

2.1. Introduction

Although many volatile organic compounds (VOCs) are non-toxic, many of them can cause harmful health and environmental effects including, but not limited to, headaches, nerve disease, or cancer.[1-2] Furthermore, VOCs play a critical role in food quality control,[3-4] explosives detection,[5-7] and medical diagnostics.[8-10] Therefore, it is very important to develop vapor-sensing techniques for detection and discrimination of various types of VOCs.

A variety of techniques, including optical sensors and colorimetric sensors, have been used for VOC analysis.[11-14] However, more recent use of electronic noses (e-nose) has gained considerable popularity[15] since e-nose devices are designed to mimic the human nose. In this regard, when the human nose encounters a scent, a signal travels from multiple receptors in the nose to the brain, which processes the receptor response pattern and identifies the scent. A mechanized analogue of an e-nose will typically comprise multiple chemically distinct coatings that act as cross reactive elements within a multisensor array.[16-17] Upon exposure to vapors, sensor-vapor interactions generate analyte specific response patterns that can be analyzed using statistical analyses such as artificial neural networks (ANN), cluster analysis, analysis of variance (ANOVA), principal component analysis (PCA), and discriminate analysis (DA). E-noses can be

*This chapter previously appeared as S. R. Vaughan, N. C. Speller, P. Chhotaray, K. S. McCarter, N. Siraj, R. L. Pérez, Y. Li, and I. M. Warner, Class specific discrimination of volatile organic compounds using a quartz crystal microbalance based multisensor array. Reprinted with permission from *Talanta*, **188**, 423–428, Elsevier, (2018).

categorized into many classes, including metal oxides, gas chromatography-mass spectrometry (GC-MS), and many others.[15] However, these approaches have distinct disadvantages; for example, GC-MS is complex, expensive, and typically requires an expert operator,[18] while metal oxides require operation at high temperatures, high power consumption, and have a limited selection of sensor coating materials.[19] To overcome these disadvantages, use of a quartz crystal microbalance (QCM) as an e-nose has been proposed due to its good precision, high sensitivity, and diverse range of sensor coating materials.[19]

The QCM is a thickness shear mode device that consists of an AT-cut quartz crystal resonator (QCR), sandwiched between two metallic electrodes and based on the reverse piezoelectric effect. In such a system, an external voltage is applied causing the QCR to oscillate, resulting in the generation of an acoustic shear wave. At the interface of a QCR and coating material, the shear wave undergoes an attenuation and phase shift, resulting in a change in frequency.[20] The operating principle of a QCM is based on the Sauerbrey equation:

$$\Delta f = -\frac{n}{c}\Delta m = -\frac{n}{c}\rho_f t_f$$

where Δf is change in resonance frequency, η is harmonic number, c is mass sensitivity which is 17.7 ngcm^{-2}Hz^{-1} for a 5 MHz AT-cut crystal as used in this study; ρ_f is the density of the film, and t_f is film thickness.[21] Essentially, change in mass on the QCR surface is directly related to change in frequency on the oscillating crystal as reflected in the above equation. Thus, change in frequency allows an estimation of the mass of analyte adsorbed onto the surface of the QCR. Since these terms are directly proportional, the

resonance frequency should decrease as mass is added to the QCR surface, which is characterized as ideal Sauerbrey behavior. In essence, the QCM has commonly been used simply as a mass detector. Selectivity and sensitivity of a QCM sensor depends on the characteristics of the coating material. In this regard, QCM sensors typically employ chemosensitive materials such as ionic liquids, imprinted polymers, and composite materials.[6, 22-24] However, there are some limitations associated with use of such materials including complex synthesis, intricate deposition procedures, and slow response times.[6, 22-26]

Phthalocyanines and their derivatives are an appealing class of sensing materials due to their flexible synthesis and ability to interact with a large number of organic vapors.[27-29] In addition, conversion of these materials into GUMBOS may allow optimization of both sensitivity and selectivity.[30] The acronym GUMBOS is derived from ***g***roup of ***u***niform ***m***aterials ***b***ased on ***o***rganic ***s***alts as coined by Warner, et al.[31] This class of compounds are similar to ionic liquids (ILs) in that both are organic salts using similar counterions; however, GUMBOS represent solid phase organic salts with melting points between 25°C and 250°C,[31] while ILs have melting points below 100°C and are typically liquid at room temperature. Both classes of compounds have tunable properties such as hydrophobicity, melting point, toxicity, etc. simply by alteration of the counterion.

Herein, a QCM-based multisensor array is described for class specific discrimination of VOCs. To achieve this goal, a novel set of GUMBOS were synthesized using copper (II) phthalocyanine tetrasulfonate as anions and four different cations as recognition elements for VOC detection. Thin films of each compound were deposited on the surface of the QCRs via use of electrospray and then exposed to a set of ten VOCs

in order to evaluate gas-sensing properties. The set of sensors exhibited cross-reactive patterns, thus rendering them as adequate candidates for development of a sensor array. The resulting data from these four sensors were then used to develop a statistical model for distinguishing four classes of compounds (alcohols, aliphatic hydrocarbons, aromatic hydrocarbons, and chloro-hydrocarbons). PCA was used to assess the dimensionality of the observed sensor data and to obtain a visual representation of separation among the four compound classes. DA was used to develop the predictive model for distinguishing among the present compound classes, using the four sensor variables directly as predictor variables. It is often necessary to reduce the dimensionality of the predictor space in an experiment because of small sample size, and PCA can be used in this regard. However, in this manuscript, and for this analysis, compound classes are predicted rather than individual compounds, and thus adequate data allows use of the four sensor variables directly as predictor variables in this DA.

2.2. Materials and Methods

2.2.1. Materials

Copper (II) phthalocyaninetetrasulfonic acid ($CuPcS_4$) tetrasodium salt, tetrabutylammonium (TBA) bromide, tetrabutylphosphonium (P_{4444}) bromide, 3-(dodecyldimethyl-ammonio)propanesulfonate (DDMA), anhydrous methanol, anhydrous 1-propanol, anhydrous dichloromethane (DCM), anhydrous chloroform, anhydrous toluene, anhydrous heptane, hexane, and anhydrous benzene were purchased from Sigma-Aldrich (St. Louis, MO USA). Tributyl-n-octylphosphonium (P_{4448}) bromide was purchased from TCI (Portland, OR USA). Xylenes was purchased from Mallinckrodt

(Paris, KY USA) and ethanol was purchased from Koptec (King of Prussia, PA USA). All chemicals were used as received without further purification.

2.2.2. Instrumentation

A Q-Sense QCM-D E4 system and associated QCRs were purchased from Biolin Scientific (Stockholm, Sweden). Each QCR is an AT-cut gold-coated quartz crystal with a diameter of 14 mm, thickness of 0.3 mm and fundamental frequency of 4.95 MHz +/- 50 kHz. Both readout equipment (Model 5878) and mass flow controllers (Model 5850E) were obtained from Brooks Instrument, LLC (Hatfield, PA, USA).

2.2.3. Synthesis and Characterization of GUMBOS

GUMBOS were synthesized using a biphasic metathesis reaction.[30] As an example of a typical synthetic procedure, $[Na]_4[CuPcS_4]$ was dissolved in water while [TBA][Br] was dissolved in DCM at a 1:4 mole ratio. Prepared solutions were mixed together and left to stir in the dark for 48 hours to obtain $[TBA]_4[CuPcS_4]$. Following completion of the reaction, the DCM layer was rinsed several times with water to remove byproducts (NaBr). DCM was removed by rotary evaporation and any residual water was removed via freeze-drying. The reaction procedure referenced above was followed to obtain remaining GUMBOS by reacting $[Na]_4[CuPcS_4]$ with $[P_{4444}][Br]$, DDMA, and $[P_{4448}][Br]$ to obtain $[P_{4444}]_4[CuPcS_4]$, $[DDMA]_4[CuPcS_4]$, and $[P_{4448}]_4[CuPcS_4]$, respectively. The final products for all GUMBOS were blue, tacky solids. Structures of starting materials are shown in Figure A1 (supporting information).

All compounds were characterized using electrospray ionization mass spectrometry (ESI-MS) and Fourier transform infrared spectrometry (FT-IR). ESI-MS was accomplished using an Agilent 6210 system in positive and negative ion modes. FT-IR

was performed using a Bruker Alpha & Tensor 27 FT-IR instrument. Thermal properties were also investigated using thermogravimetric analysis (TGA), which was completed using a Hi-Res Modulated TGA 2950 instrument (TA instruments).

2.2.4. Preparation and Characterization of Sensing Films

Prior to coating , each QCR was cleaned using RCA standard clean 1 solution (5:1:1 deionized water, 30% hydrogen peroxide, and ammonium hydroxide).[32] Stock solutions of $[TBA]_4[CuPcS_4]$, $[P_{4444}]_4[CuPcS_4]$, $[DDMA]_4[CuPcS_4]$, and $[P_{4448}]_4[CuPcS_4]$ (1 mg/mL) were prepared using DCM in 20 mL borosilicate glass scintillation vials. A fairly uniform deposition of GUMBOS onto each QCR was achieved using electrospray. Parameters for electrospray remained constant for each thin film: deposition time of 2 minutes, flowrate of 100 µL/min, current of 30 µA, voltage of 16.6 kV and a working distance of 7 cm. After coating, films were blown with nitrogen and subsequently stored in a desiccator for at least 24 hours. The change in frequency between coated and uncoated QCRs in all of the studied GUMBOS was maintained at ~ -2000 Hz. Once coated with GUMBOS, QCRs are referred to as sensors. GUMBOS thin films were analyzed using scanning electron microscopy (SEM).

2.2.5. Data Collection

In these studies, analyte vapors were generated using a flow type system. In brief, each analyte was exposed at three different instrumentally controlled dilutions of flow rate ratios (0.1, 0.2, and 0.3 F_s/F_{tot}) which correspond to 10%, 20%, and 30% of equilibrated headspace in a 20 mL vial of VOC and argon gas. This flow system consisted of two independent gas flow channels, one for sample vapors and the other for carrier gas (ultrapure argon). To begin, a stable baseline was established by purging the system with

ultrapure argon. After a stable baseline was obtained, a vial containing the VOC of interest was bubbled with argon to generate a sample of equilibrated headspace. The sample and carrier channels merged to allow dilution of the sample flow to yield respective flow rate ratios.[33] Digital mass flow controllers were used to control and adjust the total flow rate to 100 sccm. VOC vapors mixed across 1-meter length of tubing and then flowed over each sensor. Analyte vapor was removed from sensors by purging the system with argon at room temperature until the baseline was recovered. A schematic of the system described is shown in Figure 2.1.

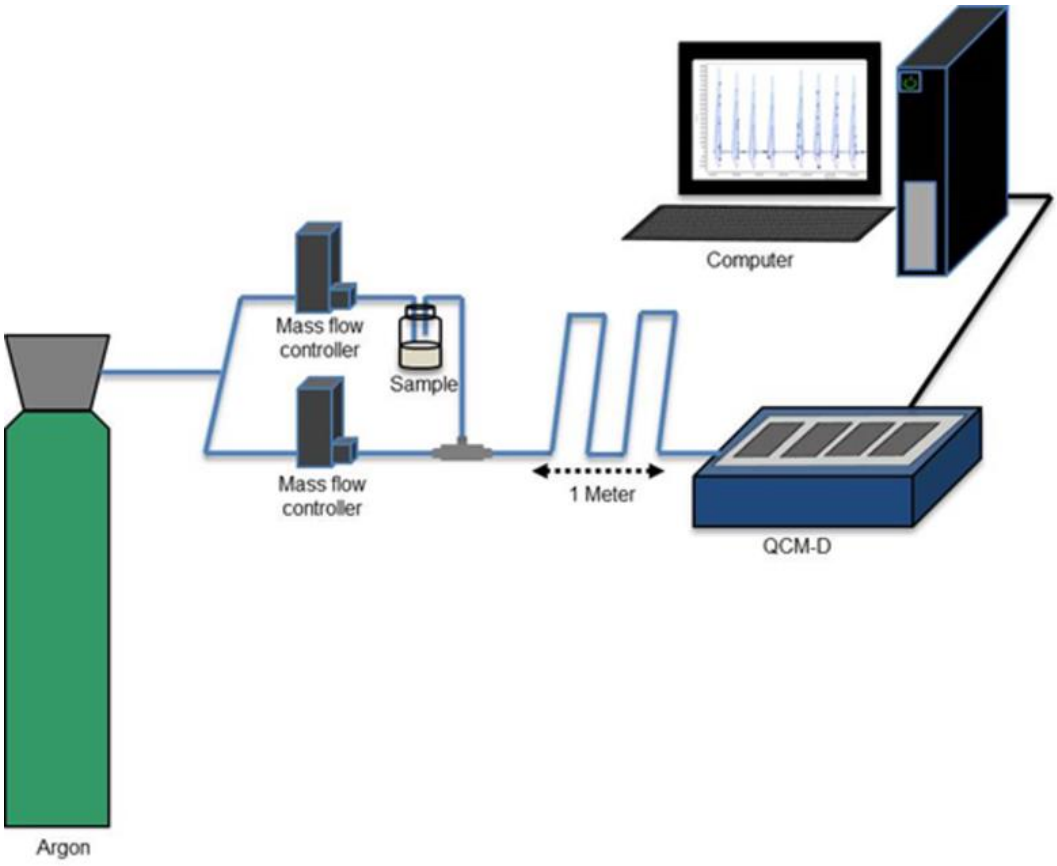

Figure 2.1. Schematic of QCM flow system.

2.2.6. Data Analysis

A single data set was acquired from vapor sensing studies expressed by change in frequency (Δf) in units of hertz (Hz). PCA was used to assess the dimensionality of the observed sensor data and to obtain a visual representation of separation among the four compound classes with respect to the principal components. DA was used to develop the predictive model for distinguishing four VOC classes, using the four sensor variables directly as predictor variables.

2.3. Results and Discussion

2.3.1. Characterization of GUMBOS

Each synthetic compound was confirmed using ESI-MS (Fig. A2 – A6) and FT-IR (Fig. A7 – A10). Thermal properties of our GUMBOS were evaluated using TGA and these curves are shown in Fig. A11 – A14. All four compounds exhibited good thermal stability. The onset temperature of decomposition for $[TBA]_4[CuPcS_4]$, $[P_{4444}]_4[CuPcS_4]$, $[DDMA]_4[CuPcS_4]$, and $[P_{4448}]_4[CuPcS_4]$ is found to be 256°C, 172°C, 175°C, and 364°C, respectively.

2.3.2. Characterization of Sensing Films

GUMBOS sensing films were analyzed using SEM. Here, the entire sensor was investigated using SEM. However, the images represent only a portion of the sensor. SEM images shown in Fig. A15 – A18 show that most of the QCRs surface are covered with GUMBOS.

2.3.3. Evaluation of Vapor Sensing Properties

Four QCM sensors with $[TBA]_4[CuPcS_4]$, $[P_{4444}]_4[CuPcS_4]$, $[DDMA]_4[CuPcS_4]$, and $[P_{4448}]_4[CuPcS_4]$, respectively, as recognition elements were inserted into QCM-D

chambers to evaluate vapor sensing properties. All sensors were introduced to a set of ten VOCs that included: methanol, ethanol, 1-propanol, dichloromethane, chloroform, xylenes, toluene, heptane, hexane, and benzene. Sensors were exposed to three different instrumentally controlled sample flow rate ratios (0.1, 0.2, and 0.3 F_s/F_{tot}) of respective VOCs at 3-minute intervals for a total exposure time of ~10 minutes and changes in resonance frequency were measured. Three replicate measurements were performed for each VOC. Plots of Δf versus flow rate ratios are depicted for each sensor, $[TBA]_4[CuPcS_4]$, $[P_{4444}]_4[CuPcS_4]$, $[DDMA]_4[CuPcS_4]$, and $[P_{4448}]_4[CuPcS_4]$ in Figures 2.2, 2.3, 2.4, and 2.5, respectively. Each sensor was determined to have a stable baseline and reversible sorption, thus rendering them reusable (data shown in Fig. A19 – A20). Furthermore, sensor responses were stable and reproducible. Due to inherent differences in chemical properties of the tested VOCs, flow rate ratios for different VOC vapors are not the same when expressed as concentrations in milligram per liter (mgL^{-1}); calculated concentrations are presented in Table A1. Thus, to compare sensitivity of each thin film towards a set of analytes, sensitivities were calculated. The sensitivity of GUMBOS has been previously defined as sensor response corresponding to 1 mgL^{-1} of an individual VOC vapor.[34] Figure 2.6 illustrates the calculated sensitivities while Tables A2 and A3 summarize calculated sensitivities and detection limits of $[TBA]_4[CuPcS_4]$, $[P_{4444}]_4[CuPcS_4]$, $[DDMA]_4[CuPcS_4]$, and $[P_{4448}]_4[CuPcS_4]$. Based on calculated sensitivities and sensor responses, these sensors demonstrated cross reactivity, which allowed for MSA fabrication.

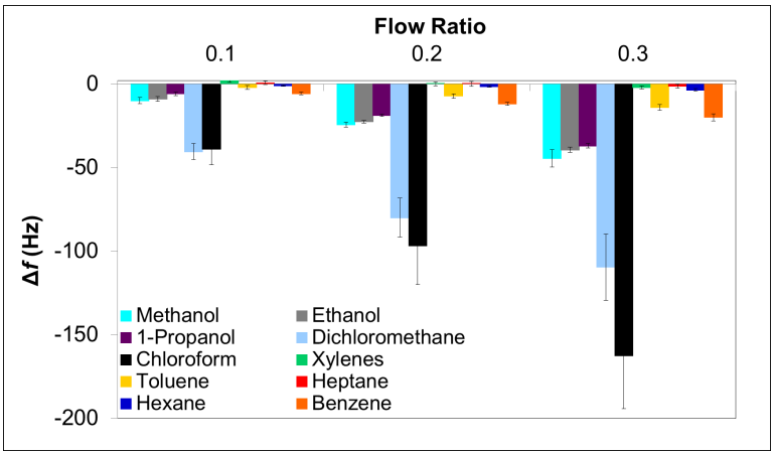

Figure 2.2. Sensor response when coated with $[TBA]_4[CuPcS_4]$ and exposed to ten VOCs at three saturated vapor pressures. Error bars represent standard deviation for three replicate measurements.

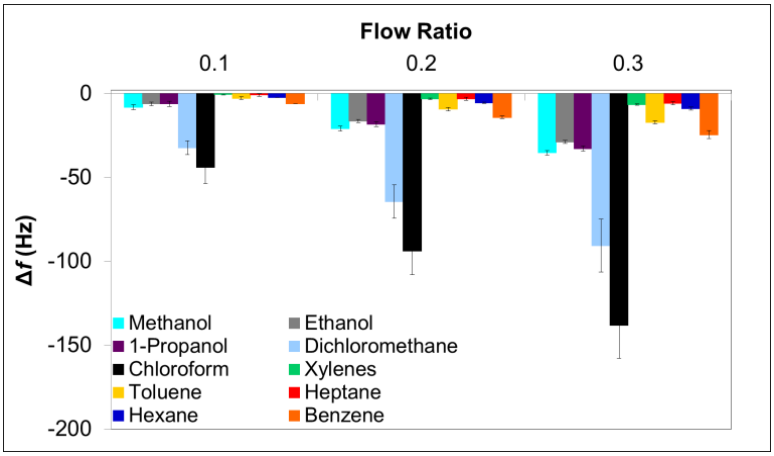

Figure 2.3. Sensor response when coated with $[P_{4444}]_4[CuPcS_4]$ and exposed to ten VOCs at three saturated vapor pressures. Error bars represent standard deviation for three replicate measurements.

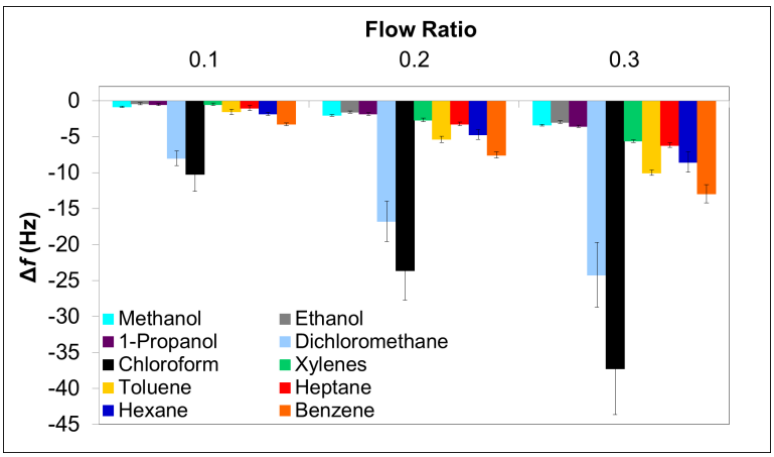

Figure 2.4. Sensor response when coated with $[DDMA]_4[CuPcS_4]$ and exposed to ten VOCs at three saturated vapor pressures. Error bars represent standard deviation for three replicate measurements.

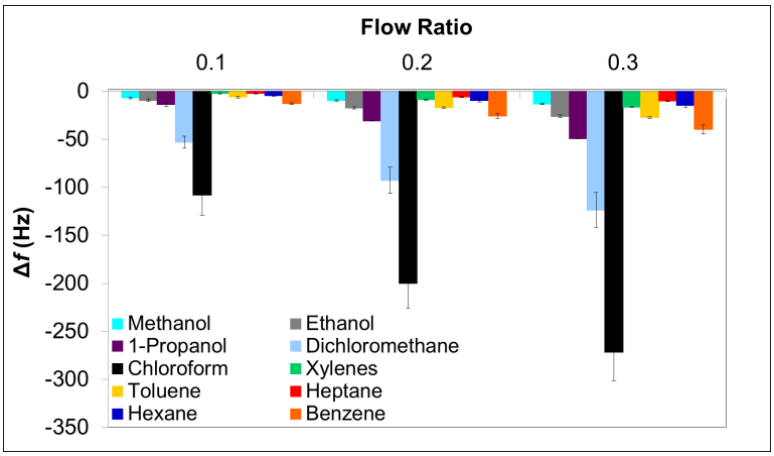

Figure 2.5. Sensor response when coated with $[P_{4448}]_4[CuPcS_4]$ and exposed to ten VOCs at three saturated vapor pressures. Error bars represent standard deviation for three replicate measurements.

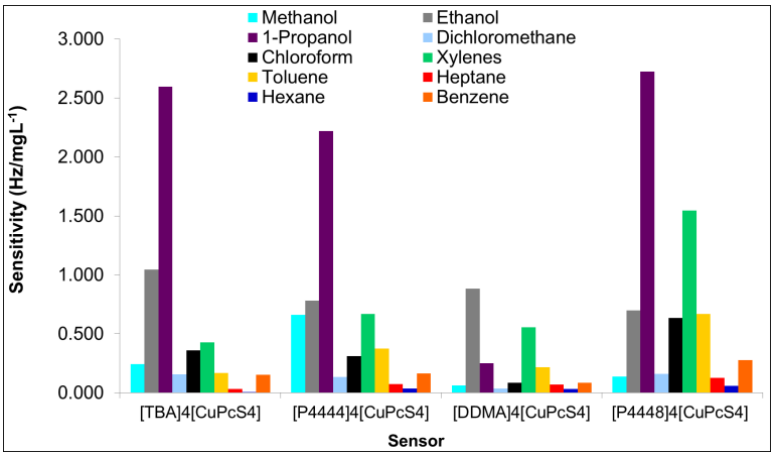

Figure 2.6. Graphical representation of calculated sensitivities of $[TBA]_4[CuPcS_4]$, $[P_{4444}]_4[CuPcS_4]$, $[DDMA]_4[CuPcS_4]$, and $[P_{4448}]_4[CuPcS_4]$ sensors.

To fabricate a MSA, the complete data set must be analyzed. Notably, each sensor produced analyte specific response patterns, but more specifically three of the four sensors exhibited class specific responses. For instance, the sensor coated with $[TBA]_4[CuPcS_4]$ in Figure 2.2, exhibited its highest sensor responses to the chlorohydrocarbons (chloroform and DCM), followed by alcohols (methanol, ethanol, and 1-propanol), aromatic hydrocarbons (benzene and toluene) and minimal response to

aliphatic hydrocarbons (hexane and heptane). Interestingly, the response of xylenes was comparable to that of the aliphatic hydrocarbons with minimal response as compared to aromatic hydrocarbons. Sensor $[P_{4444}]_4[CuPcS_4]$ exhibited similar class specific responses to that of $[TBA]_4[CuPcS_4]$; however, an increased response to hexane, heptane and xylenes as compared to $[TBA]_4[CuPcS_4]$ sensor can be seen in Figure 2.3. Similarity in sensitivities and sensor responses for $[TBA]_4[CuPcS_4]$ and $[P_{4444}]_4[CuPcS_4]$ could be attributed to chemical similarity in the cations heteroatoms and carbon chain length. As shown in Figure 2.4, the $[DDMA]_4[CuPcS_4]$ sensor demonstrated an overall lower response as compared to other sensors, with maximum change in frequency being approximately -40 Hz. It can also be seen that contrary to the $[TBA]_4[CuPcS_4]$ and $[P_{4444}]_4[CuPcS_4]$ sensors, $[DDMA]_4[CuPcS_4]$ sensor had an increased response to both aromatic and aliphatic hydrocarbons compared to alcohols. This response pattern and lower sensitivity could be attributed to the zwitterionic charge of DDMA; however, more experiments are being explored to fully understand the mechanism of this interaction. In comparison to previous sensors, the $[P_{4448}]_4[CuPcS_4]$ sensor exhibited its highest response to the chlorohydrocarbons. However, it does not show class specific responses to the remaining VOCs (Fig. 2.5). Although $[P_{4448}]_4[CuPcS_4]$ does not demonstrate class specific responses for all VOCs; it does have increased sensitivities for most analytes as compared to previous sensors. This may be attributed to the P_{4448} cation having a longer carbon chain length. These observations lead us to infer that increasing the carbon chain length of GUMBOS will likely result in a more homogenous coating on the QCR, which in turn would make the sensor more sensitive. This hypothesis is supported by the SEM images (Fig. A15 – A18).

2.3.4. Evaluation of MSA

Due to the unique responses of the reported sensors, it was hypothesized that the MSA could discriminate between these ten different VOCs by compound classes. To accomplish this, the raw Δf data collected from the four sensors were used in developing a predictive model using DA. The hypothesis that the covariance matrices associated with the four sensor variables were the same across all four compound classes was strongly rejected (p-value < 0.0001); thus, quadratic DA (QDA) was used, which fits a model that estimates the covariance matrices separately for each compound class.

The first two principal components accounted for 99.44% of the variability in the four predictors. The first principal component, which accounted for 97.09% of the variability, essentially represents the sum of the four sensor measurements. The second principal component, which accounted for an additional 2.35% of the total variation, represents a comparison between the $[DDMA]_4[CuPcS_4]$ and $[P_{4448}]_4[CuPcS_4]$ sensor measurements. Based on a plot of the first two principal component scores, shown in Figure 2.7, the principal components provided a great visual separation between chloro-hydrocarbons and alcohols, as well as between chloro-hydrocarbons and the combined classes of aliphatic hydrocarbons and aromatic hydrocarbons. However, the first two principal components provided no visual separation between the aliphatic hydrocarbons and aromatic hydrocarbons. This suggested that there may be difficulty in distinguishing between these two classes of compounds with the model produced by DA. The values for the first two principal components could be used as predictor variables in DA for developing the predictive model. However, due to the large number of observations within

each compound class, this was not necessary and the measurements from the four sensors were used directly as predictor variables.

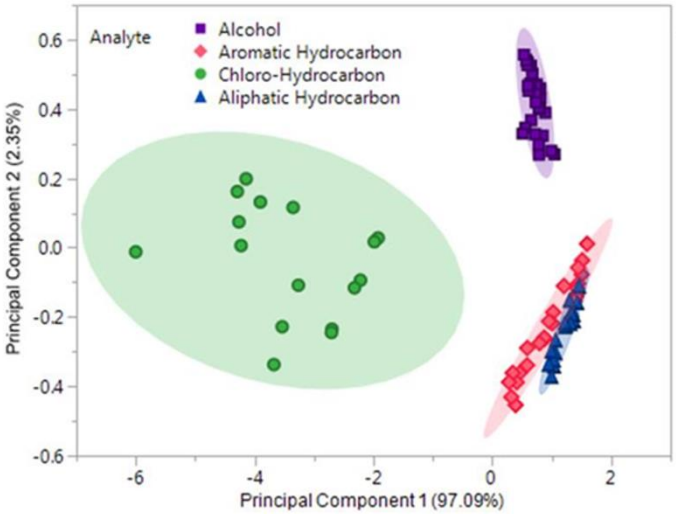

Figure 2.7. Principal component plot for discrimination of ten VOCs based on classes with respect to a four sensor MSA. Plot considers 90 total measurements consisting of three replicate measurements at three different flow ratios for each VOC (9 measurements per sample).

To assess the predictive accuracy of the resulting QDA, cross-validation classification was used. Cross-validation provides a less biased and more accurate assessment of the predictive accuracy of a model than the default resubstitution method, which is biased upwards. Using cross-validation, the QDA predictive model accurately classified, with exception of only one, all of the compounds into their correct compound classes. The one misclassification was due to an aliphatic hydrocarbon being classified as an aromatic hydrocarbon. It was previously mentioned that aliphatic hydrocarbons and aromatic hydrocarbons completely overlapped in a plot of the PCA scores (Fig. 2.7). Therefore, it was an interesting result that only one of these compounds was misclassified. Using uniform prior classification probabilities, the overall error rate was estimated to be 1.39%, corresponding to an overall accuracy rate of 98.6%.

For comparison purposes, in a QDA model using just the first principal component as a predictor, which again accounted for 97.09% of the variation in the sensor variables, the overall cross-validation classification error rate was 19.91%. In that model, two (2) of the alcohols were misclassified as hydrocarbons, seven (7) of the 27 aromatic hydrocarbons were misclassified as alcohols while another eleven (11) were misclassified as aliphatic hydrocarbons, and one (1) aliphatic hydrocarbon was misclassified as an aromatic hydrocarbon. In a QDA using the first two principal components as predictors, the overall cross-validation classification error rate dropped to 5.09%. In that model, four (4) aromatic hydrocarbons were misclassified as aliphatic hydrocarbons, and one (1) aliphatic hydrocarbon was misclassified as an aromatic hydrocarbon. Therefore, when all four sensor variables were used as predictors in the QDA, a more accurate predictive model was achieved than when the first two principal components were used as predictors.

2.4. Conclusion

In this study, four novel GUMBOS using copper (II) phthalocyanine tetrasulfonate were synthesized, and their gas-sensing properties were investigated using a QCM-based MSA. These GUMBOS showed good thermal stability, sensing characteristics, and cross-reactive responses for use in a MSA. By employing this phthalocyanine based GUMBOS multisensor array, ten different analytes were able to be discriminated into four classes with 98.6% accuracy. It should be noted that this high accuracy is achieved by using the original data set as predictor variables in QDA, as compared to the first two principal components, which is traditionally used. While the exact interaction of VOC vapors with GUMBOS sensing films is still being investigated, this work has given

considerable insight into their use as VOC sensors using a MSA. When one considers the high accuracy in discriminating classes of VOCs, this sensor array shows great potential for use in applications such as food quality control.[3-4]

2.5. References

1. Kampa, M.; Castanas, E., Human health effects of air pollution. *Environmental pollution* **2008,** *151* (2), 362-367.

2. Volatile Organic Compounds' Impact on Indoor Air Quality. https://www.epa.gov/indoor-air-quality-iaq/volatile-organic-compounds-impact-indoor-air-quality (accessed February).

3. Toniolo, R.; Pizzariello, A.; Dossi, N.; Lorenzon, S.; Abollino, O.; Bontempelli, G., Room temperature ionic liquids as useful overlayers for estimating food quality from their odor analysis by quartz crystal microbalance measurements. *Analytical chemistry* **2013,** *85* (15), 7241-7247.

4. Barié, N.; Bücking, M.; Rapp, M., A novel electronic nose based on miniaturized SAW sensor arrays coupled with SPME enhanced headspace-analysis and its use for rapid determination of volatile organic compounds in food quality monitoring. *Sensors and Actuators B: Chemical* **2006,** *114* (1), 482-488.

5. Schnorr, J. M.; van der Zwaag, D.; Walish, J. J.; Weizmann, Y.; Swager, T. M., Sensory Arrays of Covalently Functionalized Single-Walled Carbon Nanotubes for Explosive Detection. *Advanced Functional Materials* **2013,** *23* (42), 5285-5291.

6. Rehman, A.; Hamilton, A.; Chung, A.; Baker, G. A.; Wang, Z.; Zeng, X., Differential solute gas response in ionic-liquid-based QCM arrays: elucidating design factors responsible for discriminative explosive gas sensing. *Analytical chemistry* **2011,** *83* (20), 7823-7833.

7. Ponrathnam, T.; Cho, J.; Kurup, P.; Nagarajan, R.; Kumar, J., Investigation of QCM sensors with azobenzene functionalized coatings for the detection of nitroaromatics. *Journal of Macromolecular Science, Part A* **2011,** *48* (12), 1031-1037.

8. Queralto, N.; Berliner, A. N.; Goldsmith, B.; Martino, R.; Rhodes, P.; Lim, S. H., Detecting cancer by breath volatile organic compound analysis: a review of array-based sensors. *Journal of breath research* **2014,** *8* (2), 027112.

9. Chen, X.; Cao, M.; Li, Y.; Hu, W.; Wang, P.; Ying, K.; Pan, H., A study of an electronic nose for detection of lung cancer based on a virtual SAW gas sensors

array and imaging recognition method. *Measurement Science and Technology* **2005,** *16* (8), 1535.

10. Brunner, C.; Szymczak, W.; Höllriegl, V.; Mörtl, S.; Oelmez, H.; Bergner, A.; Huber, R.; Hoeschen, C.; Oeh, U., Discrimination of cancerous and non-cancerous cell lines by headspace-analysis with PTR-MS. *Analytical and bioanalytical chemistry* **2010,** *397* (6), 2315-2324.

11. Liao, H.-C.; Hsu, C.-P.; Wu, M.-C.; Lu, C.-F.; Su, W.-F., Conjugated Polymer/Nanoparticles Nanocomposites for High Efficient and Real-Time Volatile Organic Compounds Sensors. *Analytical chemistry* **2013,** *85* (19), 9305-9311.

12. Kanda, K.; Maekawa, T., Development of a WO 3 thick-film-based sensor for the detection of VOC. *Sensors and Actuators B: Chemical* **2005,** *108* (1), 97-101.

13. Elosua, C.; Matias, I. R.; Bariain, C.; Arregui, F. J., Volatile organic compound optical fiber sensors: A review. *Sensors* **2006,** *6* (11), 1440-1465.

14. Yoon, J.; Chae, S. K.; Kim, J.-M., Colorimetric sensors for volatile organic compounds (VOCs) based on conjugated polymer-embedded electrospun fibers. *Journal of the American Chemical Society* **2007,** *129* (11), 3038-3039.

15. Baldwin, E. A.; Bai, J.; Plotto, A.; Dea, S., Electronic noses and tongues: Applications for the food and pharmaceutical industries. *Sensors* **2011,** *11* (5), 4744-4766.

16. Umali, A. P.; Anslyn, E. V., A general approach to differential sensing using synthetic molecular receptors. *Current opinion in chemical biology* **2010,** *14* (6), 685-692.

17. Albert, K. J.; Lewis, N. S.; Schauer, C. L.; Sotzing, G. A.; Stitzel, S. E.; Vaid, T. P.; Walt, D. R., Cross-reactive chemical sensor arrays. *Chemical reviews* **2000,** *100* (7), 2595-2626.

18. Fens, N.; Schee, M.; Brinkman, P.; Sterk, P., Exhaled breath analysis by electronic nose in airways disease. Established issues and key questions. *Clinical & Experimental Allergy* **2013,** *43* (7), 705-715.

19. Yoo, Y. K.; Chae, M.-S.; Kang, J. Y.; Kim, T. S.; Hwang, K. S.; Lee, J. H., Multifunctionalized cantilever systems for electronic nose applications. *Analytical chemistry* **2012,** *84* (19), 8240-8245.

20. Johannsmann, D.; Reviakine, I.; Richter, R. P., Dissipation in films of adsorbed nanospheres studied by quartz crystal microbalance (QCM). *Analytical chemistry* **2009,** *81* (19), 8167-8176.

21. Sauerbrey, G., Use of quartz vibration for weighing thin films on a microbalance. *Z. phys* **1959,** *155*, 206-212.

22. Su, P.-G.; Sun, Y.-L.; Lin, C.-C., A low humidity sensor made of quartz crystal microbalance coated with multi-walled carbon nanotubes/Nafion composite material films. *Sensors and Actuators B: Chemical* **2006,** *115* (1), 338-343.

23. Fan, X.; Du, B., Selective detection of trace p-xylene by polymer-coated QCM sensors. *Sensors and Actuators B: Chemical* **2012,** *166*, 753-760.

24. Cheng, N.; Zhang, L.; Joon Kim, J.; Andrew, T. L., Vapor phase organic chemistry to deposit conjugated polymer films on arbitrary substrates. *Journal of Materials Chemistry C* **2017,** *5* (23), 5787-5796.

25. Palaniappan, A.; Li, X.; Tay, F. E.; Li, J.; Su, X., Cyclodextrin functionalized mesoporous silica films on quartz crystal microbalance for enhanced gas sensing. *Sensors and Actuators B: Chemical* **2006,** *119* (1), 220-226.

26. Burrell, A. K.; Del Sesto, R. E.; Baker, S. N.; McCleskey, T. M.; Baker, G. A., The large scale synthesis of pure imidazolium and pyrrolidinium ionic liquids. *Green Chemistry* **2007,** *9* (5), 449-454.

27. Kurosawa, S.; Kamo, N.; Matsui, D.; Kobatake, Y., Gas sorption to plasma-polymerized copper phthalocyanine film formed on a piezoelectric crystal. *Analytical Chemistry* **1990,** *62* (4), 353-359.

28. Schiebaum, K.-D.; Zhou, R.; Knecht, S.; Dieing, R.; Hanack, M.; Göpel, W., The interaction of transition metal phthalocyanines with organic molecules: a quartz-microbalance study. *Sensors and Actuators B: Chemical* **1995,** *24* (1-3), 69-71.

29. Zhou, R.; Josse, F.; Göpel, W.; Öztürk, Z.; Bekaroğlu, Ö., Phthalocyanines as sensitive materials for chemical sensors. *Applied Organometallic Chemistry* **1996,** *10* (8), 557-577.

30. Regmi, B. P.; Galpothdeniya, W. I. S.; Siraj, N.; Webb, M. H.; Speller, N. C.; Warner, I. M., Phthalocyanine-and porphyrin-based GUMBOS for rapid and sensitive detection of organic vapors. *Sensors and Actuators B: Chemical* **2015,** *209*, 172-179.

31. Warner, I. M.; El-Zahab, B.; Siraj, N., Perspectives on moving ionic liquid chemistry into the solid phase. *Analytical chemistry* **2014,** *86* (15), 7184-7191.

32. Kern, W., The evolution of silicon wafer cleaning technology. *Journal of the Electrochemical Society* **1990,** *137* (6), 1887-1892.

33. Speller, N. C.; Siraj, N.; Vaughan, S.; Speller, L. N.; Warner, I. M., QCM virtual multisensor array for fuel discrimination and detection of gasoline adulteration. *Fuel* **2017,** *199*, 38-46.

34. Capan, I.; Tarımcı, Ç.; Capan, R., Fabrication of Langmuir–Blodgett thin films of porphyrins and investigation on their gas sensing properties. *Sensors and Actuators B: Chemical* **2010,** *144* (1), 126-130.

CHAPTER 3. QUARTZ CRYSTAL MICROBALANCE BASED SENSOR ARRAYS FOR DETECTION AND DISCRIMINATION OF VOCS USING PHOSPHONIUM IONIC LIQUID COMPOSITES

3.1. Introduction

Many volatile organic compounds (VOCs) cause detrimental health and environmental effects after both acute and chronic exposure, which has led to an increase in development of new techniques for detection of these compounds.[1-3] However, it is still a challenge to detect and discriminate between closely related VOCs. In this regard, electronic noses (e-noses), which mimic the human nose, are of great interest due to their large selection of transducers.[4-5] Among possible transducers, the quartz crystal microbalance (QCM) coupled with ionic liquids (ILs) has proven to be a suitable e-nose.[6-10] The QCM is a sensitive and fast responding transducer with a large selection of sensing materials that makes it ideal for fabricating sensor arrays. ILs have proven to be good sensing materials due to their tunable properties and ability to detect a wide range of VOCs.[11-13] Briefly, ILs are a class of organic salts with melting points below 100°C, and by a simple counterion exchange, toxicity, hydrophobicity, thermal properties, etc. can be tuned.[14] Due to these redeeming qualities of ILs, and with the QCM as a transducer, IL-based QCM sensor arrays proved to be beneficial in vapor sensing studies.[15-17]

E-noses, or cross reactive sensor arrays (CRSAs), have two major sensing schemes. The most common is a multisensor array (MSA) that consists of several sensors based on chemical affinity. In this scheme, differences in each sensing material allows for interaction to a large range of VOCs. Each sensor will generate analyte specific response patterns that can be analyzed using statistical analyses techniques, such as artificial neural networks (ANN), principal component analysis (PCA), cluster analysis

(CA), discriminant analysis (DA), etc., to identify or discriminate the analyte in question. The second CRSA scheme is a virtual sensor array (VSA) that is based on a single sensor. The VSA generates multiple analyte specific response patterns and can be analyzed in the same manner as a MSA. In this regard, a VSA reduces cost and complexity of sensing materials as compared to a MSA.

QCM-based VSAs were first introduced by the Warner research group in 2015, and are based on film thickness, viscoelasticity, and harmonics.[18] Briefly, a viscoelastic material is used to coat the sensor, which results in significantly different behavioral changes under resonant conditions as compared to rigid films due to its elastic and viscous properties. This theory is based on the Sauerbrey equation:

$$\Delta f = -\frac{n}{c}\Delta m = -\frac{n}{c}\rho_f t_f \qquad (3.1)$$

where Δf is change in resonance frequency, η is harmonic number, c is mass sensitivity designated as 17.7 ngcm^{-2}Hz^{-1} for the 5 MHz AT-cut crystal used in this study; ρ_f is film density, and t_f is film thickness.[19] Thus, harmonic number, thickness, and viscoelasticity of each film will have an effect on sensor response. Harmonics are generated from the fundamental frequency at odd multiples. The quartz crystal resonators (QCRs) used in this work are capable of seven harmonics. In this regard, each harmonic response is recorded and utilized as a sensor. For QCM-based MSAs and VSAs, the selectivity and sensitivity depend on coating material.

Herein, a comparative study of QCM-based MSAs and VSAs for detection and discrimination of common chlorinated VOCs is described. To accomplish this, three phosphonium-based ILs were synthesized using trihexyltetradecylphosphonium as the cation with three different anions as coating materials for VOC detection. Phosphonium

ILs are known to have good chemical stability, viscosity, and trihexyltetradecylphosphonium, in particular, exhibits partial selectivity to a wide range of VOCs.[15, 20-21] Composite materials were then created using an IL-polymer blend with phosphonium ILs and polydimethylsiloxane (PDMS). PDMS is known to increase sensitivity of gas sensors,[22] and IL-polymer blends have been shown to increase discrimination of VOCs due to enhanced viscoelastic properties.[23-24] In order to investigate vapor sensing properties of each IL and IL-PDMS composite, thin films of each were deposited on the surface of QCRs via electrospray deposition and subsequently exposed to a set of five chlorinated VOCs. Each set of sensors (pure IL and composites) exhibited cross reactive patterns and were determined to be suitable for MSA fabrication. The resulting data from each set of sensors (pure IL sensors and composite sensors) were used to develop statistical models for discriminating five VOCs. PCA was used to assess the dimensionality of each data set and to obtain a visual representation of separation among the chlorinated VOCs. DA was used to develop the predictive models for discriminating chlorinated compounds. Lastly, each composite sensor exhibited multiple harmonic responses and each data set was used to fabricate three different VSAs.

3.2. Materials and Methods

3.2.1. Materials

Trihexyltetradecylphosphonium (P_{66614}) chloride, sodium dodecylbenzenesulfonate (DBS), chloropropane, chlorobutane, and tetrachloromethane were purchased from Sigma-Aldrich (St. Louis, MO USA). Sodium benzenesulfonate (BS) and polydimethylsiloxane (PDMS) were purchased from Acros Organics (New Jersey,

USA). Sodium 4-n-octylbenzenesulfonate (OBS) was purchased from Alfa Aesar (Haverhill, MA USA), dichloromethane (DCM) was purchased from BDH VWR Analytical (Radnor, PA USA), and chloroform was purchased from Macron Fine Chemicals (Center Valley, PA USA). All chemicals were used as purchased without further purification.

3.2.2. Instrumentation

A Q-Sense QCM-D E4 system and associated QCRs were purchased from Biolin Scientific (Stockholm, Sweden). Each QCR is an AT-cut gold-coated quartz crystal with a diameter of 14 mm, thickness of 0.3 mm and fundamental frequency of 4.95 MHz +/- 50 kHz. Both readout equipment (Model 5878) and mass flow controllers (Model 5850E) were obtained from Brooks Instrument, LLC (Hatfield, PA, USA).

3.2.3. Synthesis and Characterization of ILs

Three ILs were synthesized using a biphasic ion exchange reaction. As an example of a classic synthetic procedure, [Na][DBS] was dissolved in water, while [P_{66614}][Cl] was dissolved in DCM at a 1:1 mole ratio. Prepared solutions were mixed together and allowed to stir for 48 hours to obtain [P_{66614}][DBS]. After completion of ion exchange, NaCl (byproduct) was removed from DCM layer by washing with water several times. To achieve final product, DCM was removed using rotary evaporation followed by lyophilization to remove any residual water. The reaction procedure referenced above was used to obtain remaining ILs by reacting [P_{66614}][Cl] with [Na][BS], and [Na][OBS] to obtain [P_{66614}][BS], and [P_{66614}][OBS], respectively. All three ILs were colorless and viscous liquids. Structures of starting materials are shown in Figure B1.

Electrospray ionization mass spectrometry (ESI-MS) and Fourier transform infrared spectrometry (FT-IR) were used to characterize ILs. ESI-MS was accomplished

using an Agilent 6210 system in positive and negative ion modes. FT-IR was performed using a Bruker Alpha & Tensor 27 FT-IR instrument.

3.2.4. Preparation of IL Stock Solutions

Stock solutions of $[P_{66614}][DBS]$, $[P_{66614}][BS]$, and $[P_{66614}][OBS]$ (1 mg/mL) were prepared using DCM in 20 mL borosilicate glass scintillation vials.

3.2.5. Preparation of Composite Stock Solutions

Stock solutions of $[P_{66614}][DBS]$ (1 mg/mL) with PDMS (0.5 mg/mL), $[P_{66614}][BS]$ (1 mg/mL) with PDMS (0.5 mg/mL), and $[P_{66614}][OBS]$ (1 mg/mL) with PDMS (0.5 mg/mL) were prepared using DCM in 20 mL borosilicate glass scintillation vials.

3.2.6. Preparation of Sensing Films

Prior to coating, each QCR was cleaned using RCA standard clean 1 solution (5:1:1 deionized water, 30% hydrogen peroxide, and ammonium hydroxide).[25] An electrospray method was used for deposition of ILs and composites onto each QCR surface. Parameters for electrospray remained constant for each thin film: flowrate of 100 µL/min, current of 30 µA, voltage of 16.6 kV and a working distance of 7 cm. After coating, films were dried with nitrogen then stored in a desiccator prior to use. The change in frequency between coated and uncoated QCRs in all of the studied ILs and composites was maintained at ~ -2000 Hz. Once coated with materials, QCRs are referred to as sensors.

3.2.7. Data Collection

Each analyte was introduced at five different instrumentally controlled dilutions of flow rate ratios (0.05, 0.1, 0.2, 0.3, and 0.4 F_s/F_{tot}) which correspond to 5%, 10%, 20%, 30%, and 40% of saturated vapor pressure in a 20 mL vial of VOC and argon gas. To

achieve this, a flow system that consisted of two independent gas flow channels, one for analyte vapors and another for carrier gas, was used. Prior to data collection, the system was purged with ultrapure argon to achieve a stable baseline. Subsequently, a vial containing the VOC of choice was bubbled with argon to generate a sample of equilibrated headspace. The analyte and carrier channels merged to allow dilution of the analyte flow to yield respective flow rate ratios.[26] The total flow rate was kept constant at 100 sccm by using digital mass flow controllers. VOC vapors mixed across 1-meter length of tubing and then flowed over each sensor. To remove analyte vapors, the system was purged with argon at room temperature until the baseline was recovered.

3.2.8. Data Analysis

Multiple harmonic data was generated from vapor sensing studies expressed by change in frequency (Δf) in units of hertz (Hz). PCA was used to assess the dimensionality of the observed sensor data (MSA and VSAs) and to obtain a visual representation of separation among the chlorinated compounds with respect to the principal components. DA was used to develop the predictive model for distinguishing chlorinated VOCs, using the principal components as predictor variables.

3.3. Results and Discussion

3.3.1. Characterization of ILs

Each IL was confirmed using ESI-MS (Fig. B2 – B4) and FT-IR (Fig. B5 – B7). All three ILs were liquids at room temperature, thus thermal properties were not investigated.

3.3.2. Evaluation of IL Sensor Responses

Vapor sensing properties of $[P_{66614}][DBS]$, $[P_{66614}][BS]$, and $[P_{66614}][OBS]$ were evaluated by inserting three QCM sensors coated with respective ILs into QCM-D

chambers. Collectively sensors were exposed to a set of five chlorinated VOCs, which included dichloromethane, chloroform, chloropropane, chlorobutane, and tetrachloromethane, at five different instrumentally controlled sample flow rate ratios (0.05, 0.1, 0.2, 0.3, and 0.4 F_s/F_{tot}). Changes in resonance frequency were measured by exposing sensors to individual VOCs at indicated flow rate ratios for 3-minute intervals for a total exposure time of approximately 15 minutes. Three replicate measurements were completed for each VOC. Sensor responses for $[P_{66614}][DBS]$, $[P_{66614}][BS]$, and $[P_{66614}][OBS]$ are presented in Figure 3.1 expressed as change in frequency (Δf) versus flow rate ratios. While each sensor exhibited reversible sorption and a stable starting baseline, some sensor drift occurred over the course of the experiment. Furthermore, all sensors exhibited reproducible responses with the exception of low flow ratios (0.05 and 0.1), which resulted in large standard deviations (Figure 3.1). It should also be noted that $[P_{66614}][OBS]$ exhibited poor reproducibility in response to dichloromethane across all flow ratios. Based on pattern responses observed in Figure 3.1, fabrication of a MSA is possible, and these results will be discussed in section 3.3.4. In an attempt to increase sensor response and reproducibility at low flow ratios, the incorporation of PDMS with ILs to create composite materials was investigated.

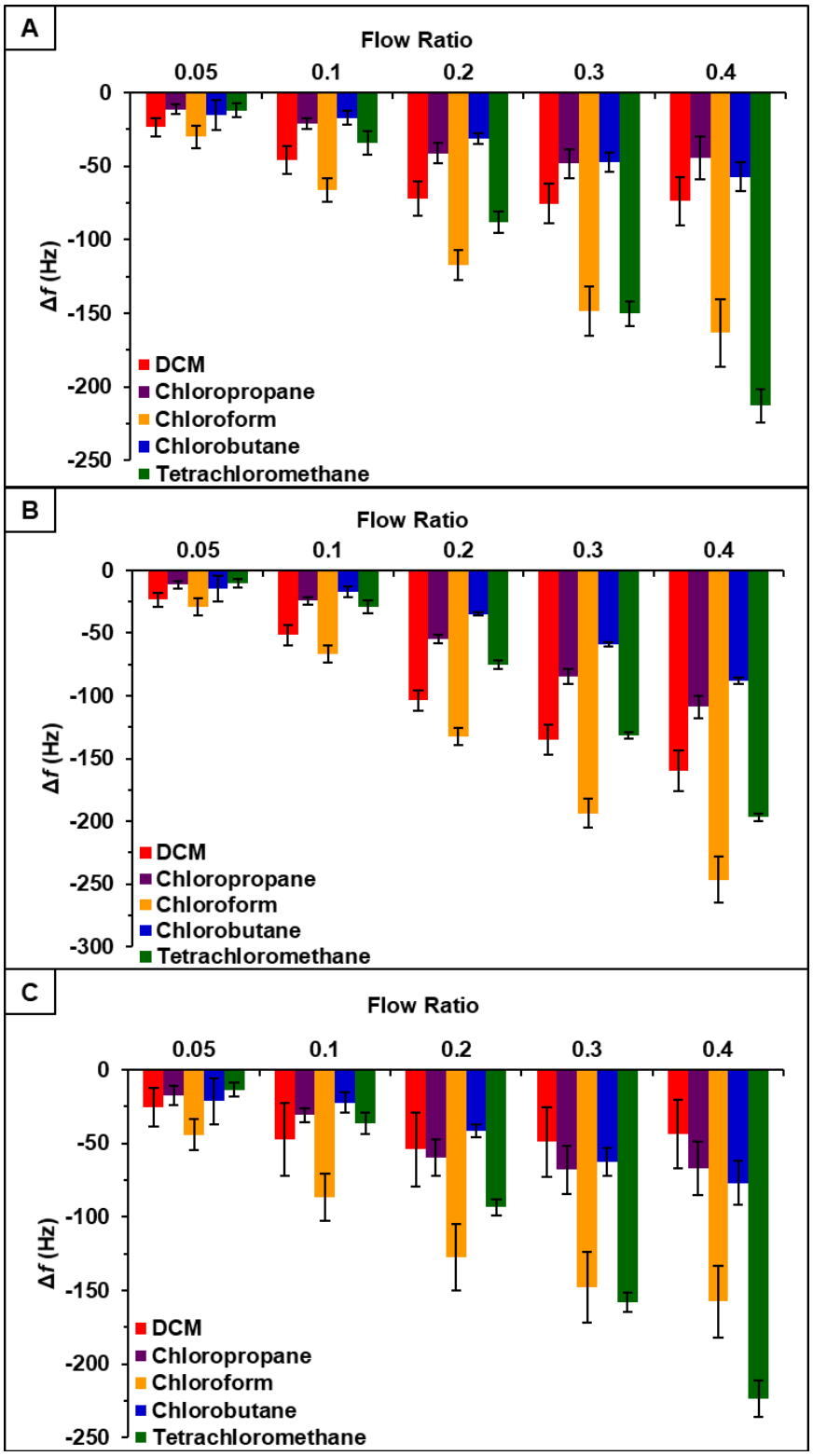

Figure 3.1. Sensor response of chlorinated VOCs at five flow ratios for A) $[P_{66614}][DBS]$, B) $[P_{66614}][BS]$, and C) $[P_{66614}][OBS]$. Error bars represent standard deviation for three replicate measurements.

3.3.3. Evaluation of Sensor Responses for Composites

It was hypothesized that incorporation of PDMS with phosphonium ILs would increase the sensor response to chlorinated compounds.[22] Thus, vapor sensing properties of $[P_{66614}]$[DBS]-PDMS, $[P_{66614}]$[BS]-PDMS, and $[P_{66614}]$[OBS]-PDMS were evaluated using similar parameters as ILs studies. Briefly, three QCM sensors coated with respective IL-polymer composites were inserted into QCM-D chambers and exposed to the same set of chlorinated VOCs at identical flow ratios. Similar to IL studies, sensors were exposed to VOCs at indicated flow ratios for 3-minute intervals for a total exposure time of approximately 15 minutes with three replicate measurements. Sensor responses for $[P_{66614}]$[DBS]-PDMS, $[P_{66614}]$[BS]-PDMS, and $[P_{66614}]$[OBS]-PDMS are presented in Figure 3.2 expressed as change in frequency (Δf) versus flow rate ratios. All sensors were found to be reusable, which is attributed to each sensor exhibiting a stable baseline and reversible sorption, as shown in Figure B8. Moreover, each sensor produced analyte specific response patterns as compared to each other, as well as to their IL counterparts.

With respect to $[P_{66614}]$[DBS], $[P_{66614}]$[DBS]-PDMS exhibited similar response patterns; however, there was an increase in overall sensor response, as well as smaller error bars with all analytes except tetrachloromethane. Overall, response patterns generated from IL-PDMS composites showed enhanced reproducibility and increased sensor response to chlorinated compounds, with the exception of tetrachloromethane.

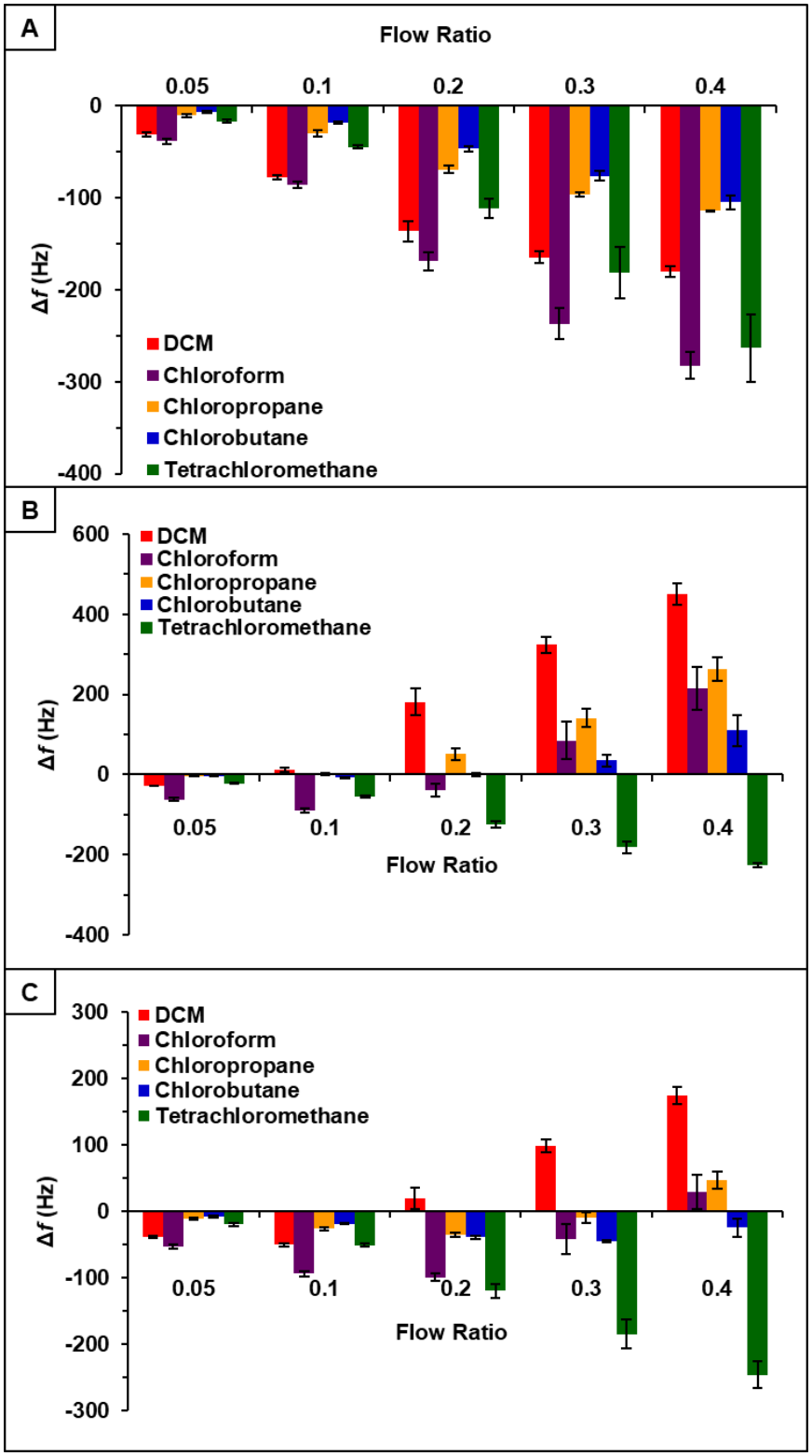

Figure 3.2. Sensor response of chlorinated VOCs at five flow ratios for A) $[P_{66614}][DBS]$-PDMS, B) $[P_{66614}][BS]$-PDMS, and C) $[P_{66614}][OBS]$-PDMS. Error bars represent standard deviation for three replicate measurements.

[P_{66614}][BS]-PDMS demonstrated an entirely different response pattern as compared to [P_{66614}][BS]. [P_{66614}][BS]-PDMS exhibited both positive and negative changes in frequency, whereas all responses were negative values in [P_{66614}][BS]. Interestingly, sensor responses for chloropropane and chlorobutane were negligible at lower flow ratios, whereas the pure IL sensor generated significantly larger responses. Notably, tetrachloromethane was the only compound to achieve negative changes in frequency over all five flow ratios. Similar to [P_{66614}][BS]-PDMS, [P_{66614}][OBS]-PDMS exhibited positive and negative changes in frequency and tetrachloromethane achieved negative values over all flow ratios. In contrast to [P_{66614}][BS]-PDMS, [P_{66614}][OBS]-PDMS exhibited an overall lower sensor response. It should be noted that composite sensors exhibited multiple harmonic responses, which was not exhibited by pure IL sensors. Figures 3.3, 3.4, and 3.5 depict sensor responses across multiple harmonics for [P_{66614}][DBS]-PDMS, [P_{66614}][BS]-PDMS, and [P_{66614}][OBS]-PDMS respectively. The positive and negative shifts in resonant frequency can be attributed to incorporation of PDMS, which changes the viscoelasticity of the sensor coating.[27] Based on pattern responses observed in Figures 3.2, 3.3, 3.4, and 3.5 fabrication of a MSA and VSA are possible and these results will be discussed in sections 3.3.4 and 3.3.5.

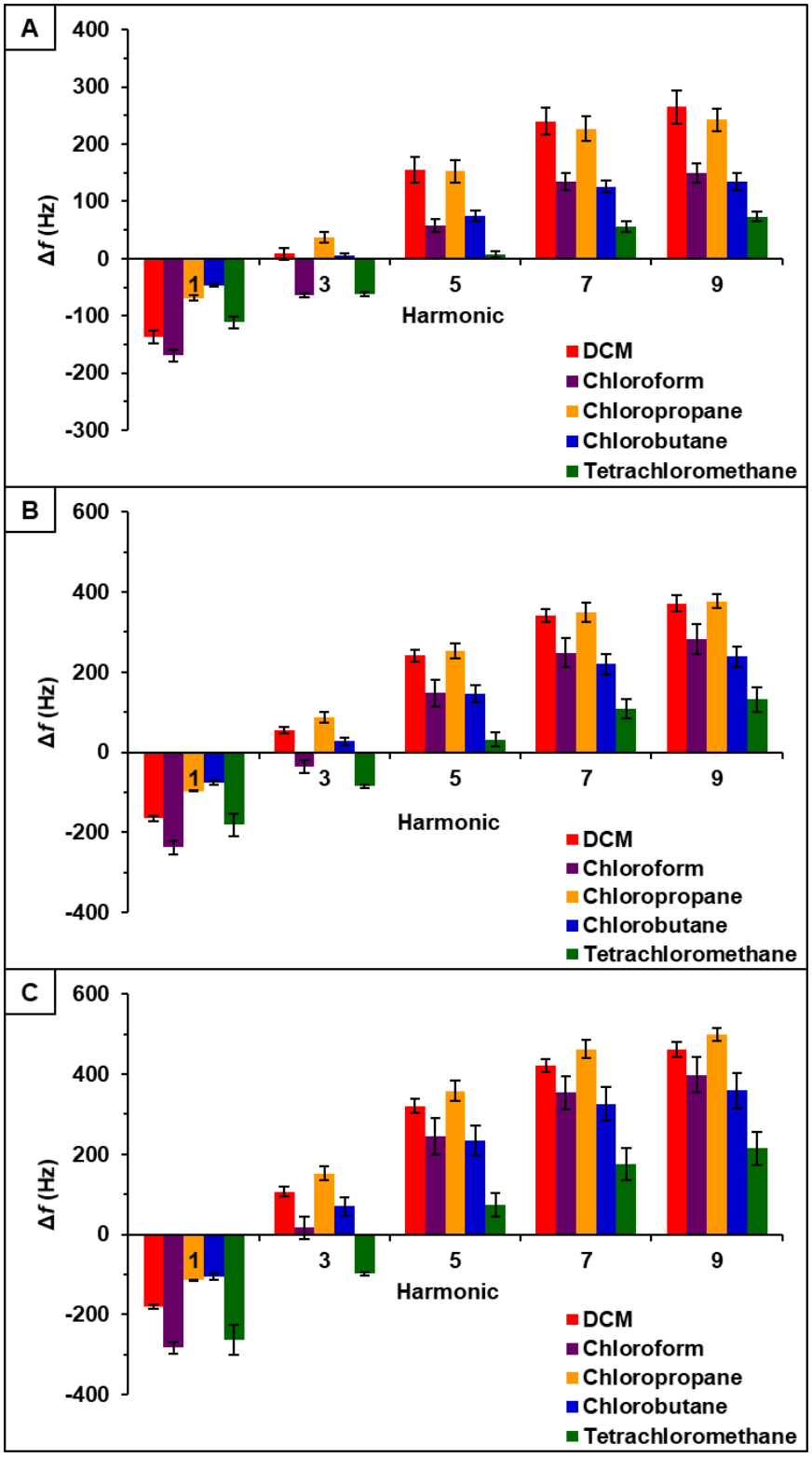

Figure 3.3. [P_{66614}][DBS]-PDMS sensor response to chlorinated VOCs at multiple harmonics at A) 0.2 flow ratio, B) 0.3 flow ratio, and C) 0.4 flow ratio. Error bars represent standard deviation for three replicate measurements.

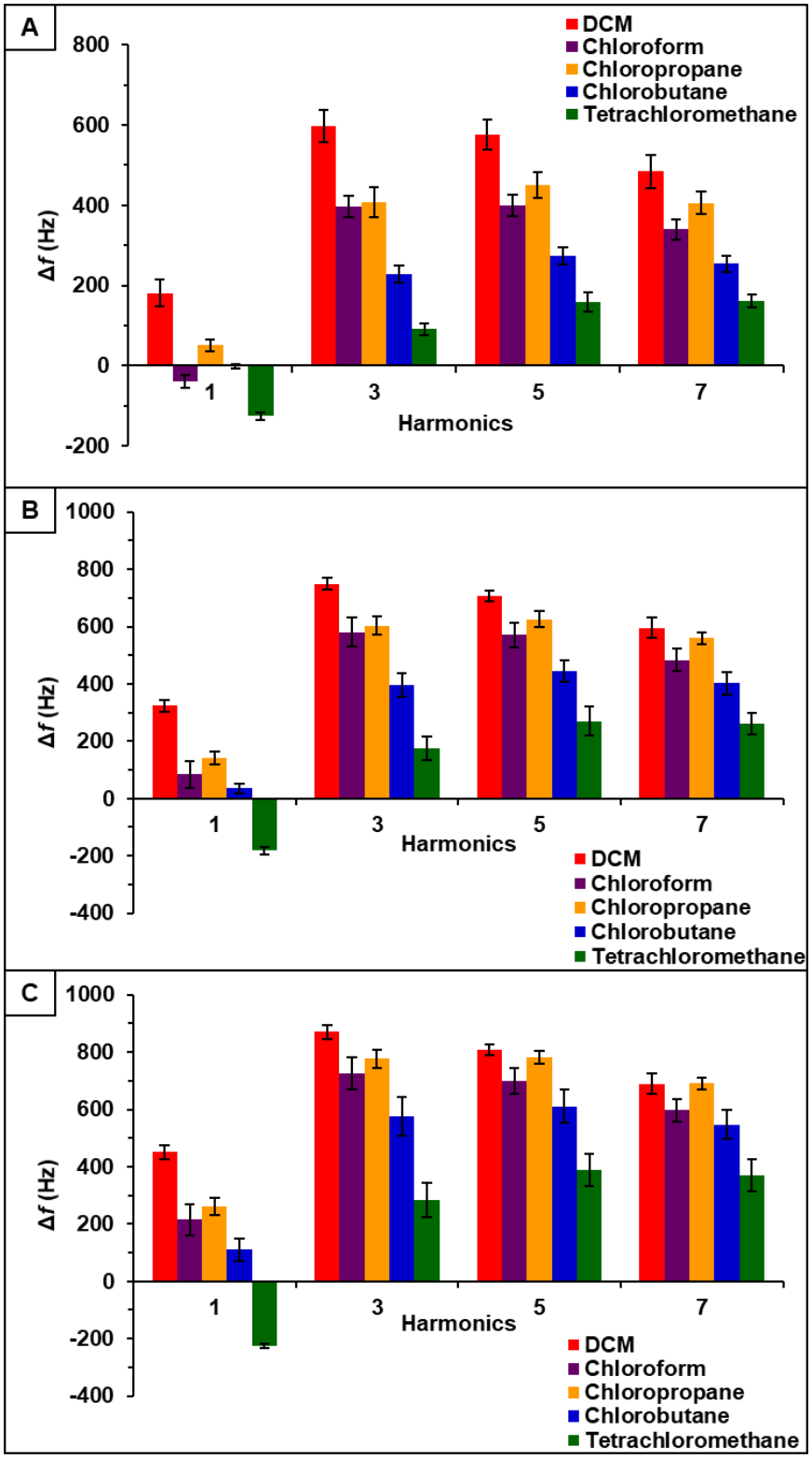

Figure 3.4. [P_{66614}][BS]-PDMS sensor response to chlorinated VOCs at multiple harmonics at A) 0.2 flow ratio, B) 0.3 flow ratio, and C) 0.4 flow ratio. Error bars represent standard deviation for three replicate measurements.

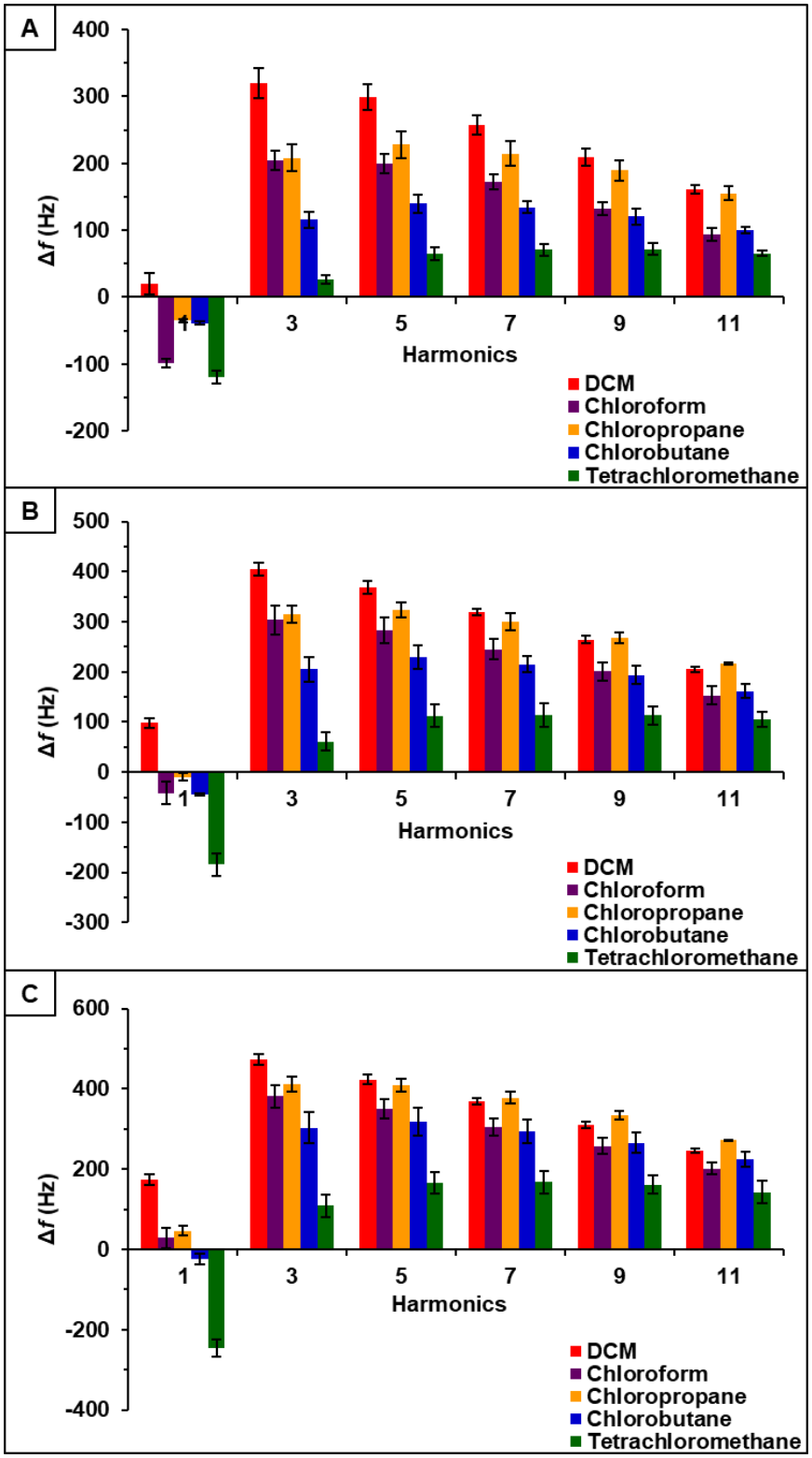

Figure 3.5. [P_{66614}][OBS]-PDMS sensor response to chlorinated VOCs at multiple harmonics at A) 0.2 flow ratio, B) 0.3 flow ratio, and C) 0.4 flow ratio. Error bars represent standard deviation for three replicate measurements.

3.3.4. Evaluation of MSAs

Based on pattern responses observed in Figures 3.1 and 3.2, fabrication of two MSAs to discriminate between the chlorinated compounds was possible. The first MSA was developed using sensor responses from pure IL sensors, [P_{66614}][DBS], [P_{66614}][BS], and [P_{66614}][OBS]. While the second array was developed using sensor responses from composite sensors, [P_{66614}][DBS]-PDMS, [P_{66614}][BS]-PDMS, and [P_{66614}][OBS]-PDMS. To achieve the first array, the raw Δf data collected from the pure IL sensors at the first harmonic were used to develop a predictive model using DA. The hypothesis that the covariance matrices associated with the three sensor variables were the same across all VOCs was strongly rejected (p-value < 0.0001). Thus, quadratic DA (QDA) was used, which fits a model that estimates the covariance matrices separately for each VOC.[26] The composite MSA was achieved using the same parameters.

For the pure IL MSA, the first two principal components accounted for 99.3% of the variability in the three predictors. The first principal component, which accounted for 92.6% of the variability, represents the sum of the three sensor responses. While the second principal component represents a comparison between [P_{66614}][BS] and [P_{66614}][OBS] responses, which accounted for 6.7% of the total variation. Figure 3.6 depicts a plot of the first two principal component scores, where some visual separation between DCM, chloroform, and tetrachloromethane is provided. However, the first two principal components do not provide any visual separation between chlorobutane and chloropropane, and there is severe overlap between chlorobutane, chloropropane and remaining VOCs.

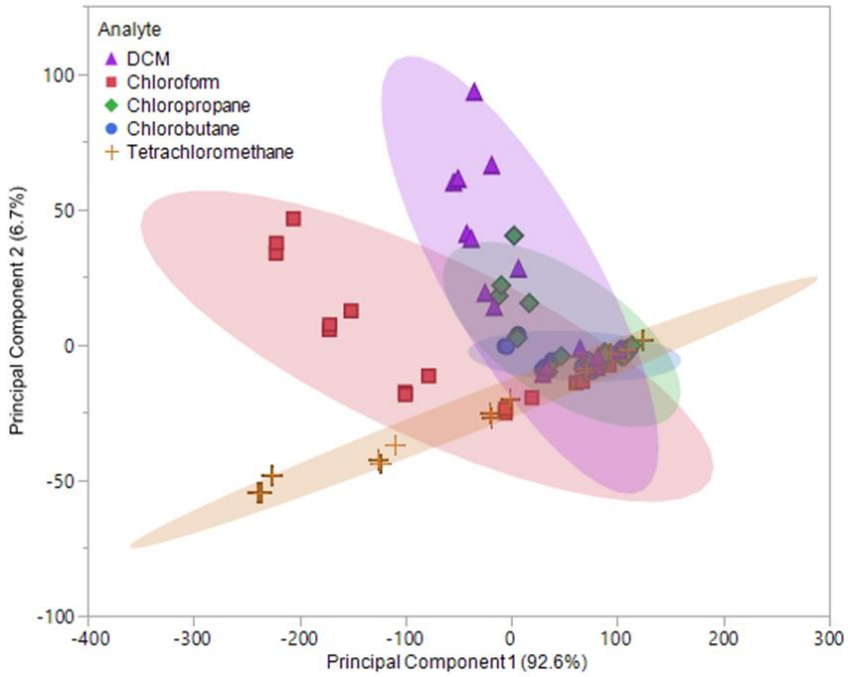

Figure 3.6. Principal component plot for discrimination of five chlorinated VOCs with respect to a three sensor MSA. Plot considers 75 total measurements consisting of three replicate measurements at five different flow ratios for each VOC (15 measurements per sample) using pure IL sensors.

Based on this plot, it is suggested that there will be difficulty distinguishing between these VOCs, especially between chlorobutane and chloropropane with the model produced by DA. The values for the first two principal components were used as predictor variables in QDA. The QDA predictive model resulted in 30 misclassifications, corresponding to an error rate of 40%. Of these misclassifications, six (6) DCM measurements were misclassified as chlorobutane, two (2) as chloropropane, one (1) chloroform measurement was misclassified as chlorobutane, one (1) as chloropropane, four (4) as tetrachloromethane, nine (9) chloropropane measurements were misclassified as chlorobutane, one (1) as DCM, one (1) chlorobutane was misclassified as chloropropane, and five (5) tetrachloromethane measurements were misclassified as chlorobutane. This corresponded to an overall accuracy of 60%. With an excess of

misclassifications and low accuracy, the discriminate scores from the QDA model were further investigated. It was found that majority of these classifications were occurring in the 0.05 and 0.1 flow ratios across all VOCs. Thus, new principal components using Δ*f* measurements from 0.2, 0.3, and 0.4 flow ratios were evaluated and used to develop an optimized QDA model.

Data obtained from 0.2 – 0.4 flow ratios showed the first two principal components accounted for 99% of the total variability in the three predictors. The first principal component accounted for 87.9% of the variability and similar to the original principal components, represents the sum of the three sensor measurements. Like the original principal components, the optimized second component represents the comparison between $[P_{66614}][BS]$ and $[P_{66614}][OBS]$ measurements, but accounts for 11.1% of the total variability. Based on the optimized PCA plot shown in Figure 3.7, an improvement in visual separation between tetrachloromethane and DCM, tetrachloromethane and chloroform, and between DCM and chloroform is provided. However, the optimized components are still unable to provide visual separation between chloropropane and chlorobutane, and an overlap of chlorobutane, chloropropane, DCM and tetrachloromethane is shown. This optimized PCA plot suggests that there may difficulties discriminating between these VOCs, but improvement in discrimination as compared to the original PCA plot in Figure 3.6. To test this theory, the optimized principal components were used as predictor variables in QDA. The optimized QDA model resulted in a total of seven (7) misclassifications, which corresponds to an error rate of 15.55%. The misclassifications consisted of one (1) DCM measurement classified as chloropropane, four (4) chloropropane classified as chlorobutane, one (1) chloropropane classified as DCM, and

one (1) chlorobutane classified as chloropropane. The overall accuracy of the optimized QDA model was found to be 84.45%, which was a large improvement compared to the original model. It should be noted that all of the tetrachloromethane and chloroform measurements were accurately classified, which was suggested by the PCA plot in Figure 3.7.

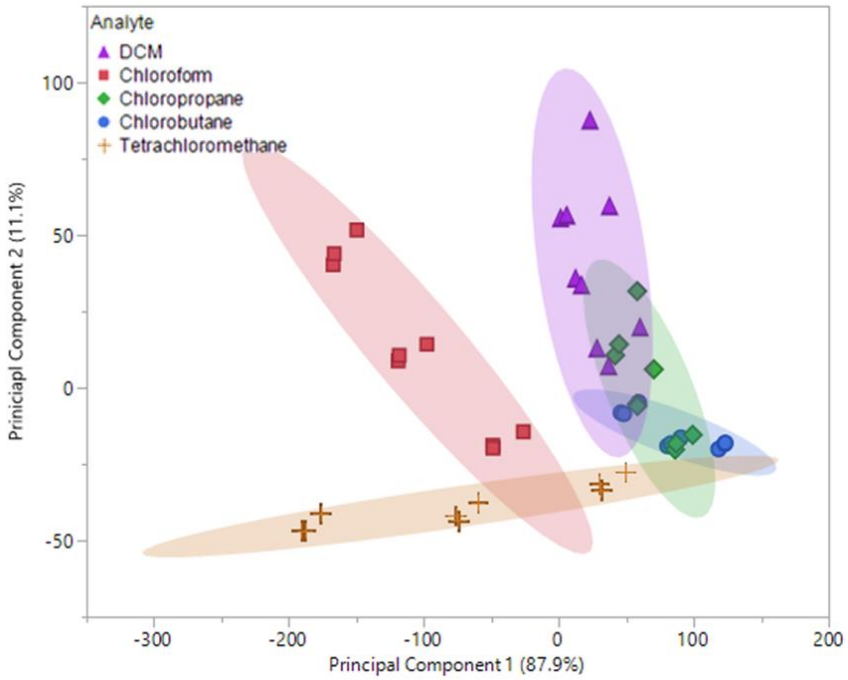

Figure 3.7. Principal component plot for discrimination of five chlorinated VOCs with respect to a three sensor MSA. Plot considers 45 total measurements consisting of three replicate measurements at three different flow ratios for each VOC (9 measurements per sample) using pure IL sensors.

Upon examination of the composite MSA, 99.5% of the total variability in the three predictors was accounted for by the first two principal components. The first principal component accounted for 81.1% of variance and represented the sum of the three sensor responses. The second principal component, which accounted for 18.4% of the variability, represented a comparison between $[P_{66614}][DBS]$-PDMS and $[P_{66614}][BS]$-PDMS

responses. Based on Figure 3.8, it was proposed that using the predicative QDA model will result in VOCs being misclassified as chloropropane or chlorobutane.

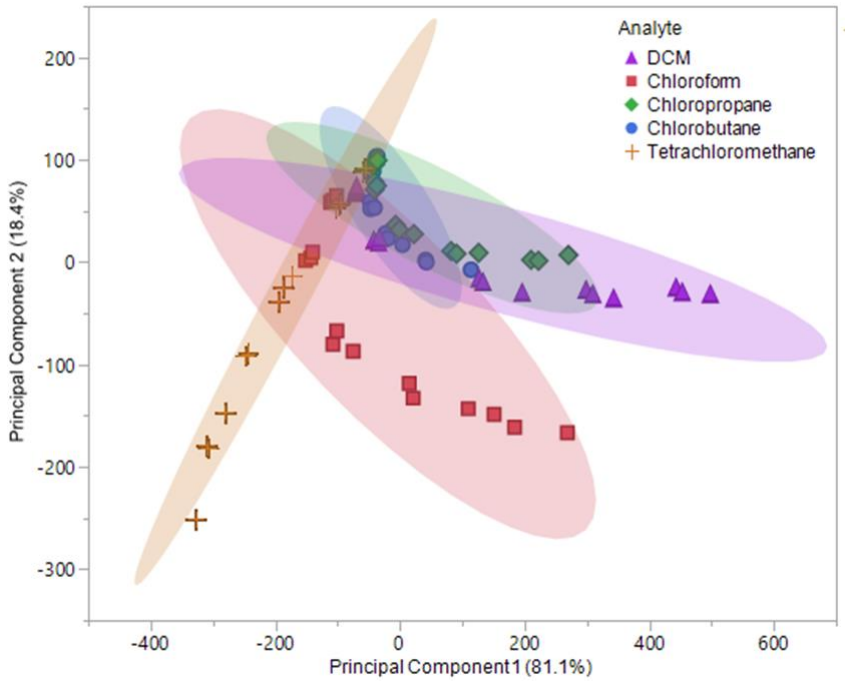

Figure 3.8. Principal component plot for discrimination of five chlorinated VOCs with respect to a three sensor MSA. Plot considers 75 total measurements consisting of three replicate measurements at five different flow ratios for each VOC (15 measurements per sample) using composite sensors.

This hypothesis is the result of significant overlap of chloropropane and chlorobutane with DCM, chloroform, and tetrachloromethane. This proposal was evaluated by using the first two principal components as predictor variables in QDA. The QDA model had an error rate of 36%, which accounted for 27 misclassifications. These misclassifications were comprised of five (5) DCM measurements classified as chlorobutane, six (6) chloroform measurements classified as tetrachloromethane, nine (9) chloropropane measurements classified as chlorobutane and three (3) as DCM, one (1) chlorobutane classified as DCM, and three (3) tetrachloromethane measurements classified as chlorobutane. This model was found to have an accuracy of 64%, which lead to further investigation of the

discriminate scores. Similar to the original pure IL MSA, most of the misclassifications were due to the lower flow ratios (0.05 and 0.1). Therefore, new principal components using Δ*f* measurements from 0.2, 0.3, and 0.4 flow ratios were evaluated and used to develop an optimized QDA model.

In this examination, the first two principal components accounted for 99.6% of the total variability in the three predictors and represented the same factors as the original components. The optimized first principal component accounted for 89.3% of the variability, while the second component accounted for 10.3%. An optimized PCA plot is depicted in Figure 3.8, where enhanced visual separation between tetrachloromethane, chloroform, and DCM is provided. Nonetheless, poor visual separation persisted between chlorobutane and chloropropane of the optimized principal components.

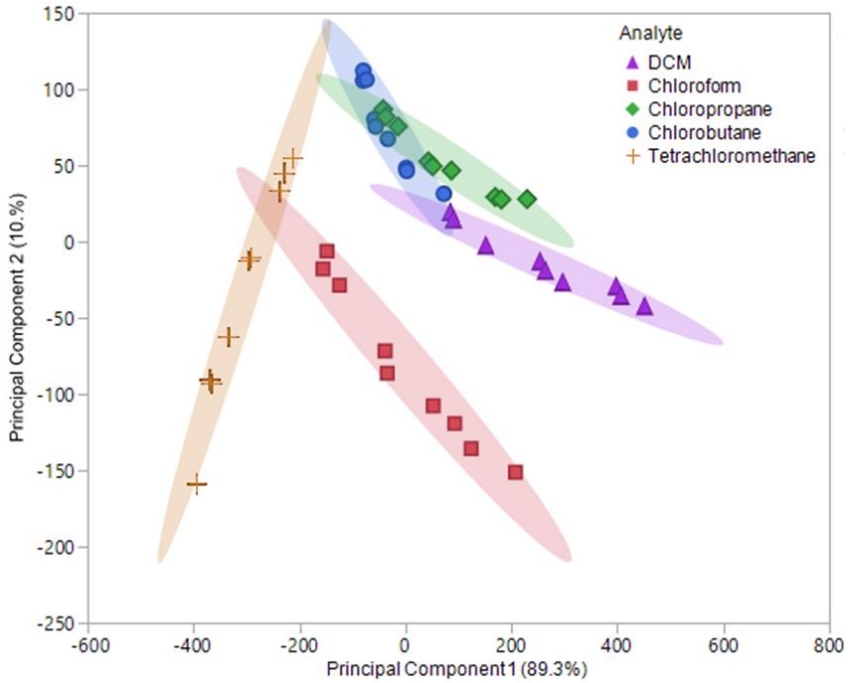

Figure 3.9. Principal component plot for discrimination of five chlorinated VOCs with respect to a three sensor MSA. Plot considers 45 total measurements consisting of three replicate measurements at three different flow ratios for each VOC (9 measurements per sample) using composite sensors.

The optimized principal components were used as predictor variables to develop the optimized QDA model. With the exception of two measurements, this model accurately discriminated between the five chlorinated VOCs and resulted in an error rate of 4.44%. The misclassification was due to two (2) chloropropane measurements being classified as chlorobutane. As previously mentioned, chloropropane and chlorobutane overlapped in the optimized PCA plot (Fig. 3.9). Thus, this misclassification was not alarming. The overall accuracy of this model was determined to be 95.56%, which is a drastic improvement from the original QDA model as well as the pure IL QDA model.

3.3.5. Evaluation of VSAs

$[P_{66614}]$[DBS]-PDMS, $[P_{66614}]$[BS]-PDMS, and $[P_{66614}]$[OBS]-PDMS exhibited sensor responses across multiple harmonics, as shown in Figures 3.3, 3.4, and 3.5 respectively. To evaluate the capability of VSAs for discrimination of chlorinated VOCs, each sensor was analyzed as an independent system. To accomplish this task, raw changes in frequency (Δf) data collected from each sensor across multiple harmonics was used to develop a predictive model using QDA. $[P_{66614}]$[DBS]-PDMS exhibited five harmonics (1^{st}, 3^{rd}, 5^{th}, 7^{th}, and 9^{th}), $[P_{66614}]$[BS]-PDMS exhibited four harmonics (1^{st}, 3^{rd}, 5^{th}, and 7^{th}), and $[P_{66614}]$[OBS]-PDMS exhibited six harmonics (1^{st}, 3^{rd}, 5^{th}, 7^{th}, 9^{th}, and 11^{th}). For each sensor the hypothesis that the covariance matrices associated with the five, four, and six sensor variables, respectively, were the same across all VOCs was strongly rejected (p-value < 0.0001). Thus, QDA was used, which fits a model that estimates the covariance matrices separately for each VOC.[26] Based on the optimization of the composite MSA, these QDA models only consider Δf measurements for 0.2, 0.3, and 0.4 flow ratios.

In regards to $[P_{66614}]$[DBS]-PDMS, four principal components were used as predictor variables to develop the QDA model. This model resulted in 100% accuracy in discriminating the five chlorinated VOCs. In contrast, $[P_{66614}]$[BS]-PDMS used three principal components as input variables for QDA, which resulted in 91.11% discrimination accuracy. These misclassifications consisted of one (1) chlorobutane measurement being classified as chloropropane, and three (3) chloropropane measurements classified as chlorobutane. Lastly, $[P_{66614}]$[OBS]-PDMS used five principal components as predictor variables for the development of the QDA model, which resulted in 100% accuracy. Due to these models using more than two principal components, and hence three-dimensional or more, it is not possible to illustrate the score plots. For simplicity, two-dimensional QDA canonical plots for each VSA are provided in Figures B9 – B11.

3.4. Conclusions

In this study, two novel phosphonium ILs and one previously reported phosphonium IL were synthesized and vapor sensing properties were investigated using a QCM-based MSA. To further evaluate the vapor sensing properties of these ILs, PDMS was incorporated to create composite materials. Incorporation of PDMS resulted in significantly different sensor responses than pure ILs. Ultimately, the composite materials vapor sensing properties were investigated using a QCM-based MSA and VSA. It was found that pure ILs and composite materials were not useful at vapor detection of chlorinated VOCs at low flow ratios (0.05 and 0.1). However, by employing the composite MSA, five chlorinated VOCs were accurately discriminated at 95.56%, which was an increase in accuracy as compared to pure ILs MSA (84.45%). It should be noted that pure ILs were not capable of VSA fabrication, while composite sensors were capable of this

endeavor. With the exception of [P_{66614}][BS]-PDMS (91.11%), the VSAs exhibited higher accuracies than the MSA at 100%. Although, further studies need to be investigated to fully understand vapor interaction with sensing materials, these studies have provided more insight on the benefits of incorporation of polymers for enhancing discrimination accuracies for QCM-based sensor arrays.

3.5. References

1. Kampa, M.; Castanas, E., Human health effects of air pollution. *Environmental pollution* **2008,** *151* (2), 362-367.

2. Adgate, J. L.; Church, T. R.; Ryan, A. D.; Ramachandran, G.; Fredrickson, A. L.; Stock, T. H.; Morandi, M. T.; Sexton, K., Outdoor, indoor, and personal exposure to VOCs in children. *Environmental health perspectives* **2004,** *112* (14), 1386-1392.

3. Delgado-Rodríguez, M.; Ruiz-Montoya, M.; Giraldez, I.; López, R.; Madejón, E.; Díaz, M. J., Use of electronic nose and GC-MS in detection and monitoring some VOC. *Atmospheric Environment* **2012,** *51*, 278-285.

4. Gardner, J. W.; Bartlett, P. N., A brief history of electronic noses. *Sensors and Actuators B: Chemical* **1994,** *18* (1), 210-211.

5. Gardner, J. W.; Bartlett, P. N., Electronic noses. Principles and applications. IOP Publishing: 2000.

6. Toniolo, R.; Pizzariello, A.; Dossi, N.; Lorenzon, S.; Abollino, O.; Bontempelli, G., Room temperature ionic liquids as useful overlayers for estimating food quality from their odor analysis by quartz crystal microbalance measurements. *Analytical chemistry* **2013,** *85* (15), 7241-7247.

7. Liu, Y.-L.; Tseng, M.-C.; Chu, Y.-H., Sensing ionic liquids for chemoselective detection of acyclic and cyclic ketone gases. *Chemical Communications* **2013,** *49* (25), 2560-2562.

8. Rehman, A.; Hamilton, A.; Chung, A.; Baker, G. A.; Wang, Z.; Zeng, X., Differential solute gas response in ionic-liquid-based QCM arrays: elucidating design factors responsible for discriminative explosive gas sensing. *Analytical chemistry* **2011,** *83* (20), 7823-7833.

9. Schäfer, T.; Di Francesco, F.; Fuoco, R., Ionic liquids as selective depositions on quartz crystal microbalances for artificial olfactory systems—a feasibility study. *Microchemical Journal* **2007,** *85* (1), 52-56.

10. Liang, C.; Yuan, C.-Y.; Warmack, R. J.; Barnes, C. E.; Dai, S., Ionic Liquids: A New Class of Sensing Materials for Detection of Organic Vapors Based on the Use of a Quartz Crystal Microbalance. *Analytical Chemistry* **2002,** *74* (9), 2172-2176.

11. Earle Martyn, J.; Seddon Kenneth, R., Ionic liquids. Green solvents for the future. In *Pure and Applied Chemistry*, 2000; Vol. 72, p 1391.

12. Galpothdeniya, W. I. S.; McCarter, K. S.; De Rooy, S. L.; Regmi, B. P.; Das, S.; Hasan, F.; Tagge, A.; Warner, I. M., Ionic liquid-based optoelectronic sensor arrays for chemical detection. *RSC Advances* **2014,** *4* (14), 7225-7234.

13. Tseng, M.-C.; Chu, Y.-H., Chemoselective gas sensing ionic liquids. *Chemical Communications* **2010,** *46* (17), 2983-2985.

14. Holbrey, J. D.; Seddon, K. R., Ionic Liquids. *Clean Products and Processes* **1999,** *1* (4), 223-236.

15. Jin, X.; Yu, L.; Garcia, D.; Ren, R. X.; Zeng, X., Ionic liquid high-temperature gas sensor array. *Analytical chemistry* **2006,** *78* (19), 6980-6989.

16. Yu, L.; Garcia, D.; Ren, R.; Zeng, X., Ionic liquid high temperature gas sensors. *Chemical Communications* **2005,** (17), 2277-2279.

17. Xu, X.; Li, C.; Pei, K.; Zhao, K.; Zhao, Z. K.; Li, H., Ionic liquids used as QCM coating materials for the detection of alcohols. *Sensors and Actuators B: Chemical* **2008,** *134* (1), 258-265.

18. Speller, N. C.; Siraj, N.; Regmi, B. P.; Marzoughi, H.; Neal, C.; Warner, I. M., Rational Design of QCM-D Virtual Sensor Arrays Based on Film Thickness, Viscoelasticity, and Harmonics for Vapor Discrimination. *Analytical Chemistry* **2015,** *87* (10), 5156-5166.

19. Sauerbrey, G., Use of quartz vibration for weighing thin films on a microbalance. *Z. phys* **1959,** *155*, 206-212.

20. Ramnial, T.; Ino, D. D.; Clyburne, J. A., Phosphonium ionic liquids as reaction media for strong bases. *Chemical Communications* **2005,** (3), 325-327.

21. Regmi, B. P.; Galpothdeniya, W. I. S.; Siraj, N.; Webb, M. H.; Speller, N. C.; Warner, I. M., Phthalocyanine-and porphyrin-based GUMBOS for rapid and sensitive detection of organic vapors. *Sensors and Actuators B: Chemical* **2015,** *209*, 172-179.

22. Wenzel, S. W.; White, R. M., Flexural plate-wave gravimetric chemical sensor. *Sensors and Actuators A: Physical* **1990,** *22* (1), 700-703.

23. Regmi, B. P.; Speller, N. C.; Anderson, M. J.; Brutus, J. O.; Merid, Y.; Das, S.; El-Zahab, B.; Hayes, D. J.; Murray, K. K.; Warner, I. M., Molecular weight sensing properties of ionic liquid-polymer composite films: theory and experiment. *Journal of Materials Chemistry C* **2014,** *2* (24), 4867-4878.

24. Regmi, B. P.; Monk, J.; El-Zahab, B.; Das, S.; Hung, F. R.; Hayes, D. J.; Warner, I. M., A novel composite film for detection and molecular weight determination of organic vapors. *Journal of Materials Chemistry* **2012,** *22* (27), 13732-13741.

25. Kern, W., The evolution of silicon wafer cleaning technology. *Journal of the Electrochemical Society* **1990,** *137* (6), 1887-1892.

26. Vaughan, S. R.; Speller, N. C.; Chhotaray, P.; McCarter, K. S.; Siraj, N.; Pérez, R. L.; Li, Y.; Warner, I. M., Class specific discrimination of volatile organic compounds using a quartz crystal microbalance based multisensor array. *Talanta* **2018,** *188*, 423-428.

27. Speller, N. C.; Siraj, N.; Vaughan, S.; Speller, L. N.; Warner, I. M., Assessment of QCM array schemes for mixture identification: citrus scented odors. *RSC Advances* **2016,** *6* (98), 95378-95386.

CHAPTER 4. IONIC LIQUID-POLYMER COMPOSITES FOR MIXTURE ANALYSIS

4.1. Introduction

Regulating beverage adulteration, also known as illegally tampering with legal beverages, has been an issue in food safety, forensics, and quality control. Depending on the amount of adulteration, severe illness or even death can occur upon consumption.[1] Alcohols are common adulterants in beverages.[1] While many are simple in their structures, isomeric forms and alcohols of various sizes can be toxic to humans and the environment. Methanol is a laboratory solvent and a component in antifreeze; however, it is the most frequently used adulterant in alcoholic beverages.[2] 1-propanol is used in brake fluid while 2-propanol is used in hand sanitizers, but both are used as adulterants in alcoholic beverages. Lastly, 1-butanol is a component in paint thinner and has been found in adulterated beverages as well.[1] Given the detrimental effects to human health and the environment, it is important to develop a simple, cost effective technique that can detect adulterant compounds, such as simple alcohols. Many techniques, including gas chromatography coupled with mass spectrometry (GC-MS) and direct analysis in real time mass spectrometry (DART-MS), have been used to detect adulterants in beverages; however, there are limitations associated with these techniques, such as cost and complexity.[1, 3-5] An alternative technique, such as a quartz crystal microbalance (QCM) based sensor array, would eliminate many of the instrumental drawbacks associated with traditional techniques due to a large selection of coating materials, simplicity, and cost effectiveness.

Traditionally, the QCM has been used as a mass detector and is fundamentally non-selective; however, when combined with a suitable coating material, a vapor sensor can be developed. Thus, sensitivity and selectivity of a QCM vapor sensor is dependent on coating material. A variety of materials such as, carbon nanotubes and calixerenes, have been used as coating materials, but are limited in sensing capabilities due to slow response times, complex synthesis, and selectivity.[6-8] To address these limitations, ionic liquids (ILs) have been found to be selective to a wide of range volatile organic compounds (VOCs) and exhibit good vapor sensing properties when coupled with QCM sensors.[9-12] It was recently discovered in the Warner Research Group, that by creating an IL-polymer composite, detection, discrimination, and molecular weight approximation of VOCs was possible.[13-14]

Herein, a QCM-based multisensor array is described for detection and analysis of 11 alcohol samples, with an ultimate objective of molecular weight discrimination within mixtures. Alcohols selected for this work were common adulterants, such as methanol, 1-propanol, 2-propanol, and 1-butanol. Ethanol was selected because it is a main component in alcoholic beverages and 2-butanol is an isomer of a common adulterant. Since methanol is the most common adulterant, the remaining five alcohol samples are made up of 1:1 ratios of respective alcohols with methanol (methanol:ethanol, methanol:1-propanol, methanol:2-propanol, methanol:1-butanol, methanol:2-butanol). A set of four IL-polymer composites that were previously used to detect alcohols[13-14] were used as coating materials for detection of alcohols and change of frequency (Δf) and dissipation (ΔD) were measured. The set of sensors exhibited cross-reactive response patterns, and ratios of $\Delta f/\Delta D$ were used to develop a statistical model for discriminating

between 11 alcohol samples. Principal component analysis (PCA) was used to evaluate the dimensionality of the observed sensor data and to obtain a visual representation of separation among 11 alcohol samples. Discriminant analysis (DA) was used to develop a predictive model for discriminating between alcohol samples using the four $\Delta f/\Delta D$ sensor responses directly as predictor variables.

4.2. Materials and Methods

4.2.1. Materials

Poly (methyl methacrylate) (PMMA molecular weight ~ 500,000 Da) was purchased from Polysciences, Inc. (Washington, PA, USA). 1-n-butyl-2,3-dimethylimidazolium trifluoromethanesulfonate ([BM_2Im][OTf]) and 1-n-butyl-2,3-dimethylimidazolium hexafluorophosphate ([BM_2Im][PF_6]) were purchased from Ionic Liquids Technologies, Inc. (Heilbronn, Germany). 1-butylpyridinium hexafluorophosphate ([BPyr][PF_6]) was purchased from Acros Organics (New Jersey, USA). 1-hexyl-3-methylimidazolium bis(trifluoromethylsulfonyl)imide ([HMIm][NTf_2]) was obtained from a previous study and synthesized using a previously reported procedure.[14] 1-propanol, 2-propanol, and 2-butanol were purchased from Sigma-Aldrich (St. Louis, MO USA). Methanol and dichloromethane (DCM) were purchased from BDH VWR Analytical (Radnor, PA USA), ethanol was purchased from Koptec (King of Prussia, PA USA), and 1-butanol was purchased from Fisher Scientific (Hampton, New Hampshire, USA). All chemicals were used as received without further purification.

4.2.2. Instrumentation

A Q-Sense QCM-D E4 system and associated quartz crystal resonators (QCRs) were purchased from Biolin Scientific (Stockholm, Sweden). Each QCR is an AT-cut gold-

coated quartz crystal with a diameter of 14 mm, thickness of 0.3 mm and fundamental frequency of 4.95 MHz +/- 50 kHz. Both readout equipment (Model 5878) and mass flow controllers (Model 5850E) were obtained from Brooks Instrument, LLC (Hatfield, PA, USA).

4.2.3. Preparation of Composite Stock Solutions

Stock solutions of composites were prepared using 1 mg/mL of respective IL with 0.5 mg/mL of PMMA dissolved in DCM in 20mL borosilicate glass scintillation vials. The resulting composites were [HMIm][NTf_2]-PMMA, [BM_2Im][OTf]-PMMA, [BM_2Im][PF_6]-PMMA, and [BPyr][PF_6]-PMMA.

4.2.4. Preparation of Sensing Films

RCA standard clean 1 solution (5:1:1 deionized water, 30% hydrogen peroxide, and ammonium hydroxide)[15] was used to clean QCRs prior to deposition of composites. Quartz crystal resonators (QCR) were coated using electrospray deposition. Parameters for electrospray remained constant for each QCR: flowrate of 100 µL/min, current of 30 µA, voltage of 16.6 kV and a working distance of 7 cm. After electrospraying, the QCRs were dried using nitrogen and stored in a desiccator until testing. The change in frequency between coated and uncoated QCRs with composites was maintained at approximately -2000 Hz. Once materials are deposited on the surface, QCRs are referred to as sensors.

4.2.5. Data Collection

A flow system was used to expose sensors to each analyte at three different instrumentally controlled dilutions of flow rate ratios (0.2, 0.3, and 0.4 F_s/F_{tot}) which correspond to 20%, 30%, and 40% of equilibrated headspace in a 20 mL vial of sample and argon gas. The flow system consisted of two independent gas flow channels, one for

sample vapors and the other for carrier gas (ultrapure argon). Before collecting data, the system was purged with carrier gas to achieve a stable baseline. Once a baseline was obtained, a vial containing the sample of choice was bubbled with argon to generate a sample of equilibrated headspace. The sample and carrier channels merged to allow dilution of the analyte flow to yield respective flow rate ratios.[16] The total flow rate was maintained at 100 sccm by using digital mass flow controllers. Sample vapors were allowed to mix across 1-meter length of tubing and subsequently flowed over each sensor. To remove sample vapors, the system was purged with carrier gas at room temperature until the baseline was recovered.

4.2.6. Data Analysis

Two predicative models were developed using change in frequency (Δf) alone and in combination with change in dissipation (ΔD). PCA was used to assess the dimensionality of the observed sensor data and to obtain a visual representation of separation among pure alcohols and 1:1 mixture of alcohols with respect to the principal components. DA was used to develop the predictive models for discriminating between 11 alcohol samples using the four sensor variables directly as predictor variables.

4.3. Results and Discussion

4.3.1. Evaluation of Vapor Sensing Properties

Four QCM sensors coated with [HMIm][NTf_2]-PMMA, [BM_2Im][PF_6]-PMMA, [BM_2Im][OTf]-PMMA, and [BPyr][PF_6]-PMMA were inserted into QCM-D chambers to evaluate their vapor sensing capabilities. All sensors were exposed to six pure alcohols (methanol, ethanol, 1-propanol, 2-propanol, 1-butanol, 2-butanol) and a 1:1 ratio of respective alcohols with methanol (methanol:ethanol, methanol:1-propanol, methanol:2-

propanol, methanol:1-butanol, methanol:2-butanol) at three instrumentally controlled sample flow rate ratios (0.2, 0.3, and 0.4 F_s/F_{tot}). Changes in frequency (Δf) and dissipation (ΔD) were measured by exposing sensors to individual samples at indicated flow ratios for 3-minute intervals for a total exposure time of approximately 9 minutes in triplicate. Δf and ΔD sensor responses for [HMIm][NTf_2]-PMMA, [BM_2Im][PF_6]-PMMA, [BM_2Im][OTf]-PMMA, and [BPyr][PF_6]-PMMA are depicted in Figures 4.1, 4.2, 4.3, and 4.4, respectively.

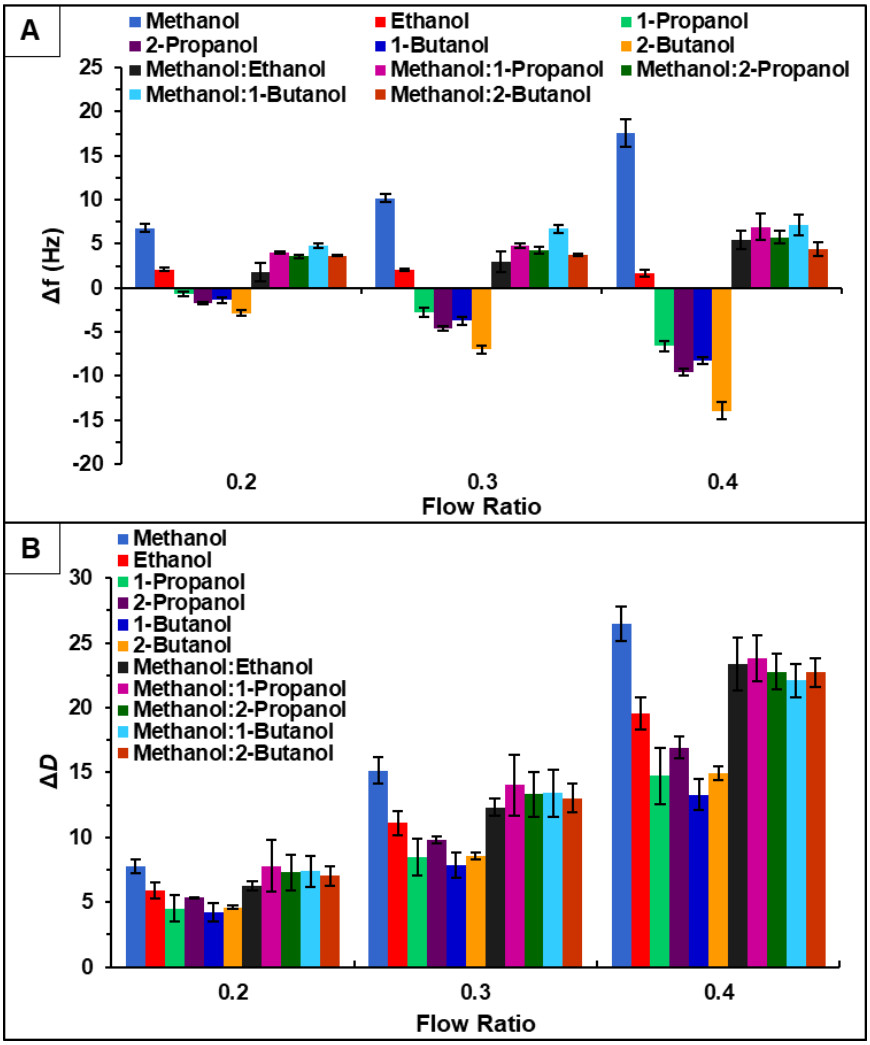

Figure 4.1. [HMIm][NTf_2]-PMMA sensor response of 11 alcohol samples at three flow ratios for A) Δf, and B) ΔD. Error bars represent standard deviation for three replicate measurements.

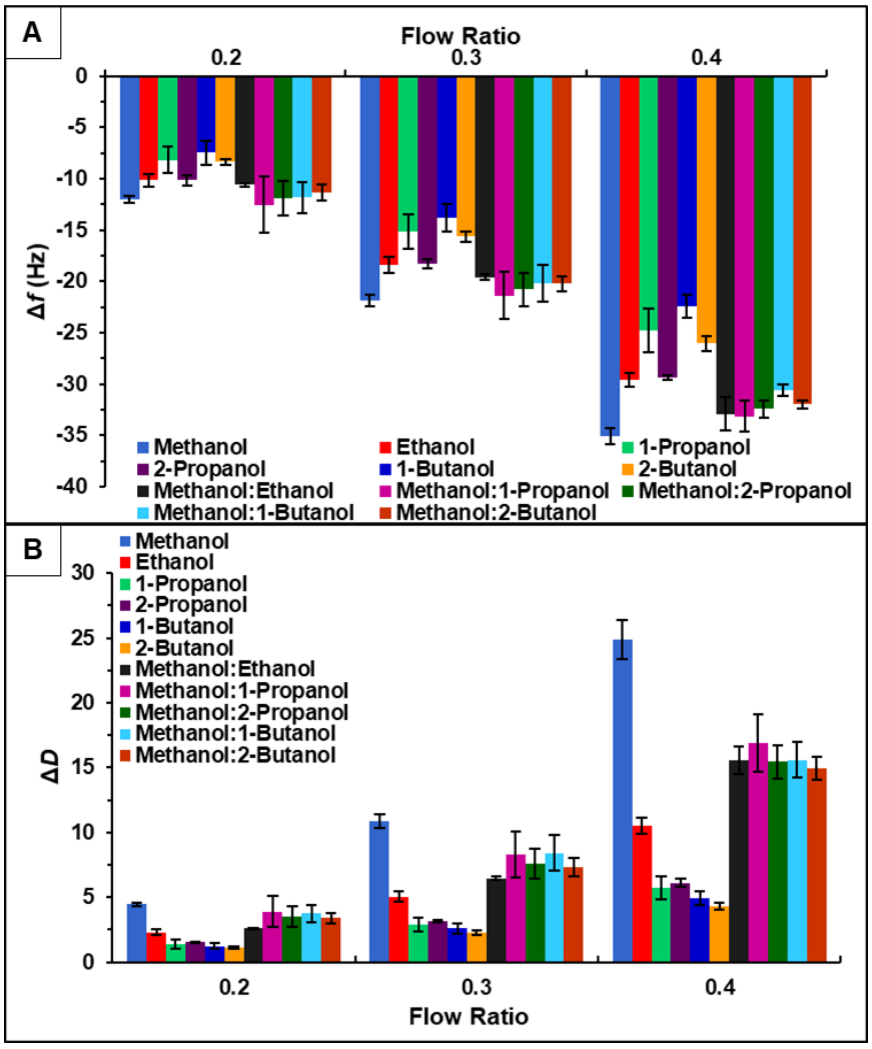

Figure 4.2. [BM_2Im][PF_6]-PMMA sensor response of 11 alcohol samples at three flow ratios for A) Δ*f*, and B) Δ*D*. Error bars represent standard deviation for three replicate measurements.

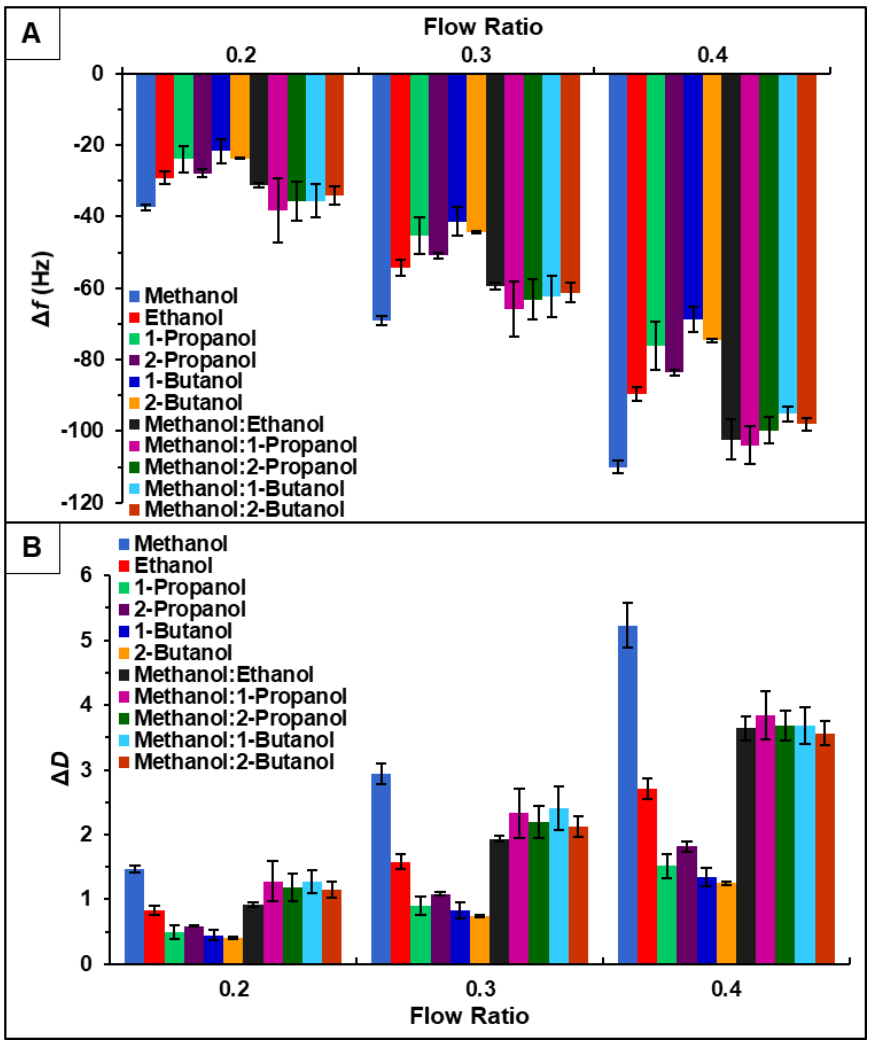

Figure 4.3. [BM$_2$Im][OTf]-PMMA sensor response of 11 alcohol samples at three flow ratios for A) Δ*f*, and B) Δ*D*. Error bars represent standard deviation for three replicate measurements.

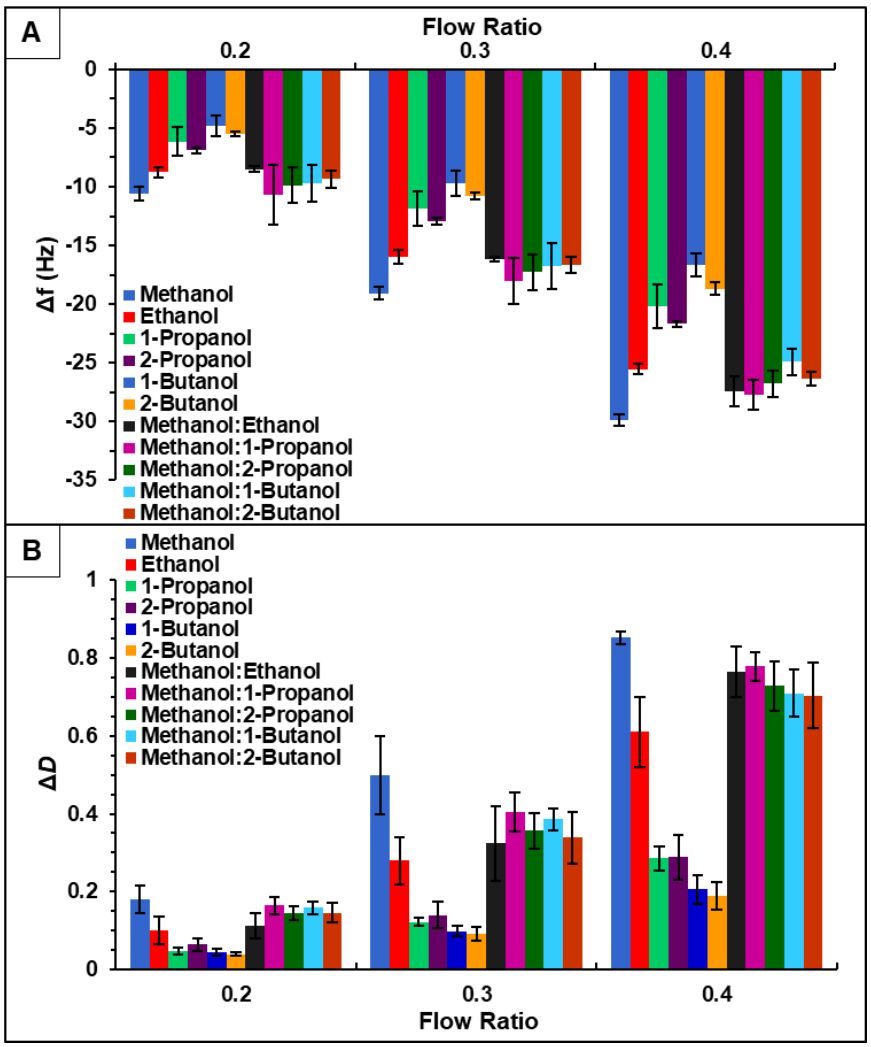

Figure 4.4. [BPyr][PF_6]-PMMA sensor response of 11 alcohol samples at three flow ratios for A) Δ*f*, and B) Δ*D*. Error bars represent standard deviation for three replicate measurements.

With the exception of [HMIm][NTf_2]-PMMA, which exhibited slight sensor drift, each sensor displayed stable baselines. Although, [HMIm][NTf_2]-PMMA exhibited some sensor drift, each sensor was found to be reusable and exhibited reversible sorption as seen in Figure C1. Furthermore, all sensors generated analyte specific response patterns. It was originally hypothesized that alcohol mixtures at 1:1 ratios would exhibit additive responses of their respective alcohols. However, this was not seen in any of the four sensors. For instance, in Figure 4.1 at 0.4 flow ratio, methanol generated a response of approximately

15 Hz and ethanol is generated a response of about 2 Hz. An additive response for the methanol:ethanol mixture is expected to generate a response of about 17 Hz, but the actual response generated was approximately 5 Hz. This behavior is shown in all sensor responses (Figures 4.1, 4.2, 4.3, and 4.4). In fact, the mixture responses are similar to each other, but vary from respective alcohols with the exception of methanol. This may be attributed to methanol being the most volatile alcohol and when mixtures are being exposed to the sensors, methanol is adsorbing to the sensors before the second alcohol component does. However, experiments are ongoing to fully understand the mechanism of this interaction.

Figure 4.5 allows the entire Δf data set to be analyzed visually. In this figure, [HMIm][NTf_2]-PMMA exhibits the lowest overall sensor response, and is the only sensor to generate both positive and negative sensor responses. [BM_2Im][PF_6]-PMMA and [BPyr][PF_6]-PMMA exhibit similar sensor response patterns, which is likely attributed to the PF_6 counterion. Upon further examination, [BM_2Im][OTf]-PMMA demonstrates the overall highest sensor response. This could be attributed to the OTf counter-anion, which is the only difference between previous sensor. Sensor responses, however, are drastically different. Although [BM_2Im][PF_6]-PMMA and [BPyr][PF_6]-PMMA exhibit similar Δf sensor responses, a closer look at ΔD sensor responses reveals that each sensor exhibits different response patterns. Based on this observation, it was hypothesized that new analyte specific response patterns could be observed by plotting $\Delta f/\Delta D$ versus flow ratio. Based on pattern responses shown in Figures 4.6, 4.7, 4.8, and 4.9, it was determined that MSA development was possible.

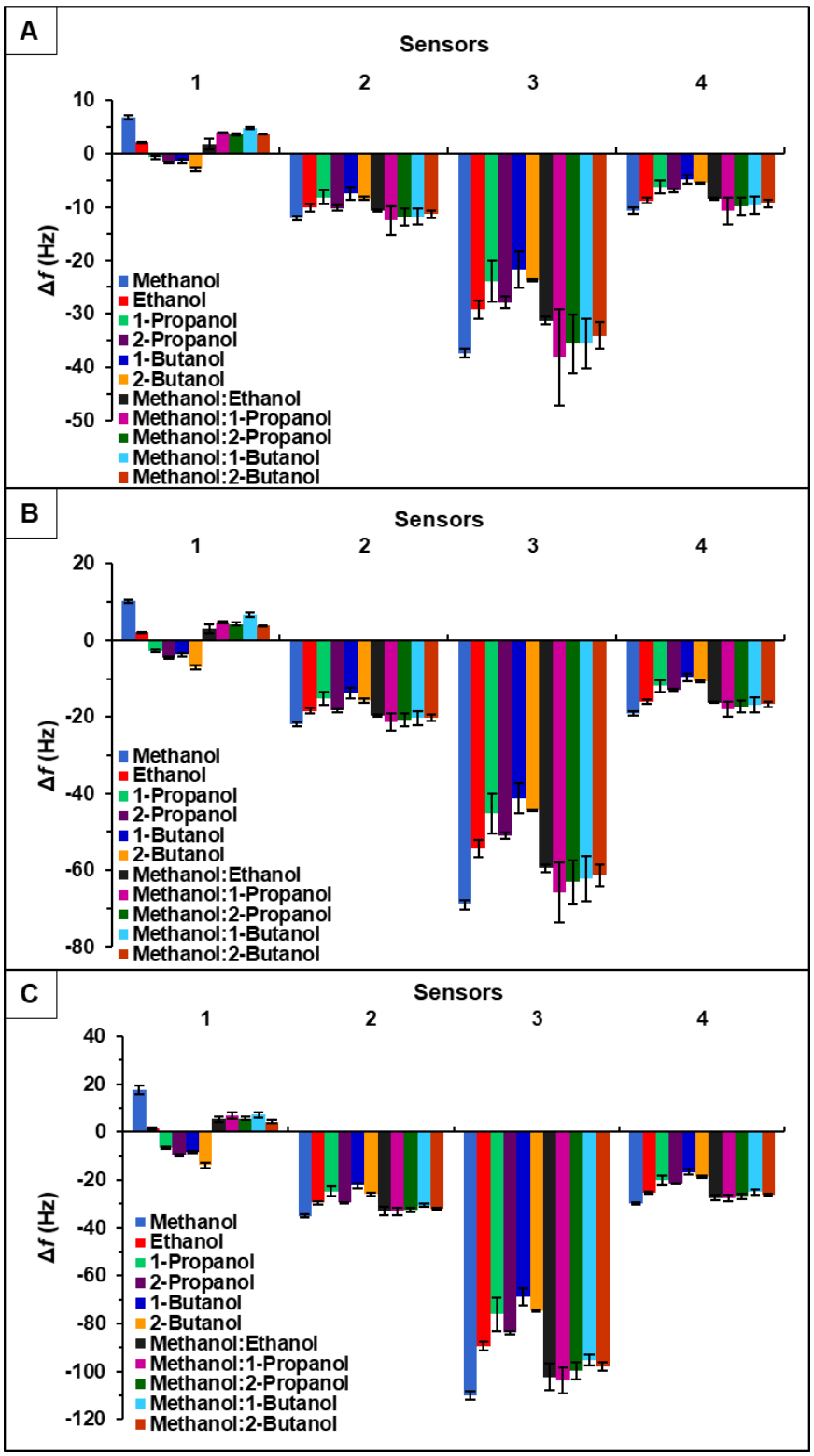

Figure 4.5. Comparison of sensor responses of 11 alcohol samples for A) 0.2 flow ratio, B) 0.3 flow ratio, and C) 0.4 flow ratio. 1, 2, 3, and 4, represent [HMIm][NTf_2]-PMMA, [BM_2Im][PF_6]-PMMA, [BM_2Im][OTf]-PMMA, and [BPyr][PF_6]-PMMA, respectively. Error bars represent standard deviation for three replicate measurements.

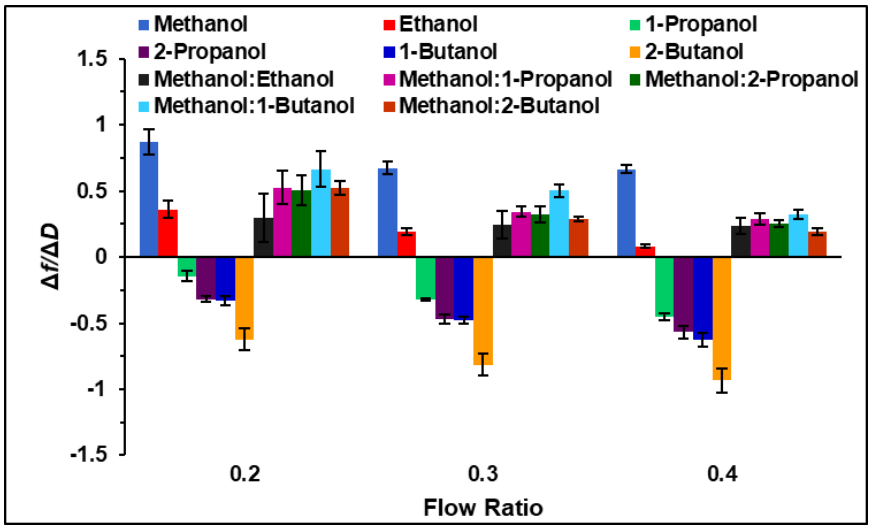

Figure 4.6. [HMIm][NTf_2]-PMMA Δ*f*/Δ*D* sensor response of 11 alcohol samples at three flow ratios. Error bars represent standard deviation for three replicate measurements.

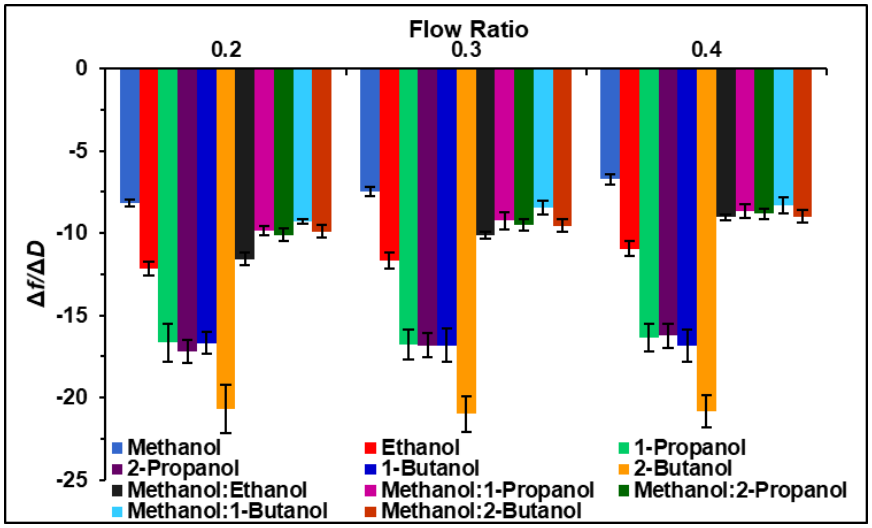

Figure 4.7. [BM_2Im][PF_6]-PMMA Δ*f*/Δ*D* sensor response of 11 alcohol samples at three flow ratios. Error bars represent standard deviation for three replicate measurements.

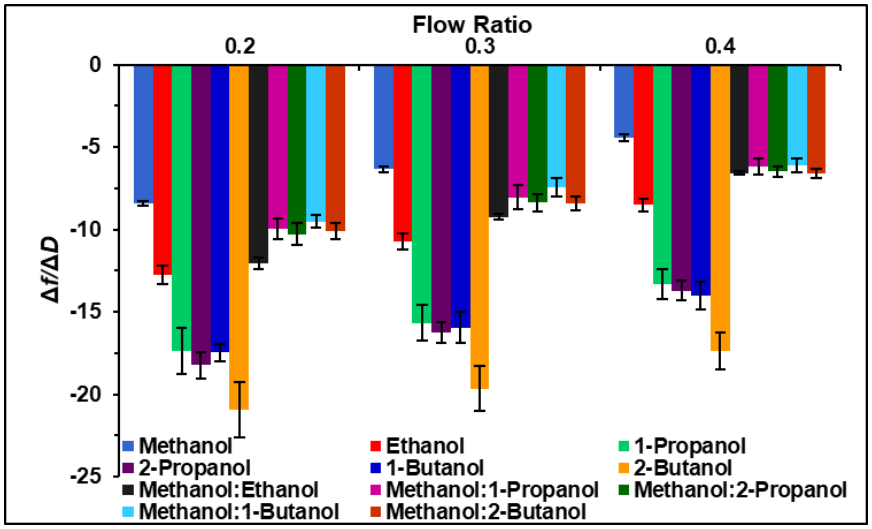

Figure 4.8. [BM_2Im][OTf]-PMMA $\Delta f/\Delta D$ sensor response of 11 alcohol samples at three flow ratios. Error bars represent standard deviation for three replicate measurements.

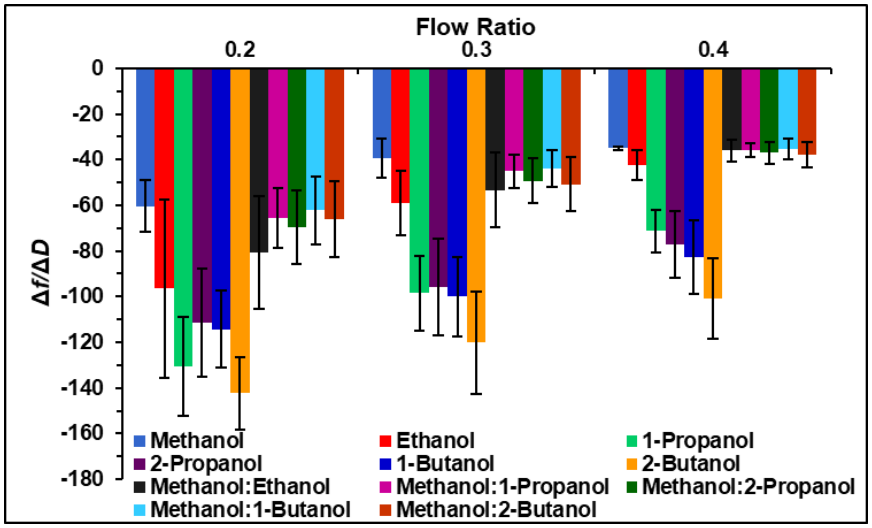

Figure 4.9. [BPyr][PF_6]-PMMA $\Delta f/\Delta D$ sensor response of 11 alcohol samples at three flow ratios. Error bars represent standard deviation for three replicate measurements.

4.3.2. Evaluation of MSA

Figures 4.6, 4.7, 4.8, and 4.9 suggest that MSA fabrication to discriminate between the six pure alcohol samples and five alcohol mixtures is possible. The raw $\Delta f/\Delta D$ data collected from the four sensors were used to develop a predictive model using DA. More specifically, quadratic DA (QDA) was used because it assumes that the covariance matrices are different for each alcohol sample.

It was determined that the first two principal components accounted for 99.9% of the total variability in the four predictors. The first principal component, which accounted for 98.9% of variability, represents the sum of the four sensor measurements. The second principal component, which accounted for an additional 1.06% of the total variation, represents a comparison between [HMIm][NTf_2] and [BPyr][PF_6] sensor measurements. Based on a plot of the first two principal component scores (Figure 4.10), the principal components provided no visual separation between the 11 alcohol samples.

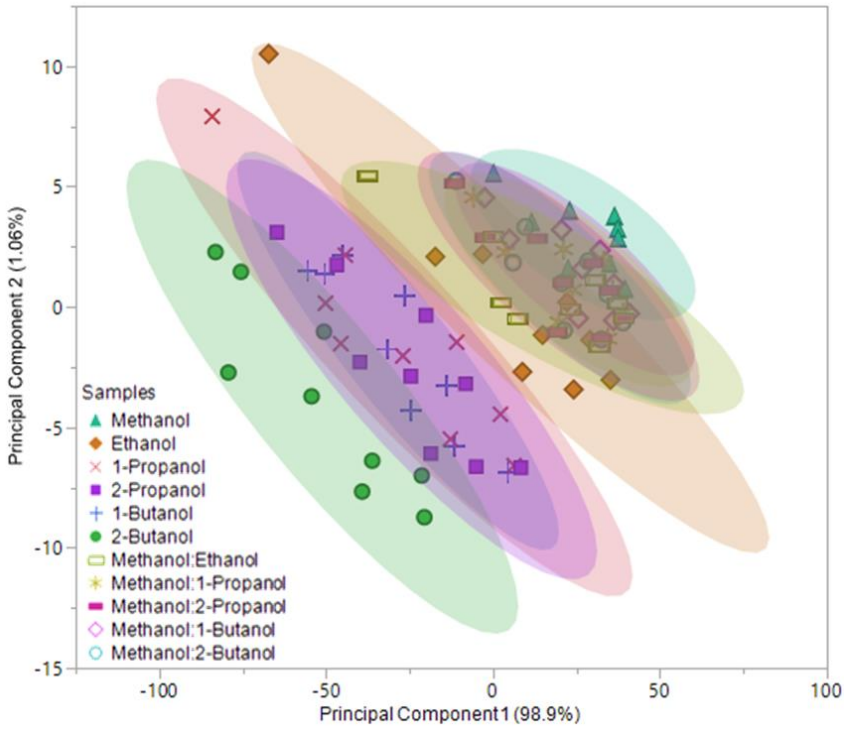

Figure 4.10. Principal component plot for discrimination of 11 alcohol samples with respect to a four sensor MSA. Plot considers 99 total measurements consisting of three replicate measurements at three different flow ratios for each sample (9 measurements per sample).

This overlap of data values indicated that the MSA would be unable to discriminate between any of the 11 alcohol samples. To evaluate the accuracy of this observation, a QDA predictive model was developed using $\Delta f/\Delta D$ measurements from the four sensors

directly as predictor variables. The subsequent QDA model resulted in 15 misclassifications, which corresponds to an error rate of 15.15%. In this model, one (1) 2-propanol measurement was misclassified as 1-butanol, one (1) methanol:ethanol measurement was misclassified as methanol:2-propanol, one (1) as methanol:2-butanol, one (1) methanol:1-propanol measurement was misclassified as methanol:2-butanol, two (2) as methanol:2-propanol, one (1) as methanol:ethanol, one (1) methanol:2-propanol measurement was misclassified as methanol:1-propanol while another four (4) were misclassified as methanol:2-butanol, one (1) methanol:1-butanol was misclassified as methanol:2-propanol, and one (1) methanol:2-butanol measurement was misclassified as methanol:2-propanol. This predictive model resulted in an overall accuracy rate of 84.85%.

To verify the necessity of the combination of these two values, a QDA model using only Δ*f* measurements from the four sensors as predictor variables was developed. This predictive model resulted in an overall error rate of 27.27%, which corresponds to a total of 27 misclassifications. These misclassifications consisted of one (1) ethanol measurement classified as methanol:ethanol, one (1) 1-propanol measurement classified as 2-propanol, two (2) 1-butanol measurements classified as 2-butanol, three (3) methanol:ethanol measurements classified as methanol:2-propanol, one (1) methanol:1-propanol measurement classified as methanol:1-butanol and one (1) as methanol:ethanol, one (1) methanol:2-propanol measurement classified as methanol:ethanol, one (1) methanol:1-butanol measurement classified as methanol:2-propanol, and two (2) methanol:2-butanol measurements classified as methanol:ethanol. The overall accuracy rate for this model was found to be 72.73%. Therefore, combining

Δ*f* and Δ*D* measurements for use as sensor responses directly as predictor variables in QDA, resulted in a more accurate predictive model than using Δ*f* sensor responses alone.

4.4. Conclusion

This work is a blueprint for development of a QCM-based MSA for discrimination of pure alcohol samples and 1:1 mixtures of alcohol samples. To achieve this, a MSA was fabricated using four previously synthesized IL-polymer composites as coating materials. Overall, these composites showed good sensing characteristics and cross-reactive responses to six pure alcohol samples and five alcohol mixtures. However, it was found that a higher degree of discrimination between samples could be obtained from these sensors by using Δ*f*/Δ*D* measurements rather than Δ*f* measurements than Δ*f* alone. The MSA was developed using Δ*f*/Δ*D* measurements from all four sensors as predictor variables in QDA, which resulted in an 84.85% accuracy in discriminating 11 alcohol samples. This was an improvement as compared to the QDA model using Δ*f* measurements as predictor variables, which resulted in 72.73% accuracy. Currently, more analyses are being explored to identify the components of the alcohol mixtures, and these results show promise for use in discriminating and identifying complex mixtures for adulteration of beverages.

4.5. References

1. Sisco, E.; Dake, J., Detection of Low Molecular Weight Adulterants in Beverages by Direct Analysis in Real Time Mass Spectrometry. *Anal Methods* **2016,** *8* (14), 2971-2978.

2. Magnusdottir, K.; Kristinsson, J.; Jóhannesson, B., Adulterated alcoholic beverages. *Laeknabladid* **2010,** *96* (10), 626-628.

3. Rothenbacher, T.; Schwack, W., Rapid and nondestructive analysis of phthalic acid esters in toys made of poly (vinyl chloride) by direct analysis in real time single-quadrupole mass spectrometry. *Rapid Communications in Mass*

Spectrometry: An International Journal Devoted to the Rapid Dissemination of Up-to-the-Minute Research in Mass Spectrometry **2009,** *23* (17), 2829-2835.

4. Jackson, D. S.; Crockett, D. F.; Wolnik, K. A., The indirect detection of bleach (sodium hypochlorite) in beverages as evidence of product tampering. *Journal of forensic sciences* **2006,** *51* (4), 827-831.

5. Yarita, T.; Nakajima, R.; Otsuka, S.; Ihara, T.; Takatsu, A.; Shibukawa, M., Determination of ethanol in alcoholic beverages by high-performance liquid chromatography–flame ionization detection using pure water as mobile phase. *Journal of Chromatography A* **2002,** *976* (1-2), 387-391.

6. KALCHENKO, V. I.; KOSHETS, I. A.; MATSAS, E. P.; KOPYLOV, O. N.; SOLOVYOV, A.; KAZANTSEVA, Z. I.; SHIRSHOV, Y. M., Calixarene-based QCM sensors array and its response to volatile organic vapours *Materials Science* **2002,** *20* (3), 73-88.

7. Wang, F.; Gu, H.; Swager, T. M., Carbon nanotube/polythiophene chemiresistive sensors for chemical warfare agents. *Journal of the American Chemical Society* **2008,** *130* (16), 5392-5393.

8. Abraham, J. K.; Philip, B.; Witchurch, A.; Varadan, V. K.; Reddy, C. C., A compact wireless gas sensor using a carbon nanotube/PMMA thin film chemiresistor. *Smart Materials and Structures* **2004,** *13* (5), 1045.

9. Rehman, A.; Hamilton, A.; Chung, A.; Baker, G. A.; Wang, Z.; Zeng, X., Differential solute gas response in ionic-liquid-based QCM arrays: elucidating design factors responsible for discriminative explosive gas sensing. *Analytical chemistry* **2011,** *83* (20), 7823-7833.

10. Schäfer, T.; Di Francesco, F.; Fuoco, R., Ionic liquids as selective depositions on quartz crystal microbalances for artificial olfactory systems—a feasibility study. *Microchemical Journal* **2007,** *85* (1), 52-56.

11. Tseng, M.-C.; Chu, Y.-H., Chemoselective gas sensing ionic liquids. *Chemical Communications* **2010,** *46* (17), 2983-2985.

12. Xu, X.; Li, C.; Pei, K.; Zhao, K.; Zhao, Z. K.; Li, H., Ionic liquids used as QCM coating materials for the detection of alcohols. *Sensors and Actuators B: Chemical* **2008,** *134* (1), 258-265.

13. Regmi, B. P.; Monk, J.; El-Zahab, B.; Das, S.; Hung, F. R.; Hayes, D. J.; Warner, I. M., A novel composite film for detection and molecular weight determination of organic vapors. *Journal of Materials Chemistry* **2012,** *22* (27), 13732-13741.

14. Speller, N. C.; Siraj, N.; McCarter, K. S.; Vaughan, S.; Warner, I. M., QCM VIRTUAL SENSOR ARRAY: VAPOR IDENTIFICATION AND MOLECULAR WEIGHT APPROXIMATION. *Sensors and Actuators B: Chemical* **2017**.

15. Kern, W., The evolution of silicon wafer cleaning technology. *Journal of the Electrochemical Society* **1990,** *137* (6), 1887-1892.

16. Vaughan, S. R.; Speller, N. C.; Chhotaray, P.; McCarter, K. S.; Siraj, N.; Pérez, R. L.; Li, Y.; Warner, I. M., Class specific discrimination of volatile organic compounds using a quartz crystal microbalance based multisensor array. *Talanta* **2018,** *188*, 423-428.

CHAPTER 5. CONCLUSIONS AND FUTURE WORK

5.1. Conclusions

Volatile organic compounds (VOCs) are a group of carbon-based organic chemicals that are emitted from both natural and artificial sources. VOCs are present in everyday life and many of them are known to cause adverse environmental and health effects. For this reason, detecting and analyzing these vapors is of great concern. In this regard, electronic noses (e-nose) have been used for vapor sensors. A variety of transducers with suitable coating materials have been investigated; however, within this dissertation the quartz crystal microbalance (QCM) has been employed as an e-nose. Ionic liquids (ILs) and a ***g***roup of ***u***niform ***m***aterials ***b***ased on ***o***rganic ***s***alts (GUMBOS) were selected as coating materials due to their appealing properties, such as tunable physicochemical properties, simple synthesis, and negligible volatility. Although QCM-based vapor sensors have shown great potential for detecting VOCs, they are not capable of discrimination between different VOCs. Thus, ionic materials coated QCM-based sensor arrays were employed for this dissertation. In Chapter 1, an introduction to VOCs, e-noses, sensor arrays, statistical techniques, ILs, GUMBOS, and theory of the QCM is reported.

Chapter 2 described the synthesis of four novel phthalocyanine-based GUMBOS for use as coating materials in a QCM-based multisensor array (MSA). Vapor sensing properties of these GUMBOS was investigated by exposing the MSA to a set of ten VOCs. It was found that by employing this phthalocyanine-based GUMBOS MSA, ten different analytes were discriminated into four classes with an accuracy of 98.6%. These studies present the first QCM-based MSA to discriminate VOCs by classes.

In Chapter 3, two sensing schemes for detection and discrimination of chlorinated VOCs was presented. In this work, phosphonium ILs were synthesized and vapor sensing properties were examined and compared to phosphonium IL-polymer composites. Pure IL sensors were used to develop a QCM-based MSA, while IL-polymer composites were used to develop a MSA and virtual sensor arrays (VSAs). It was found that by employing the composite MSA, five chlorinated VOCs were accurately discriminated at 95.56%, which was an increase in accuracy in comparison to pure ILs MSA (84.45%). Two out of three VSAs discriminated chlorinated VOCs with 100% accuracy. These studies have provided more insight on the benefits of incorporating polymers in coating materials for enhanced discrimination accuracies of QCM-based sensor arrays.

Development of a QCM-based MSA for discrimination of pure alcohol samples and 1:1 mixtures of alcohol samples was described in Chapter 4. IL-polymer composites were prepared and their gas-sensing properties were investigated. Using change in frequency and dissipation ratio ($\Delta f/\Delta D$) measurements, an MSA was developed from all four sensors as predictor variables in a predictive model, which resulted in an 84.85% accuracy in discriminating 11 alcohol samples. These studies show promise for use in discriminating and identifying complex mixtures for adulteration of beverages.

5.2. Future Work

The work described in this dissertation demonstrates the capability of QCM-based vapor sensor arrays with GUMBOS and ILs as coating materials for accurate discrimination of VOCs. However, further research needs to be investigated in the area of vapor sensors for the identification of individual components within a complex mixture. The QCM-based sensor array presented in Chapter 4 is the first attempt at discriminating

and identifying individual components within a known mixture. Future work for this project is aimed at developing another predictive model that is capable of identifying components within a binary mixture. Once this is accomplished, more complex mixtures may be analyzed.

In addition, the QCM as an e-nose is an attractive technology due to its simplicity, and sensitivity; however, it is a slightly bulky instrument. Thus, it is of great interest to develop a miniaturized QCM. This would allow for “on the field testing” of QCM-based sensor arrays for detection of VOCs in real time. Our group is currently working in collaboration with Professor Jinwoo Choi in LSU’s Electrical Engineering Department to consult and assist in analysis and development of a miniaturized QCM.

APPENDIX A. SUPPORTING INFORMATION FOR CHAPTER 2

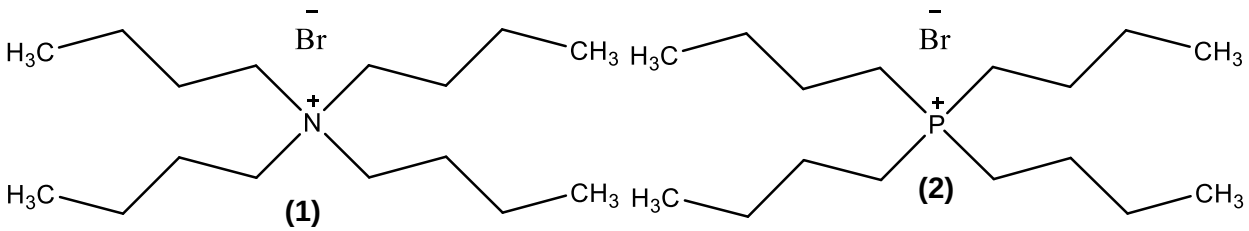

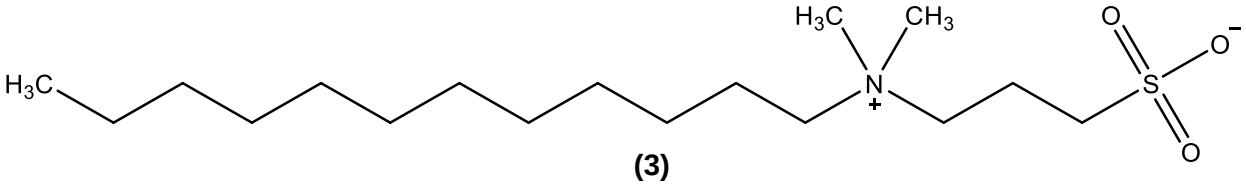

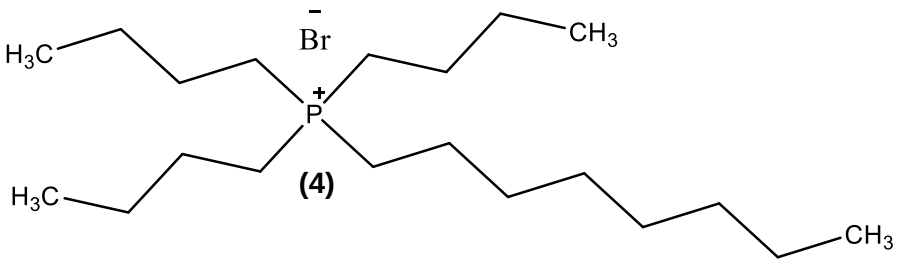

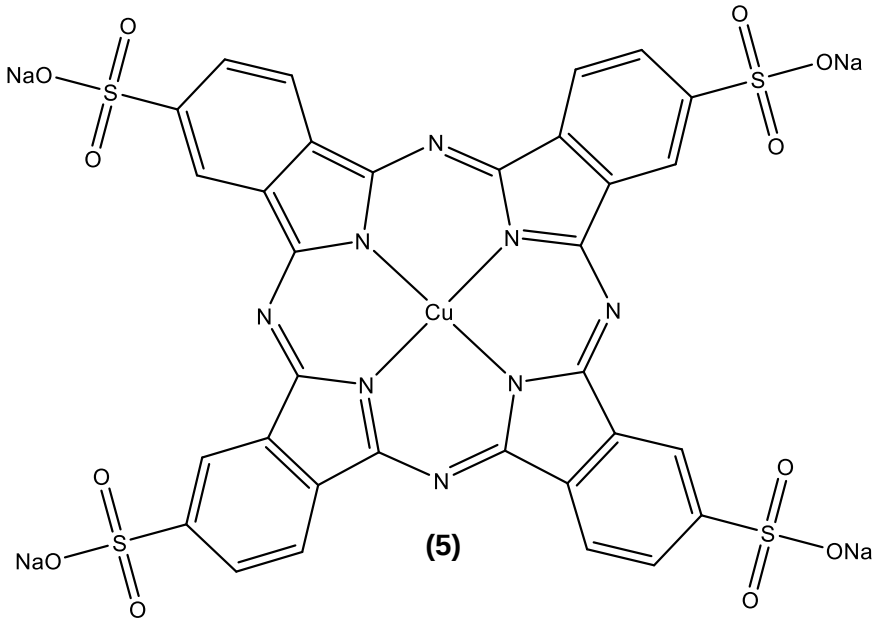

Figure A1. Structures of compounds used to synthesize GUMBOS. 1) Tetrabutylammonium bromide (TBA), 2) Tetrabutylphosphonium bromide (P_{4444}), 3) 3-(dodecyldimethyl-ammonio)propanesulfonate (DDMA), 4) Tributyl-*n*-octylphosphonium bromide (P_{4448}), and 5) copper (II) phthalocyaninetetrasulfonic acid ($CuPcS_4$) tetrasodium salt.

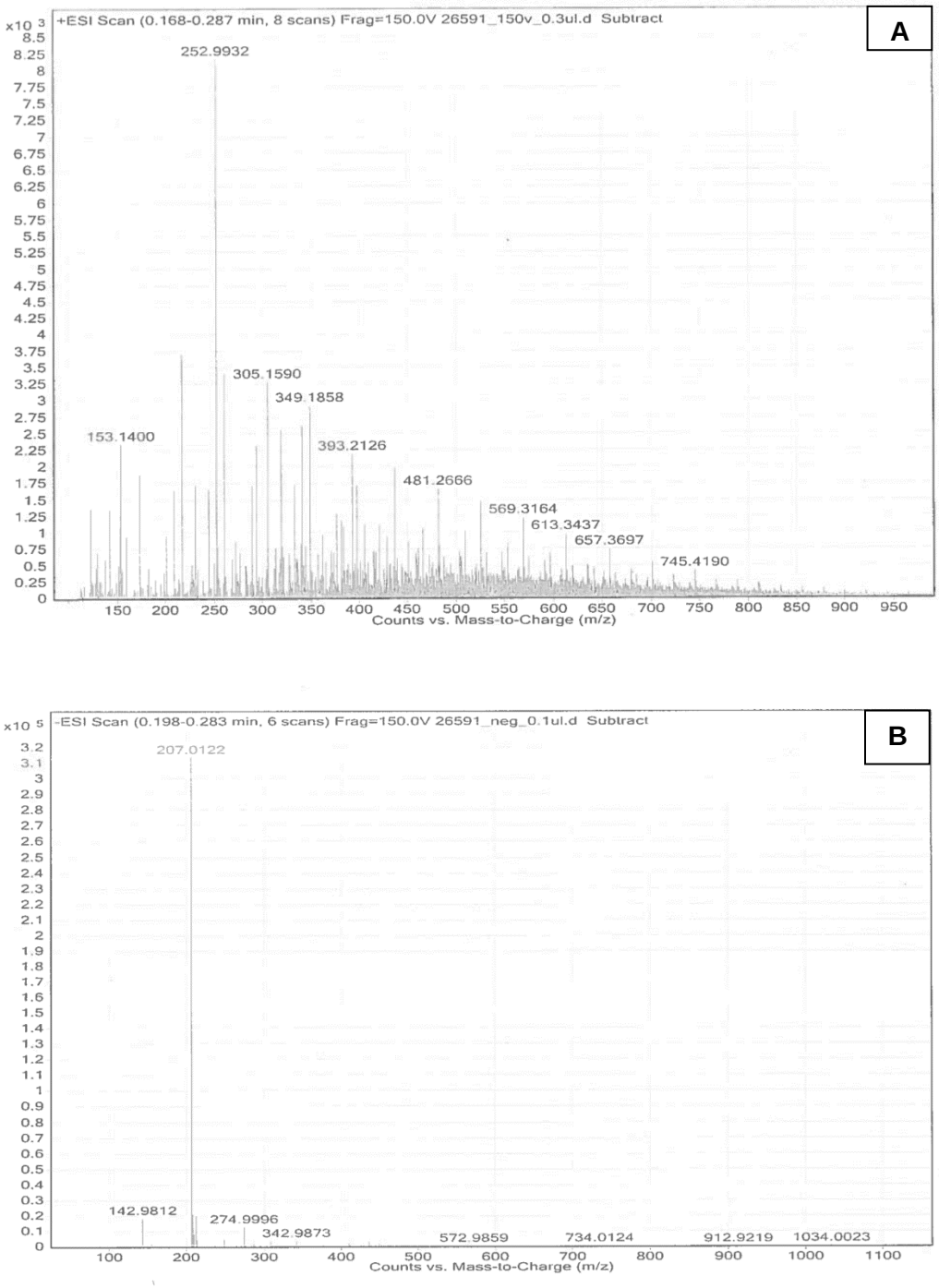

Figure A2. Electrospray ionization mass spectrometry (ESI-MS) spectra for $CuPcS_4$, where A) is in positive mode and B) is in negative mode. Solvent used was water.

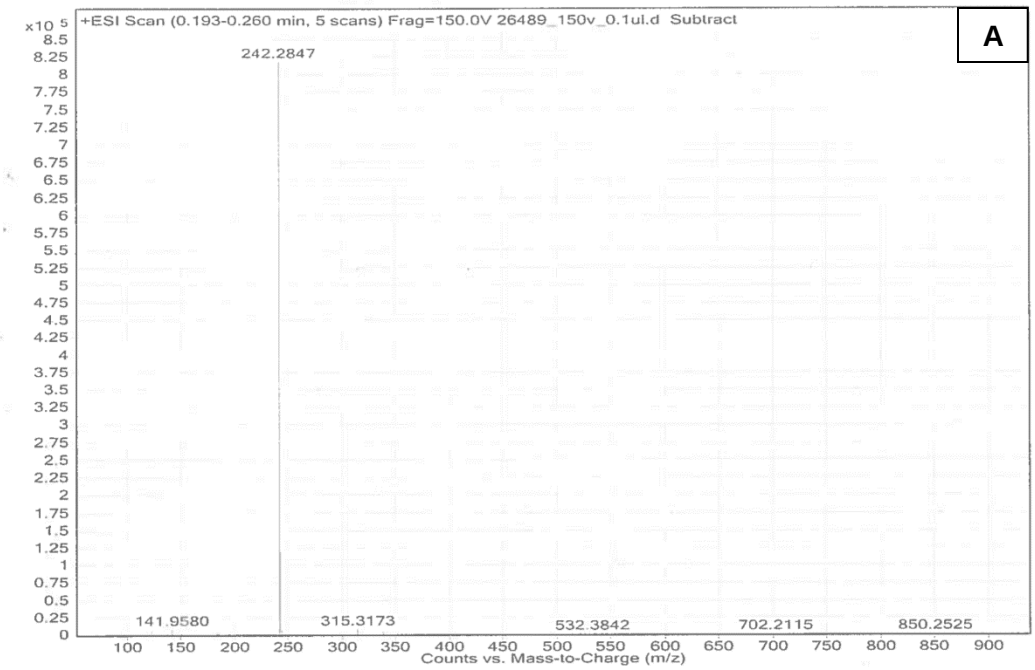

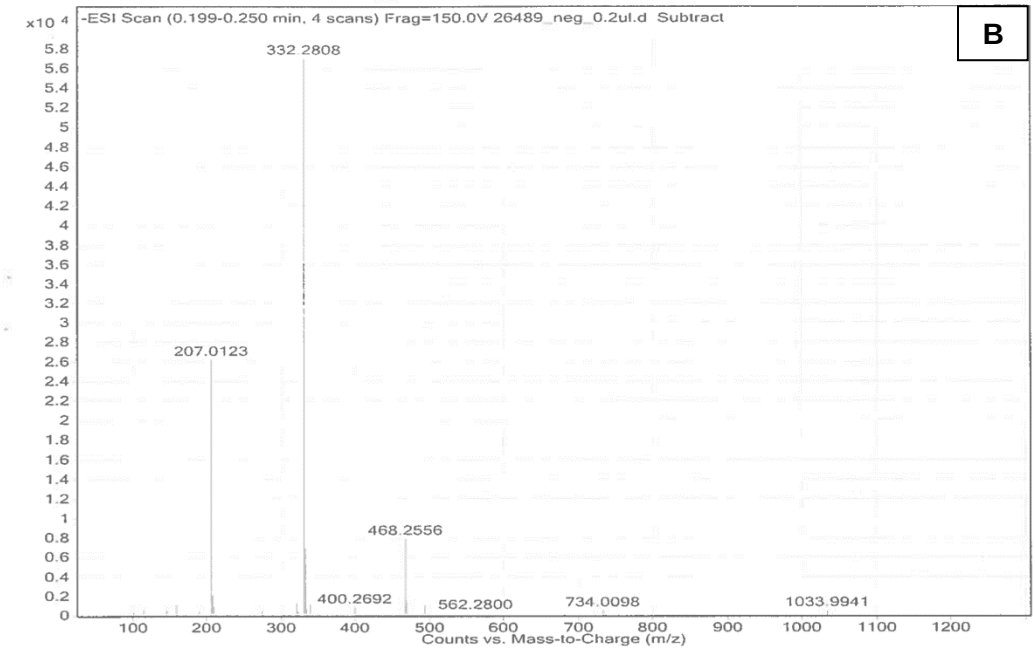

Figure A3. Electrospray ionization mass spectrometry (ESI-MS) spectra for $[TBA]_4[CuPcS_4]$ where A) is in positive mode and B) is in negative mode. Solvent used was DCM.

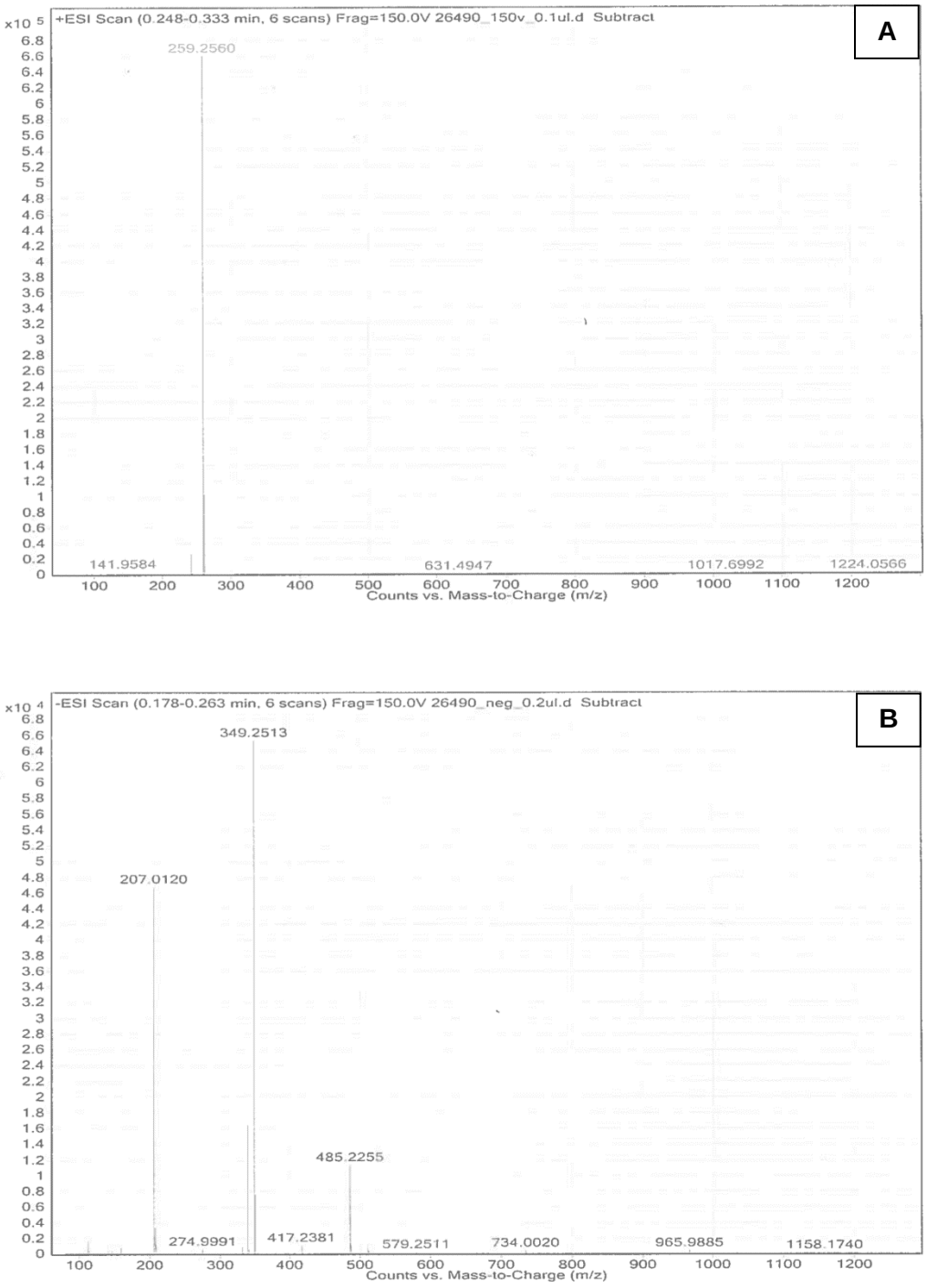

Figure A4. Electrospray ionization mass spectrometry (ESI-MS) spectra for $[P_{4444}]_4[CuPcS_4]$ where A) is in positive mode and B) is in negative mode. Solvent used was DCM.

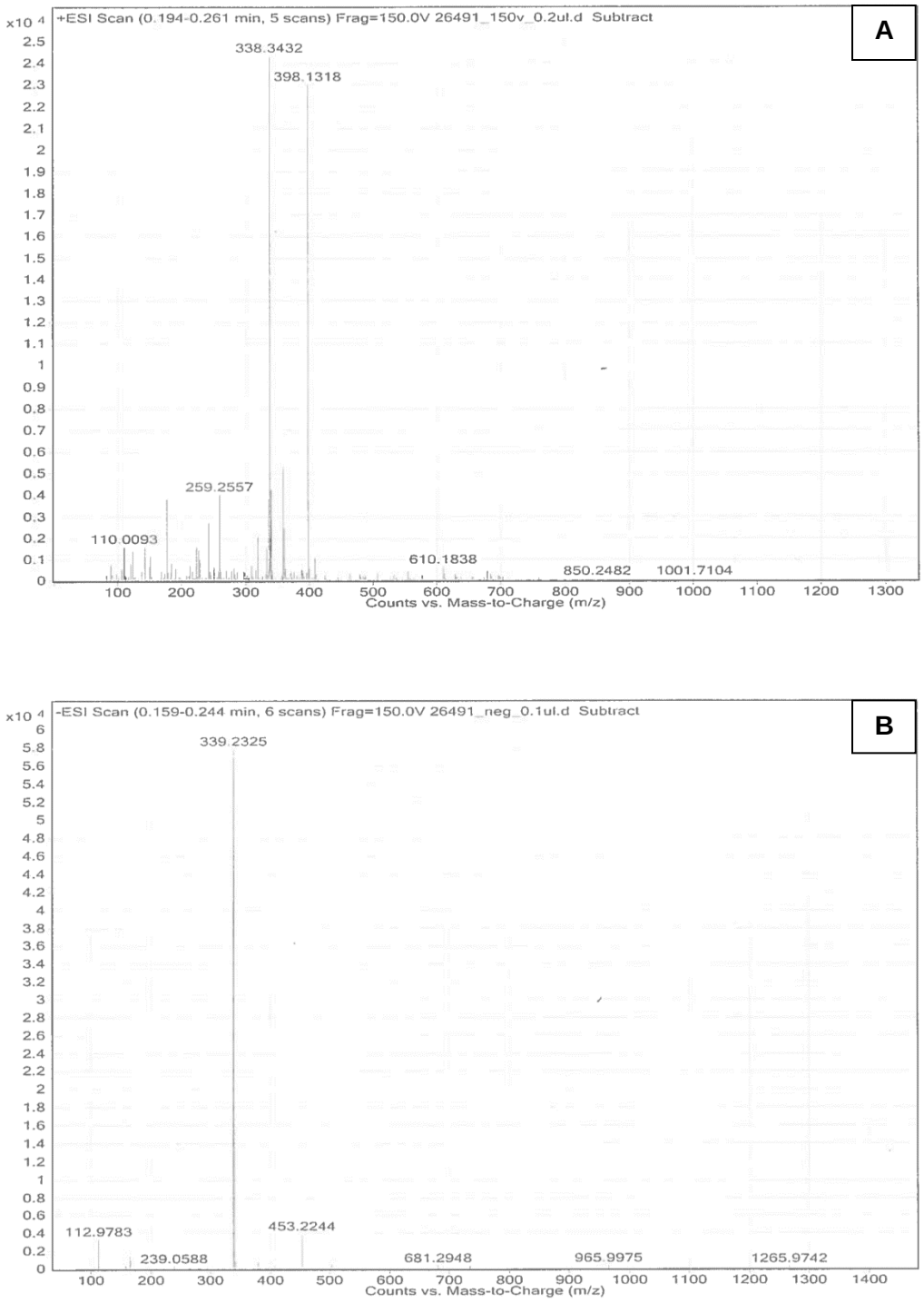

Figure A5. Electrospray ionization mass spectrometry (ESI-MS) spectra for $[DDMA]_4[CuPcS_4]$ where A) is in positive mode and B) is in negative mode. Solvent used was DCM.

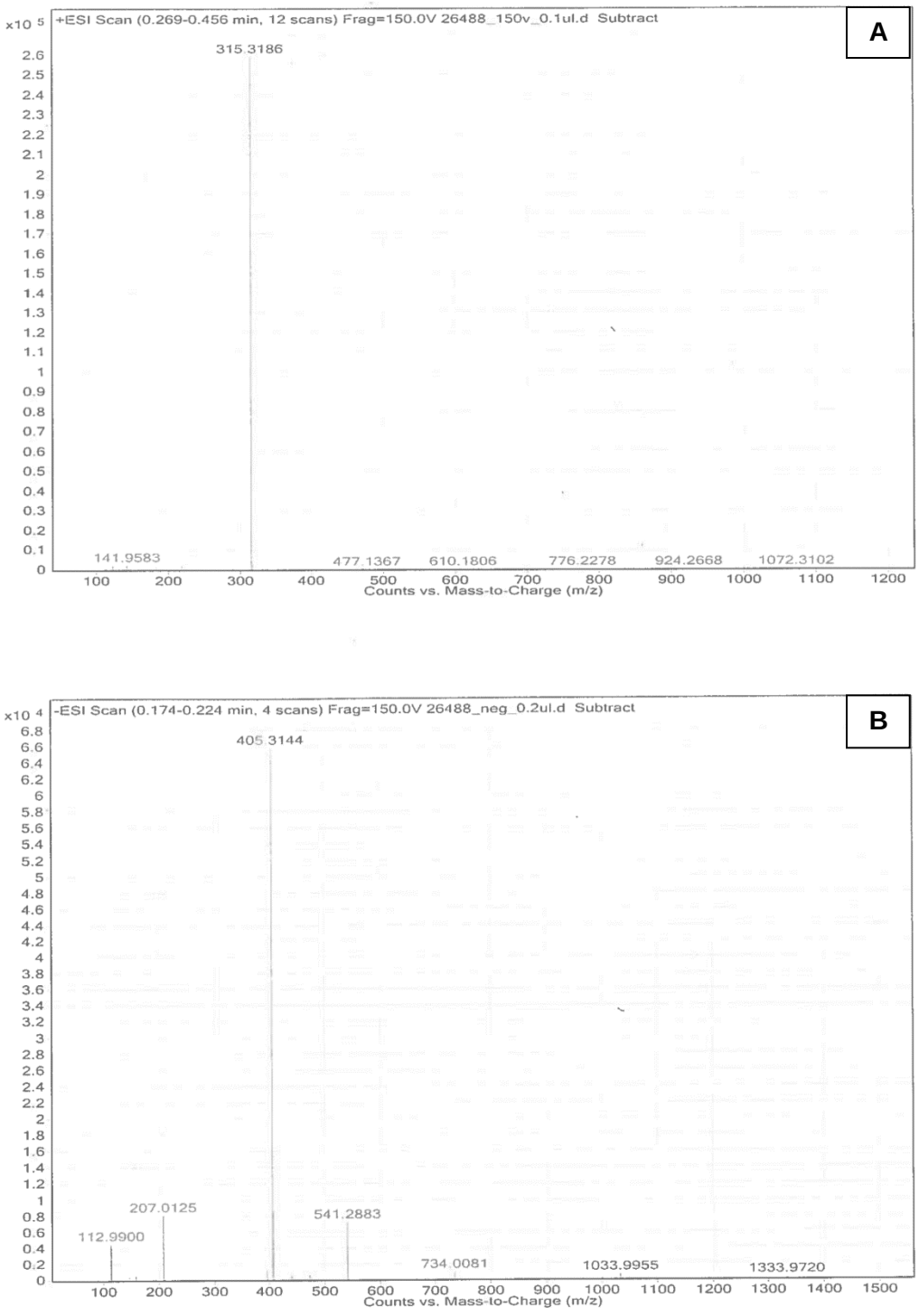

Figure A6. Electrospray ionization mass spectrometry (ESI-MS) spectra for $[P_{4448}]_4[CuPcS_4]$ where A) is in positive mode and B) is in negative mode. Solvent used was DCM.

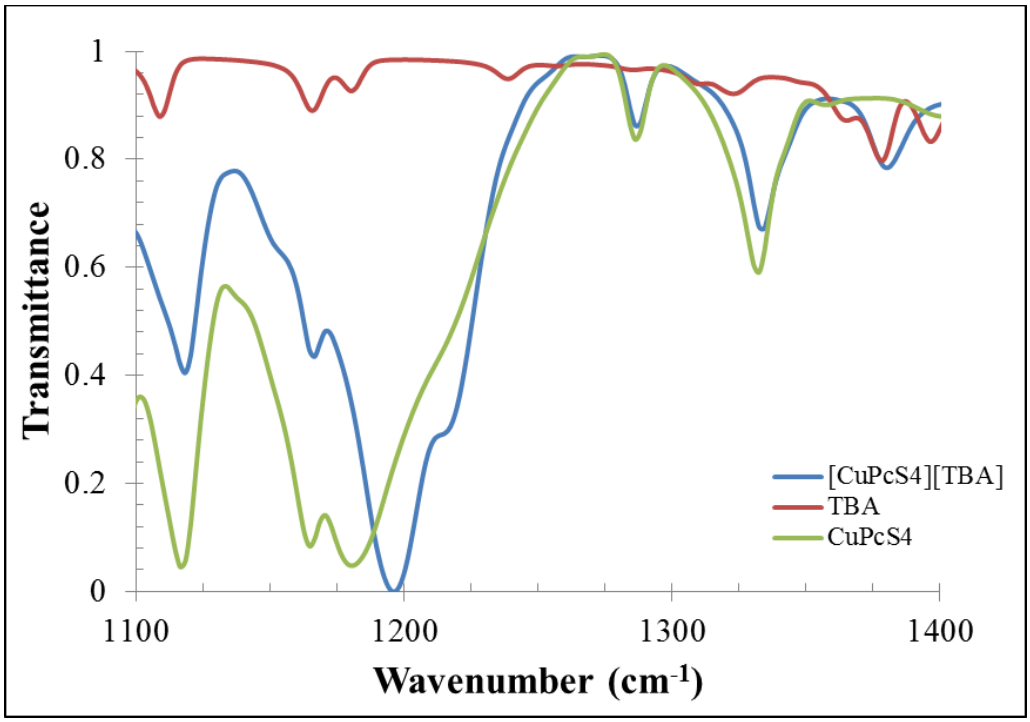

Figure A7. Fourier transform infrared (FT-IR) spectra for $[TBA]_4[CuPcS_4]$. S=O stretching in $CuPcS_4$ ~1184 shifts to ~1197 in $[TBA]_4[CuPcS_4]$.

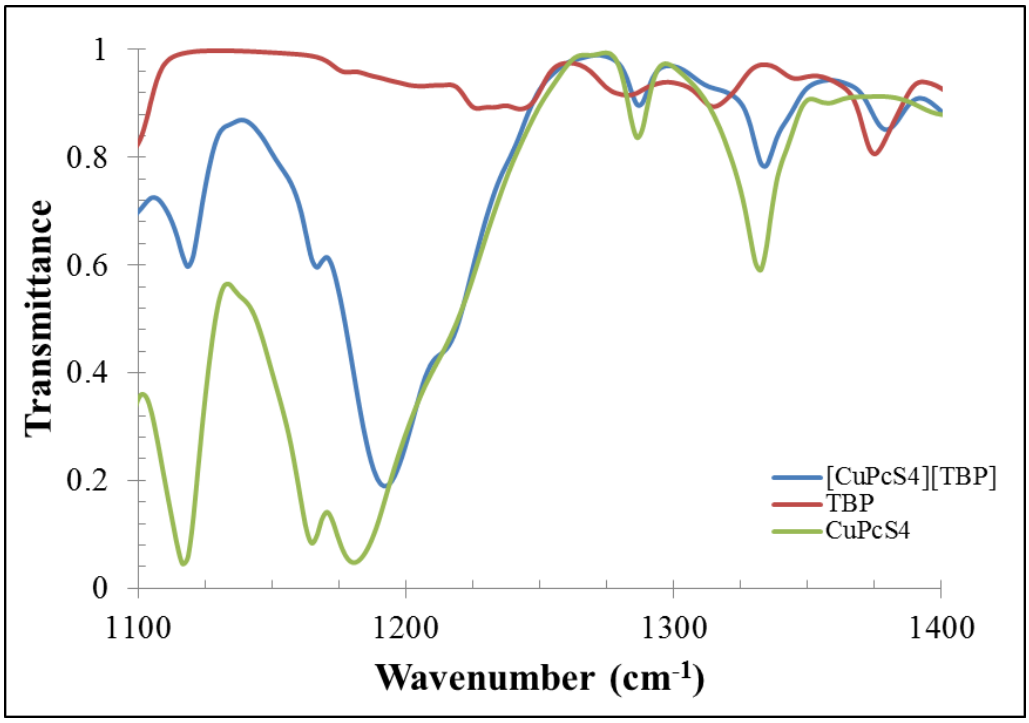

Figure A8. Fourier transform infrared (FT-IR) spectra for $[P_{4444}]_4[CuPcS_4]$. S=O stretching in $CuPcS_4$ ~1184 shifts to ~1195 in $[P_{4444}]_4[CuPcS_4]$.

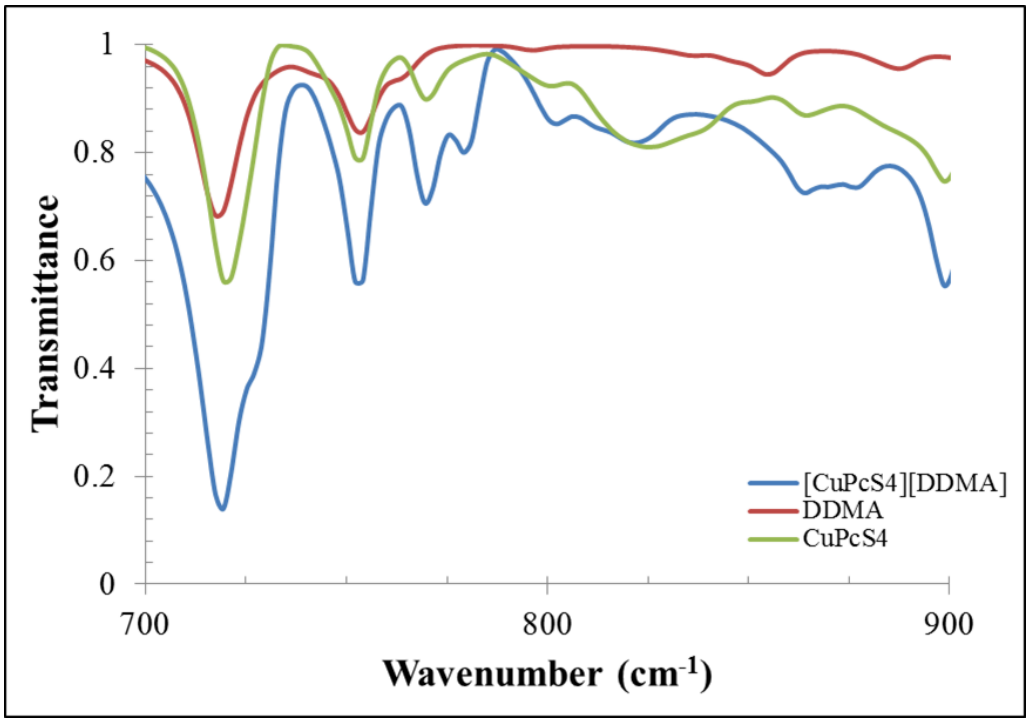

Figure A9. Fourier transform infrared (FT-IR) spectra for $[DDMA]_4[CuPcS_4]$.

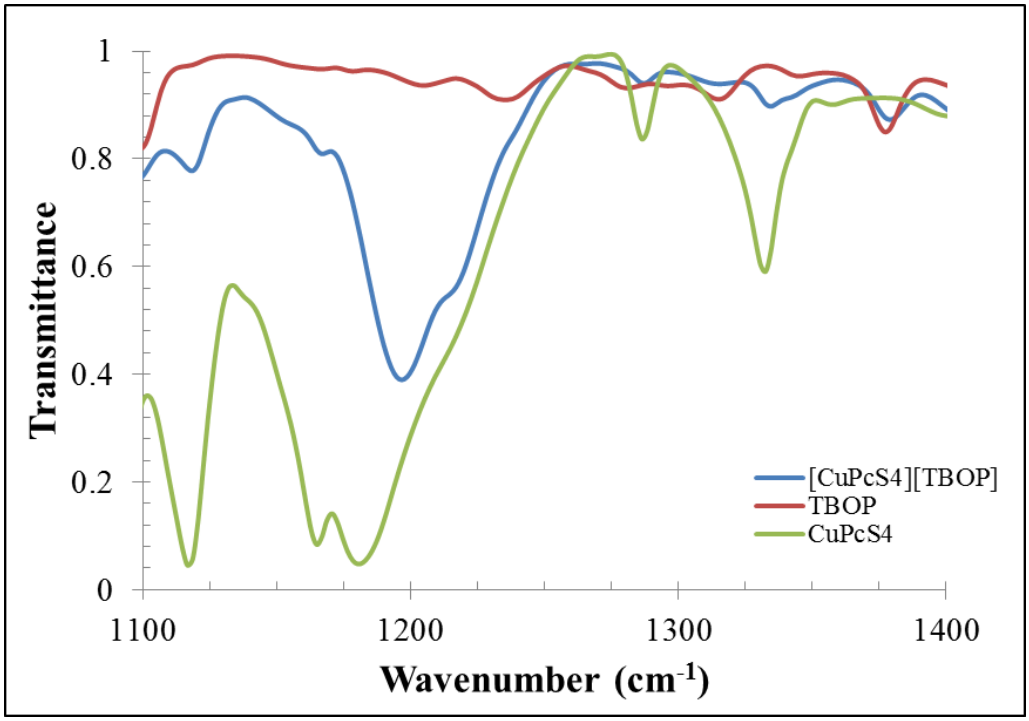

Figure A10. Fourier transform infrared (FT-IR) spectra for $[P_{4448}]_4[CuPcS_4]$. S=O stretching in $CuPcS_4$ ~1184 shifts to ~1199 in $[P_{4448}]_4[CuPcS_4]$.

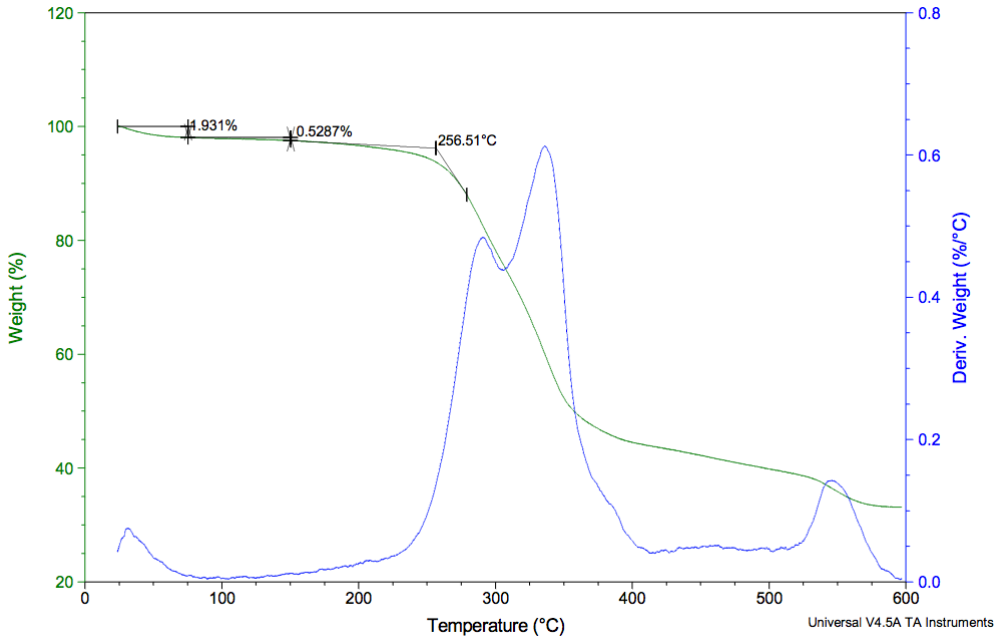

Figure A11. Thermogravimetric analysis (TGA) curve for $[TBA]_4[CuPcS_4]$.

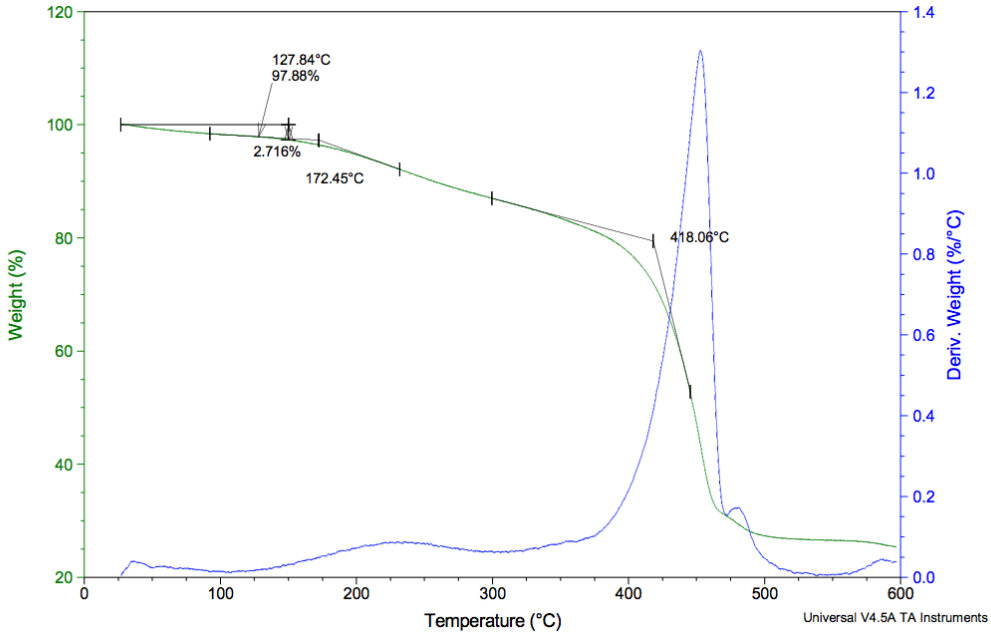

Figure A12. Thermogravimetric analysis (TGA) curve for $[P_{4444}]_4[CuPcS_4]$.

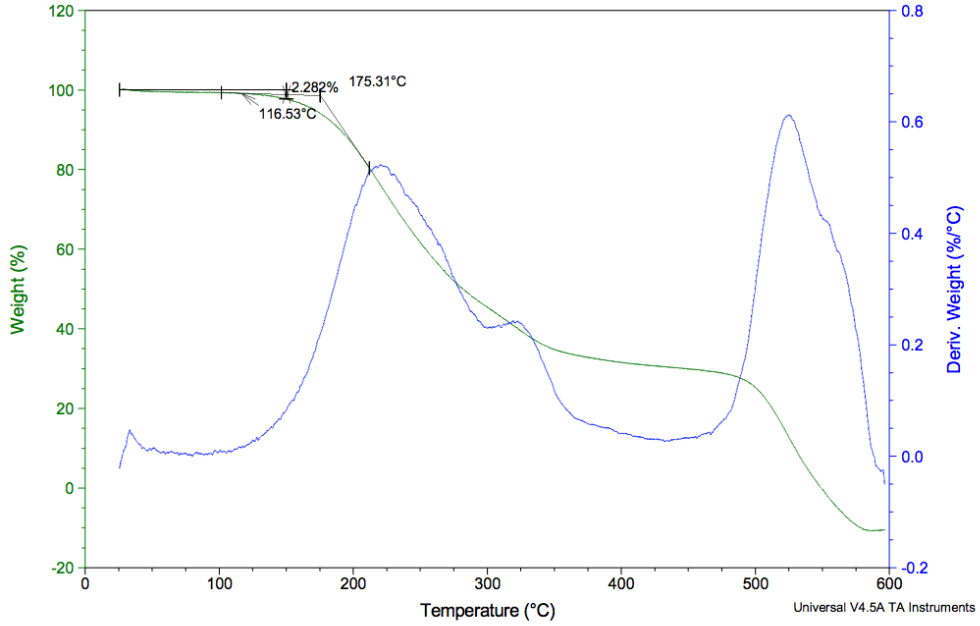

Figure A13. Thermogravimetric analysis (TGA) curve for $[DDMA]_4[CuPcS_4]$.

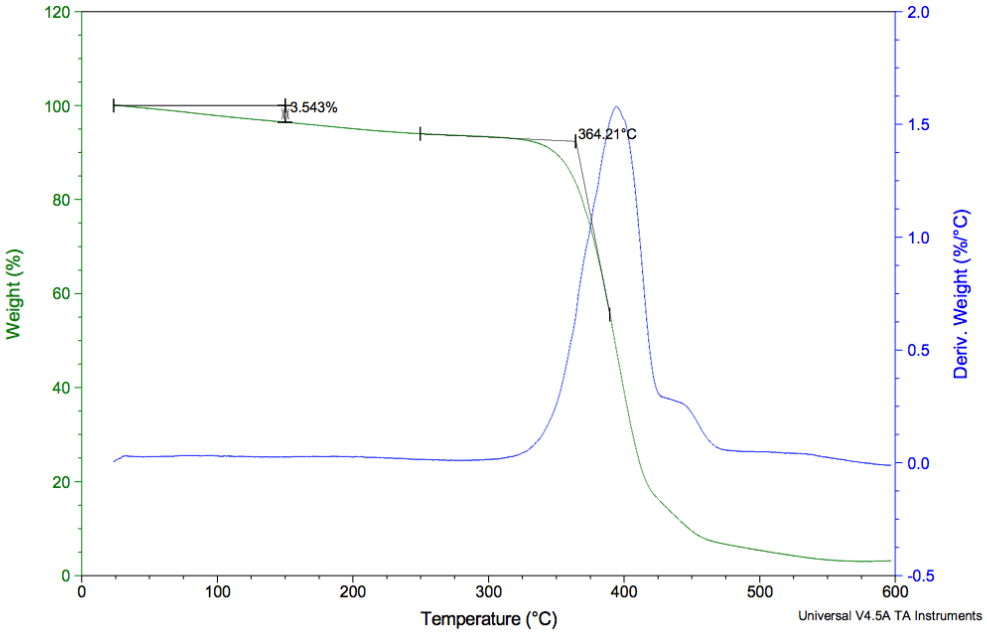

Figure A14. Thermogravimetric analysis (TGA) curve for $[P_{4448}]_4[CuPcS_4]$.

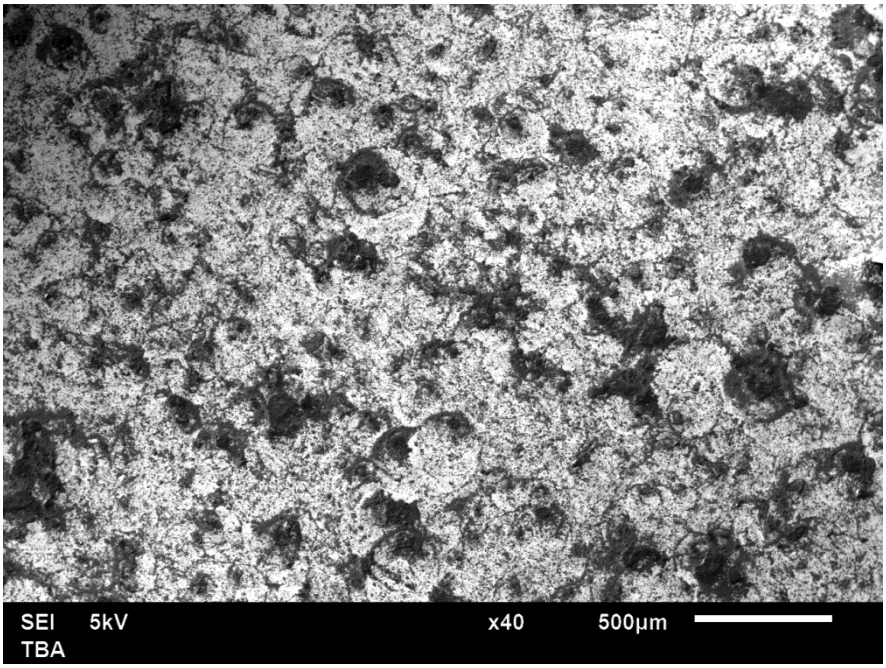

Figure A15. Scanning electron microscopy (SEM) image for $[TBA]_4[CuPcS_4]$.

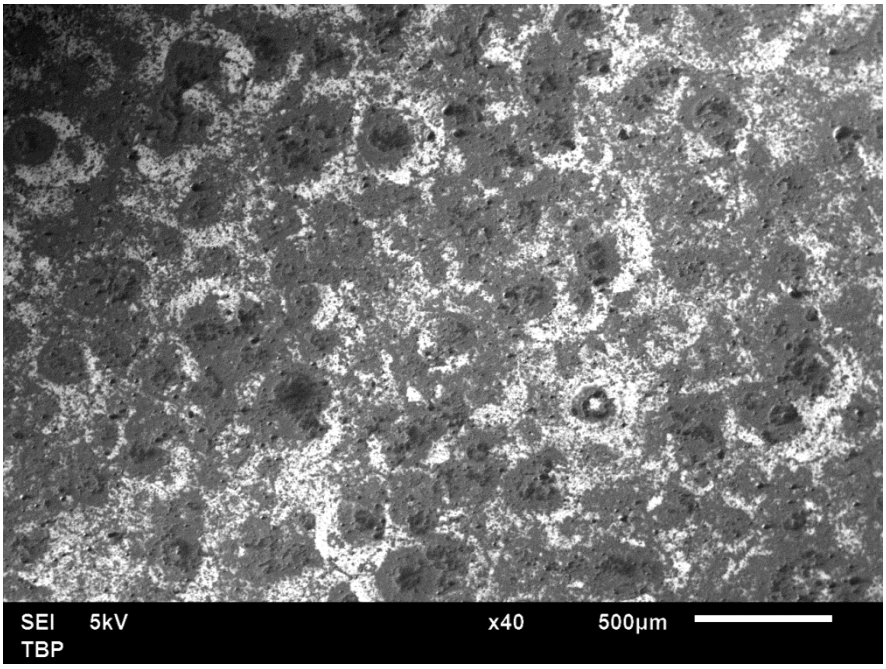

Figure A16. Scanning electron microscopy (SEM) image for $[P_{4444}]_4[CuPcS_4]$.

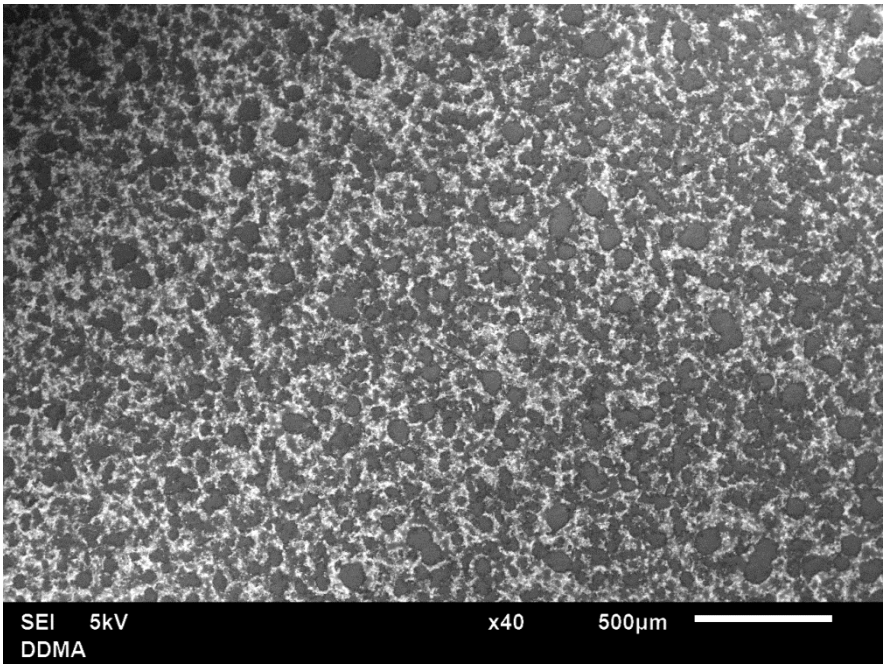

Figure A17. Scanning electron microscopy (SEM) image for $[DDMA]_4[CuPcS_4]$.

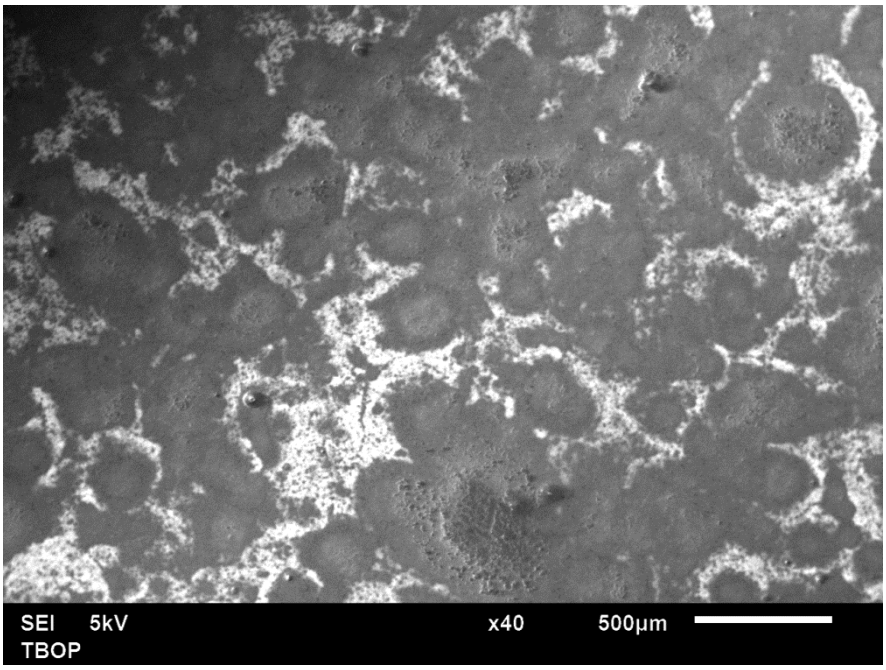

Figure A18. Scanning electron microscopy (SEM) image for $[P_{4448}]_4[CuPcS_4]$.

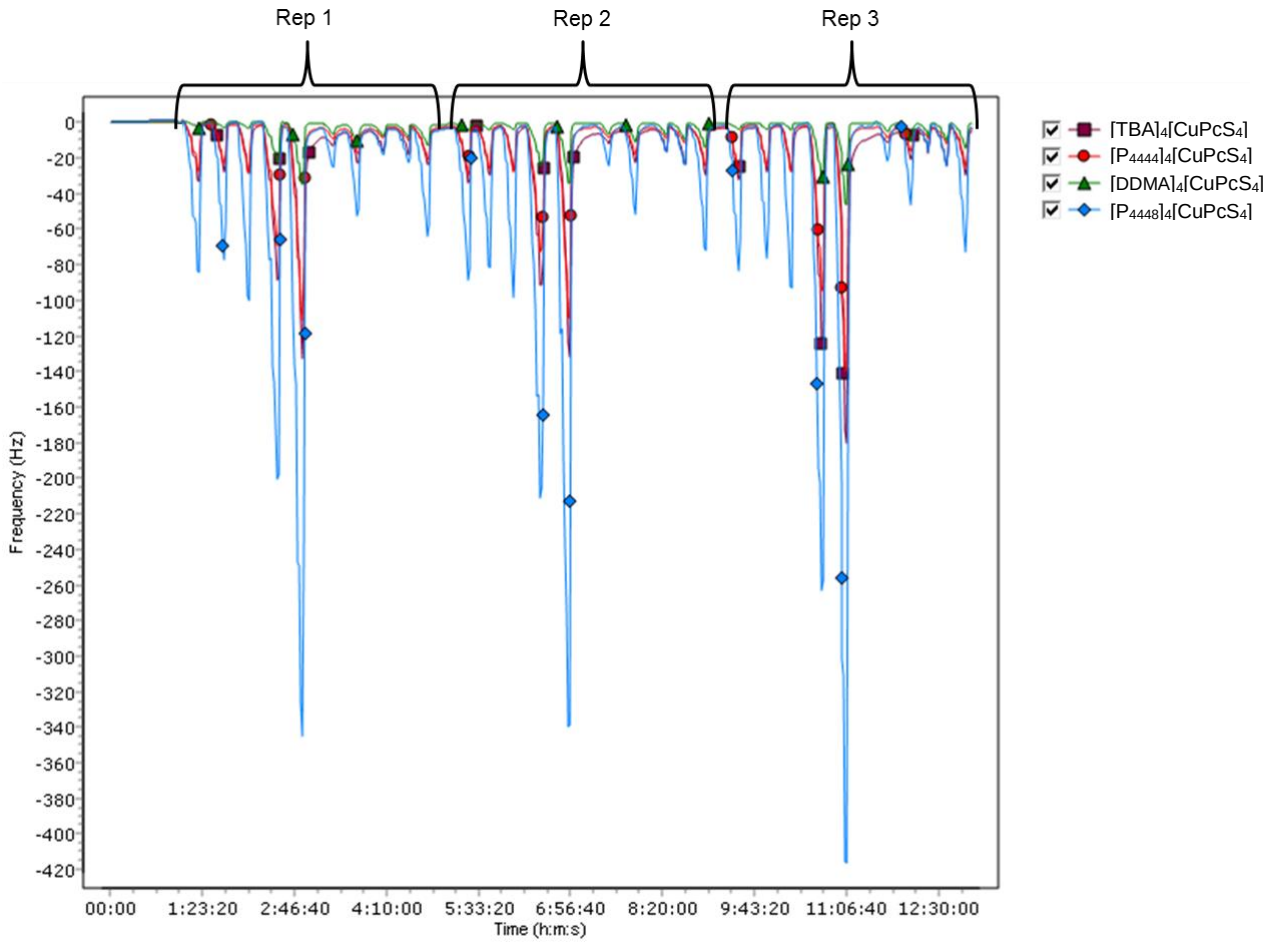

Figure A19. Sensorgram for three replicate measurements of set of ten VOCs at multiple flow ratios for all four sensors.

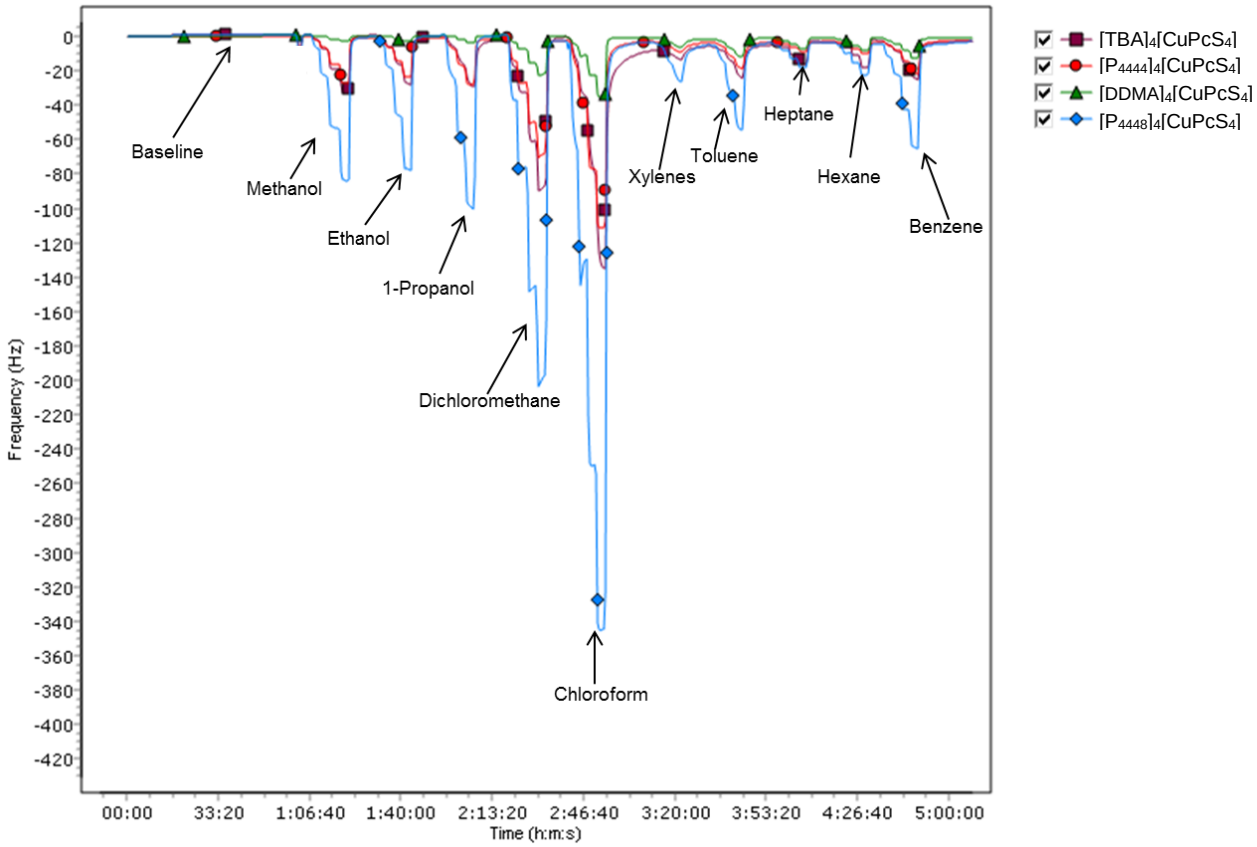

Figure A20. Inset of sensorgram in Fig. S19 for first replicate measurement. Arrows indicate the VOC being measured at multiple flow ratios in 3-minute increments.

Table A1. Analyte concentration ranges.

Class	Analyte	Concentration (mgL^{-1})
***n*-alcohols**	Methanol	41 – 82
	Ethanol	18 – 47
	1-Propanol	8 – 20
Chlorohydrocarbons	Dichloromethane	425 – 861
	Chloroform	161 – 405
Aromatic Hydrocarbons	Xylene	6 – 15
	Toluene	12 – 41
	Benzene	41 – 126
Hydrocarbons	Heptane	20 – 75
	Hexane	88 – 258

Table A2. Summary of calculated sensitivities for all sensors.

Analyte	$[TBA]_4[CuPcS_4]$	$[P_{4444}]_4[CuPcS_4]$	$[DDMA]_4[CuPcS_4]$	$[P_{4448}]_4[CuPcS_4]$
	Sensitivity (Hz/mgL^{-1})	**Sensitivity (Hz/mgL^{-1})**	**Sensitivity (Hz/mgL^{-1})**	**Sensitivity (Hz/mgL^{-1})**
Methanol	0.245	0.662	0.062	0.139
Ethanol	1.046	0.783	0.885	0.700
1-Propanol	2.595	2.221	0.252	2.724
Dichloromethane	0.159	0.134	0.037	0.162
Chloroform	0.362	0.310	0.085	0.635
Xylenes	0.428	0.669	0.555	1.547
Toluene	0.169	0.376	0.218	0.669
Heptane	0.034	0.075	0.071	0.128
Hexane	0.006	0.036	0.032	0.060
Benzene	0.155	0.165	0.087	0.279

Table A3. Summary of calculated detection limits for all sensors.

Analyte	$[TBA]_4[CuPcS_4]$	$[P_{4444}]_4[CuPcS_4]$	$[DDMA]_4[CuPcS_4]$	$[P_{4448}]_4[CuPcS_4]$
	Detection Limit (mgL^{-1})	**Detection Limit (mgL^{-1})**	**Detection Limit (mgL^{-1})**	**Detection Limit (mgL^{-1})**
Methanol	3.79	0.237	5.40	6.35
Ethanol	0.8883	0.201	0.379	1.26
1-Propanol	0.3581	0.0707	1.33	0.324
Dichloromethane	5.85	1.17	9.07	5.45
Chloroform	2.57	0.507	3.93	1.39
Xylenes	2.17	0.235	0.605	0.570
Toluene	5.50	0.418	1.54	1.32
Heptane	27.5	2.10	4.72	6.89
Hexane	147.5	4.41	10.7	14.6
Benzene	5.99	0.951	3.87	3.16

APPENDIX B. SUPPORTING INFORMATION FOR CHAPTER 3

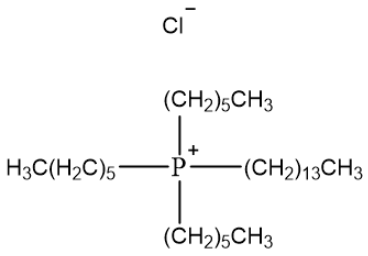

Trihexyltetradecylphosphonium chloride
(P_{66614})

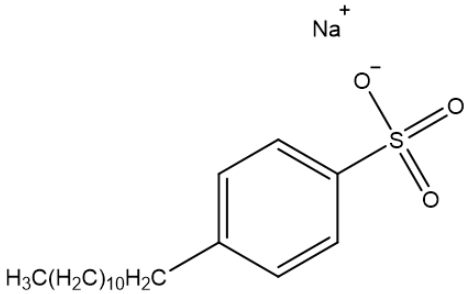

Sodium dodecylbenzenesulfonate (DBS)

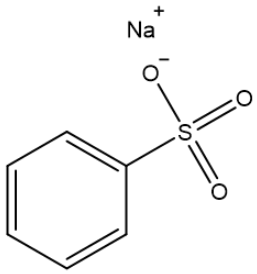

Sodium benzenesulfonate (BS)

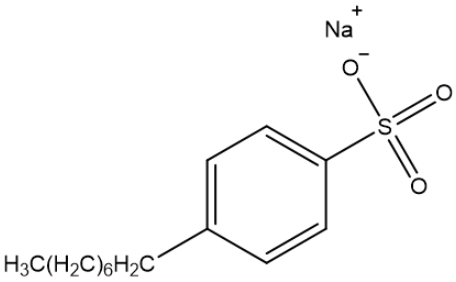

Sodium 4-n-octylbenzenesulfonate
(OBS)

Figure B1. Structures of starting materials used to synthesize ILs.

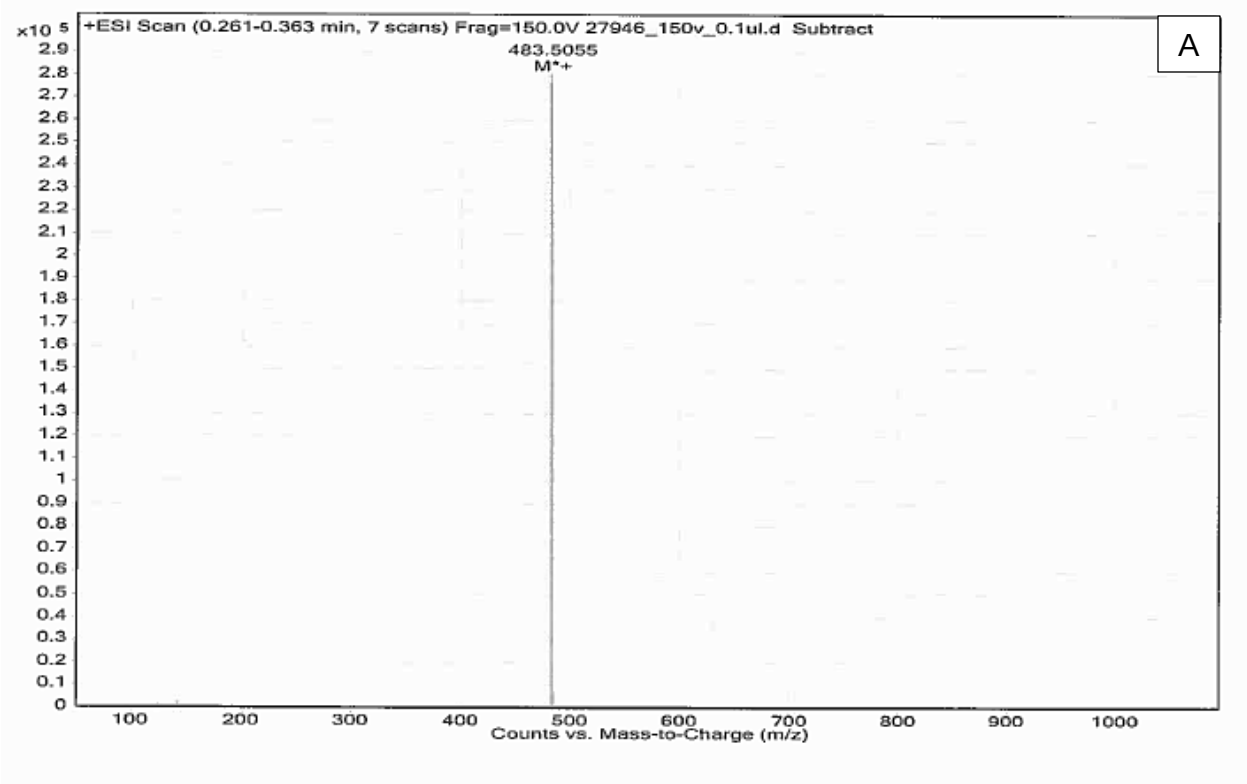

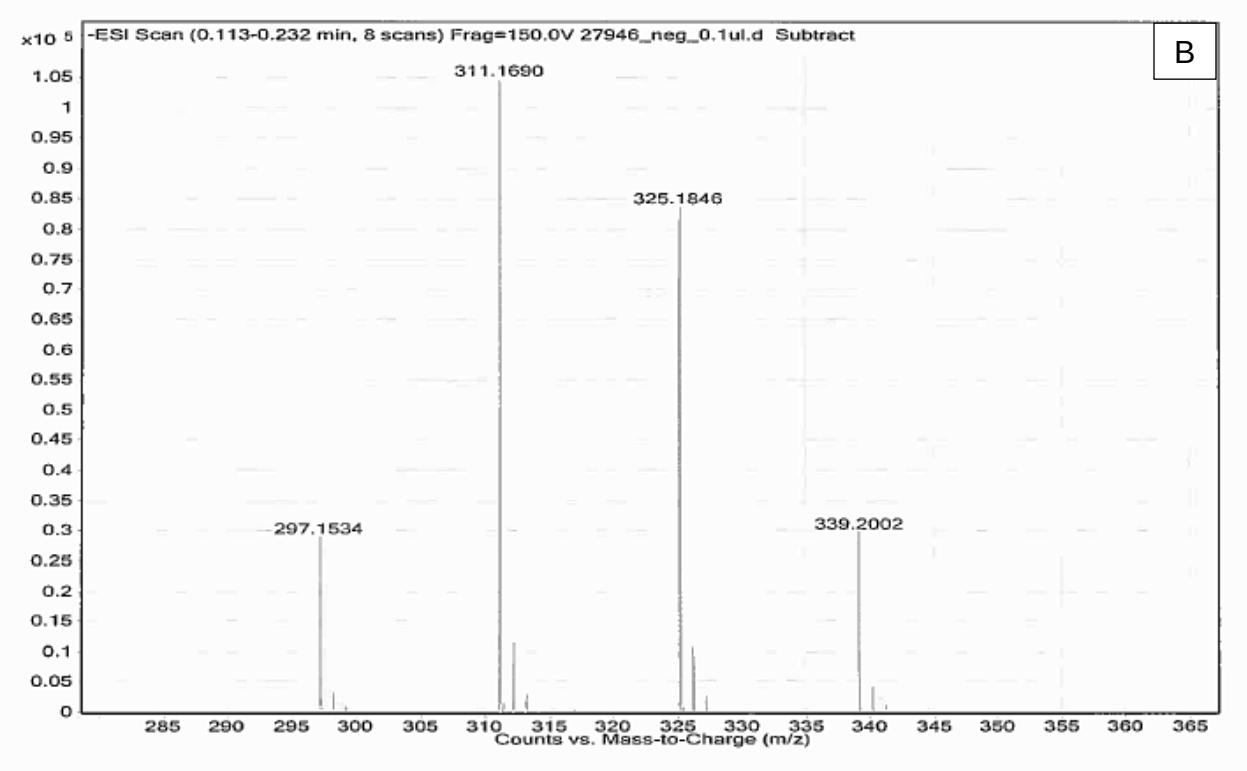

Figure B2. Electrospray ionization mass spectrometry (ESI-MS) spectra for $[P_{66614}][DBS]$, where A) is in positive mode and B) is in negative mode. Solvent used was DCM.

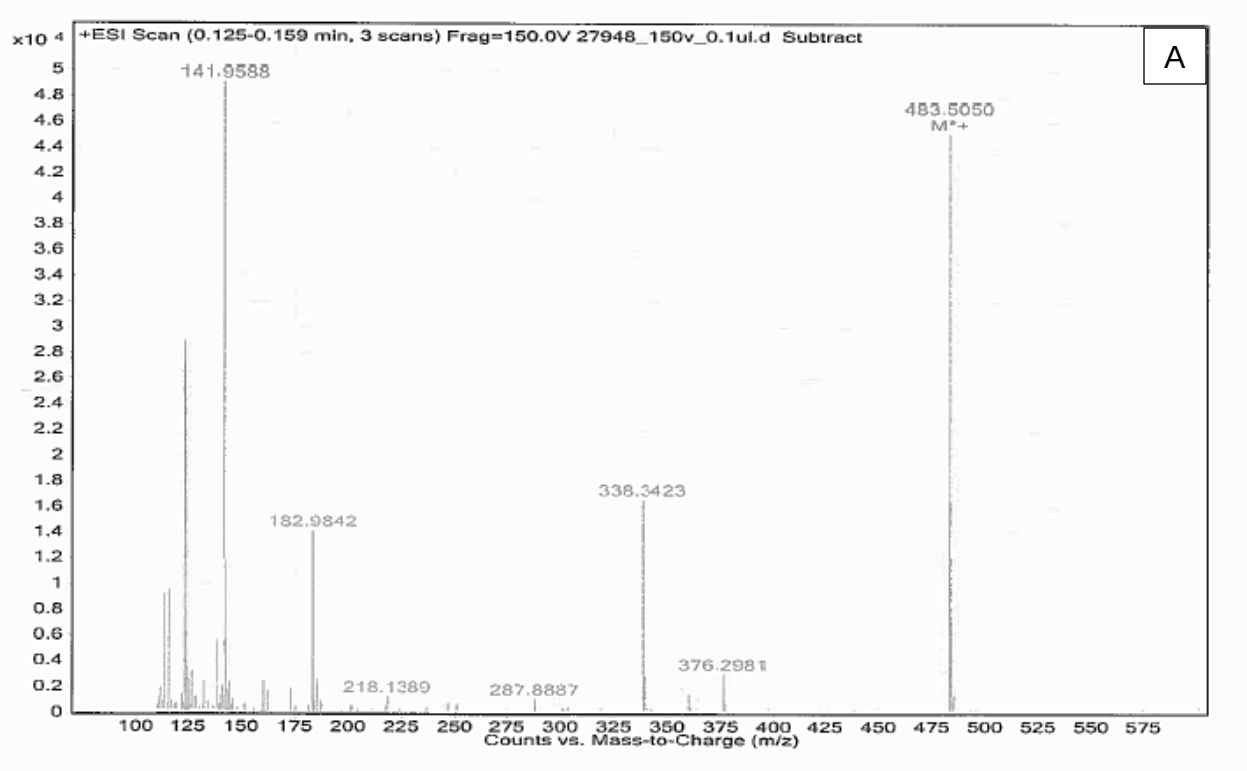

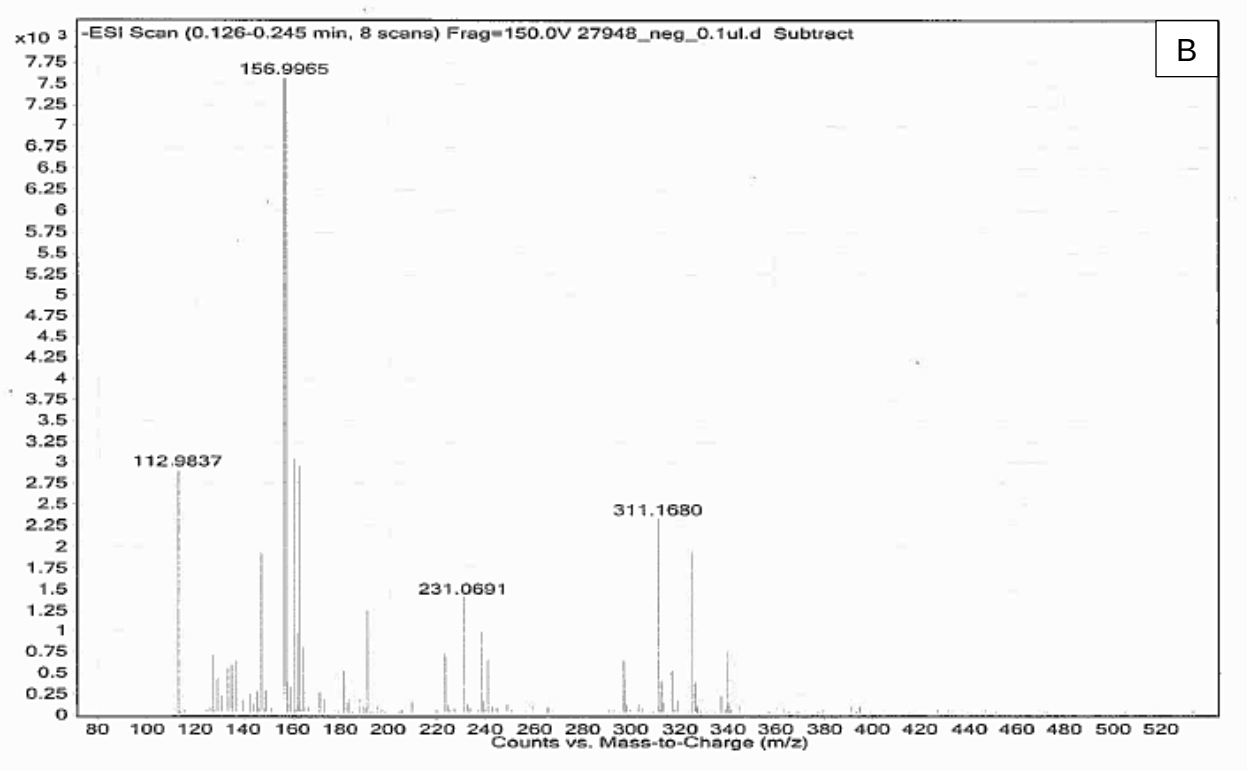

Figure B3. Electrospray ionization mass spectrometry (ESI-MS) spectra for $[P_{66614}][BS]$, where A) is in positive mode and B) is in negative mode. Solvent used was DCM.

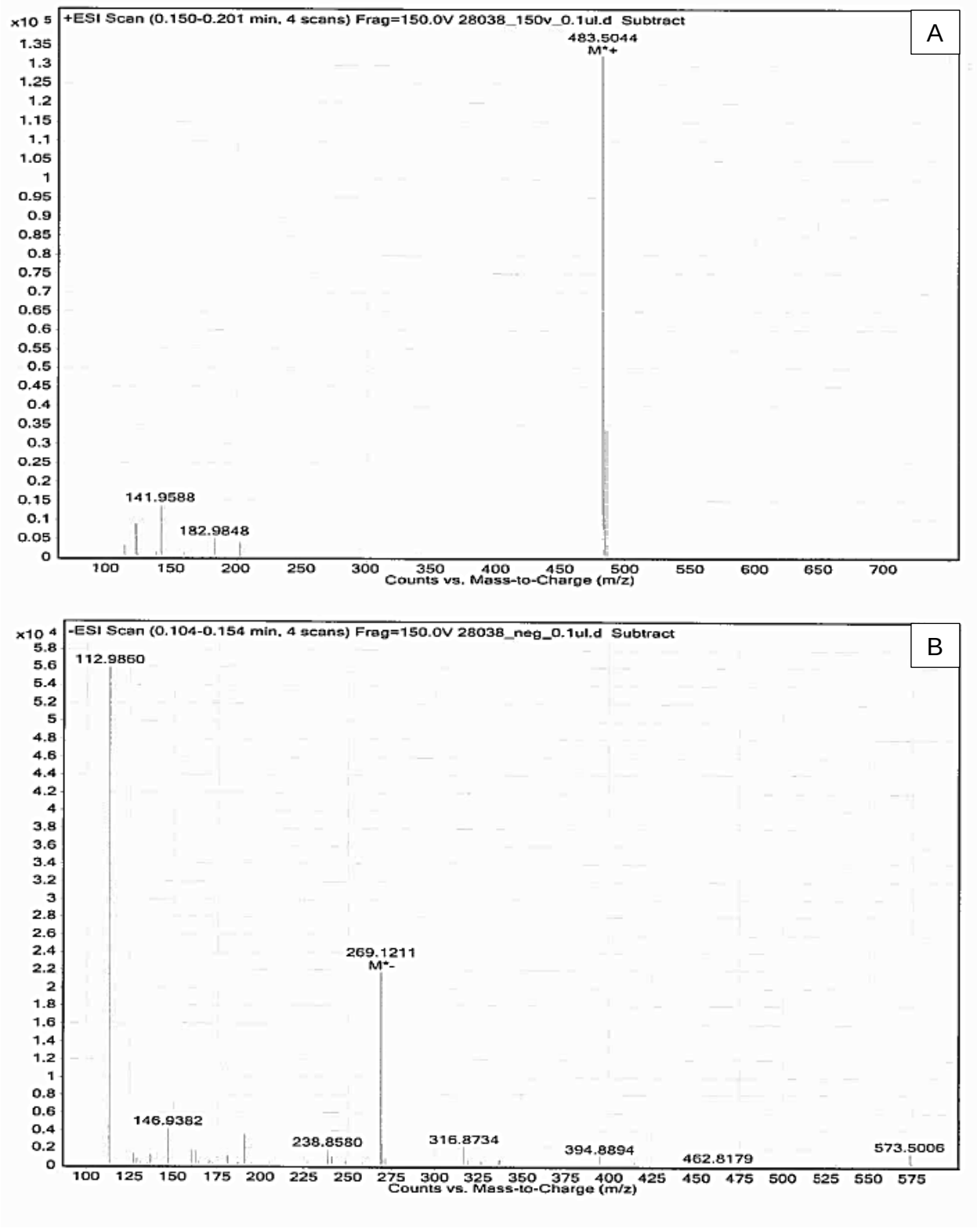

Figure B4. Electrospray ionization mass spectrometry (ESI-MS) spectra for $[P_{66614}][OBS]$, where A) is in positive mode and B) is in negative mode. Solvent used was DCM.

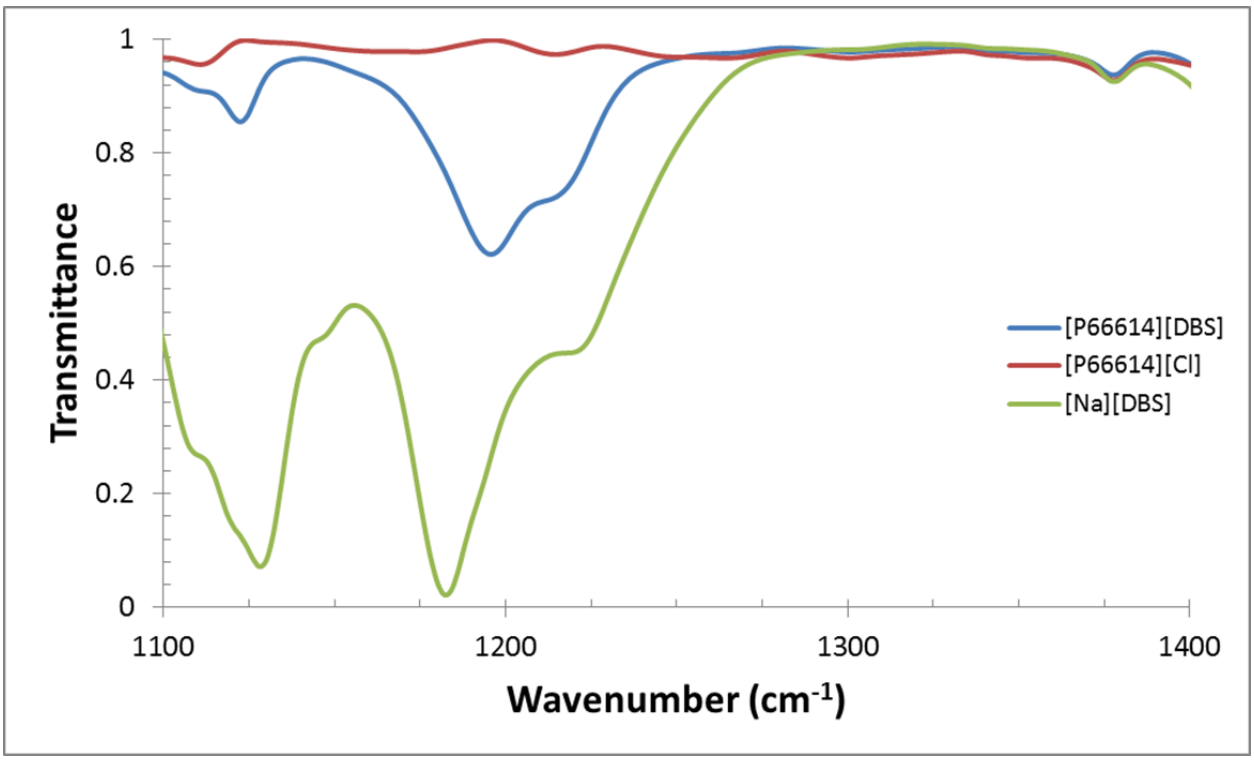

Figure B5. Fourier transform infrared (FT-IR) spectra for [P_{66614}][DBS]. S=O stretching in DBS ~1182 shifts to ~1195 in [P_{66614}][DBS].

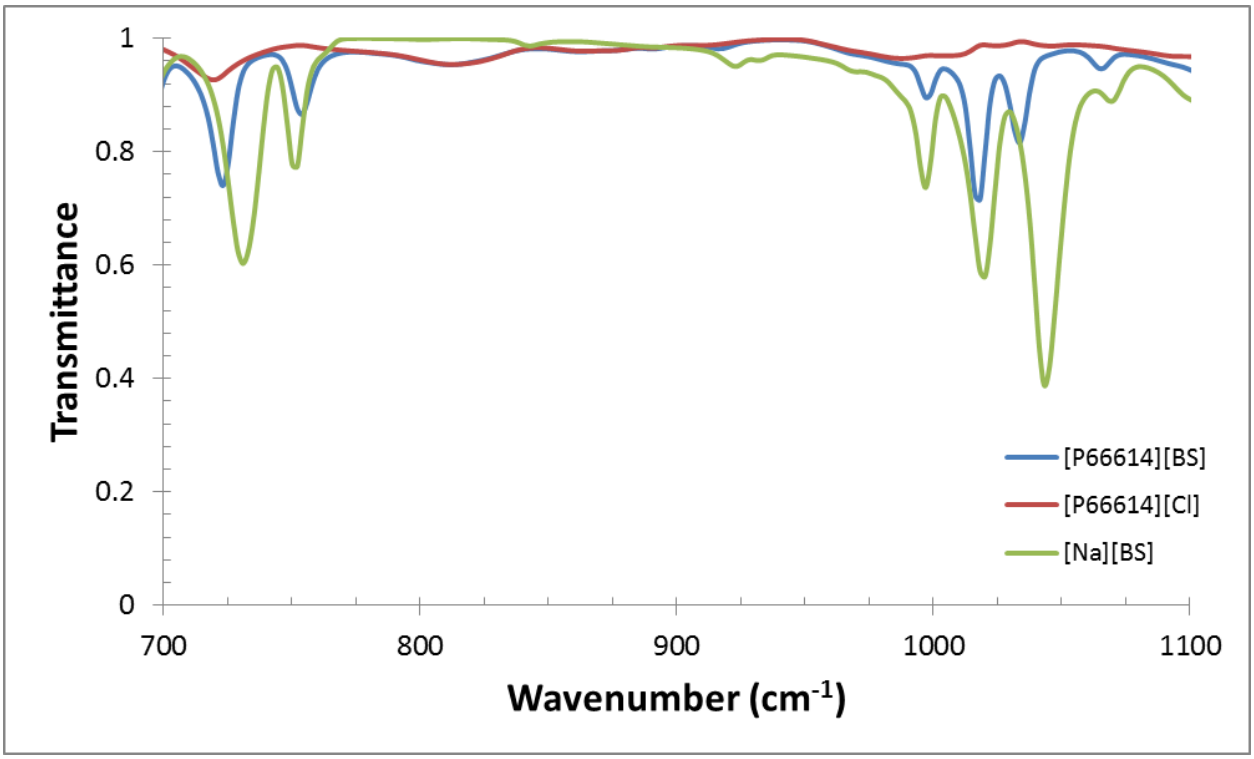

Figure B6. Fourier transform infrared (FT-IR) spectra for [P_{66614}][BS]. S-O stretching in BS ~732 shifts to ~725 and ~750 shifts to ~755 in [P_{66614}][BS].

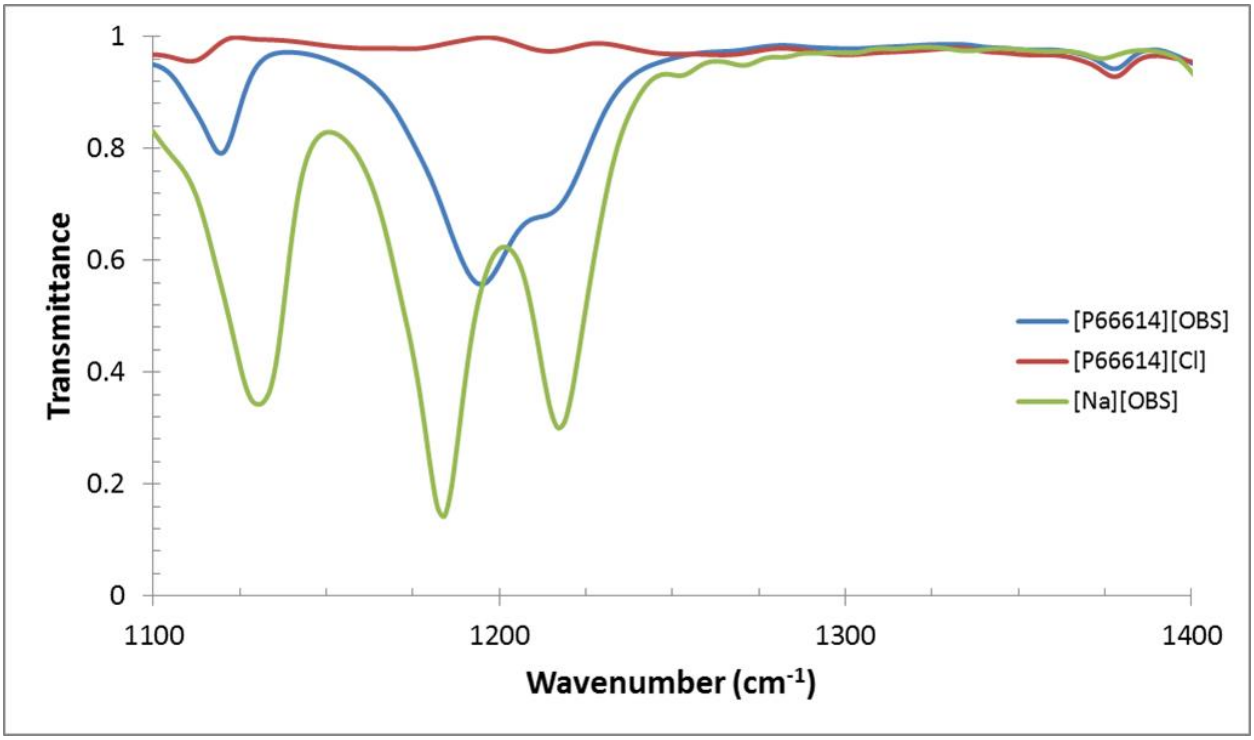

Figure B7. Fourier transform infrared (FT-IR) spectra for $[P_{66614}][OBS]$. S=O stretching in OBS ~1184 shifts to ~1195 in $[P_{66614}][OBS]$.

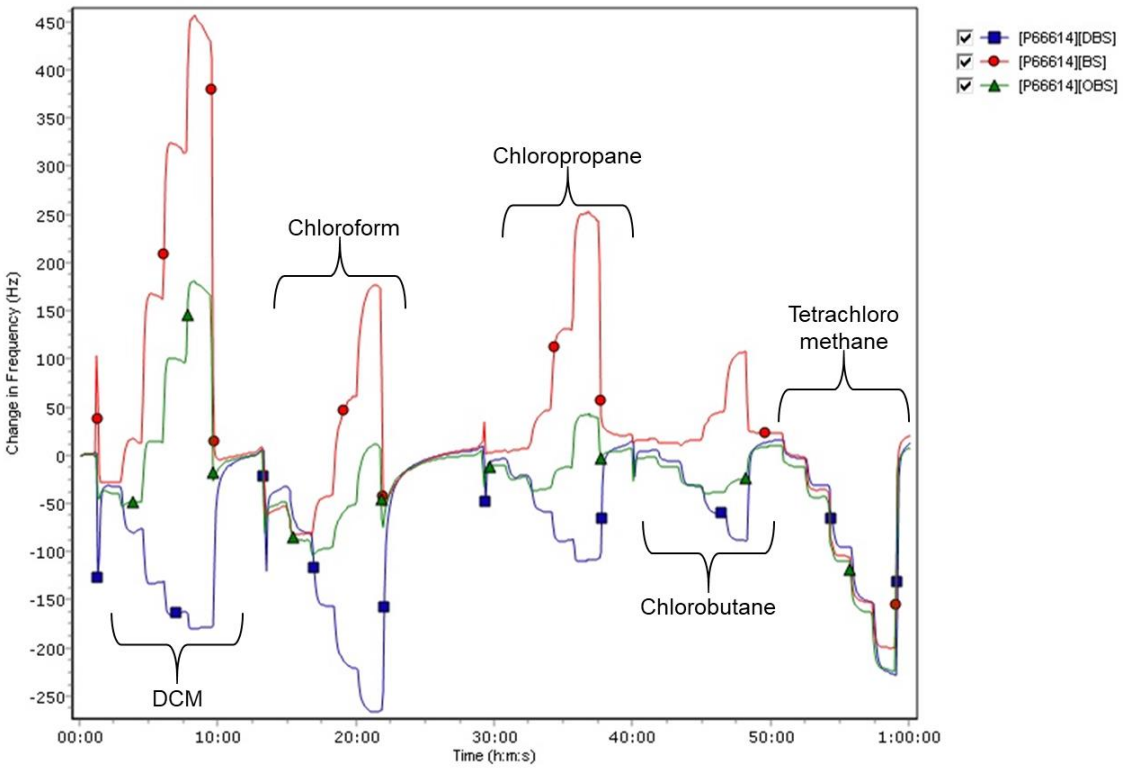

Figure B8. Sensorgram for first replicate measurement. Braces indicate the VOC being measured at multiple flow ratios in 3-minute increments.

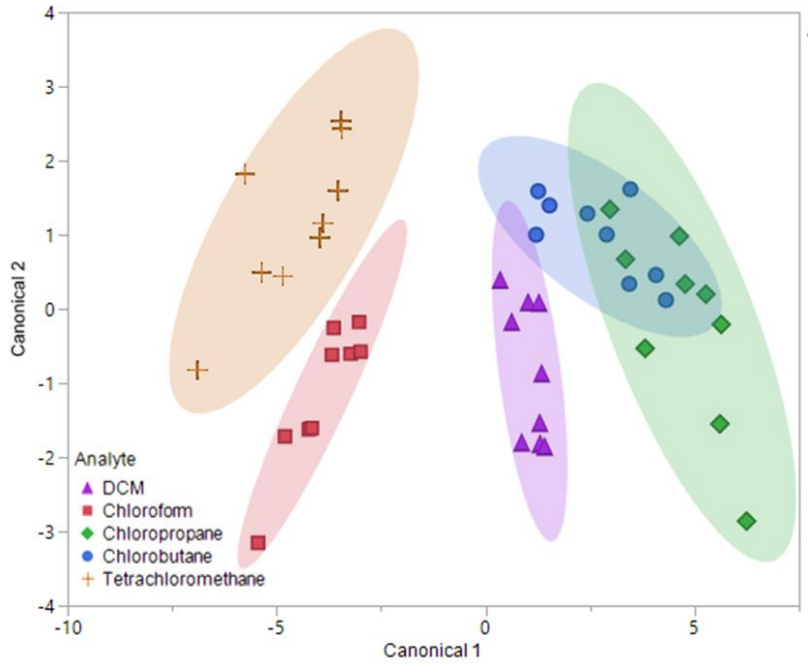

Figure B9. Canonical plot for discrimination of five chlorinated VOCs with respect to a five sensor VSA. Plot considers 45 total measurements consisting of three replicate measurements at three different flow ratios for each VOC (9 measurements per sample) using [P_{66614}][DBS]-PDMS.

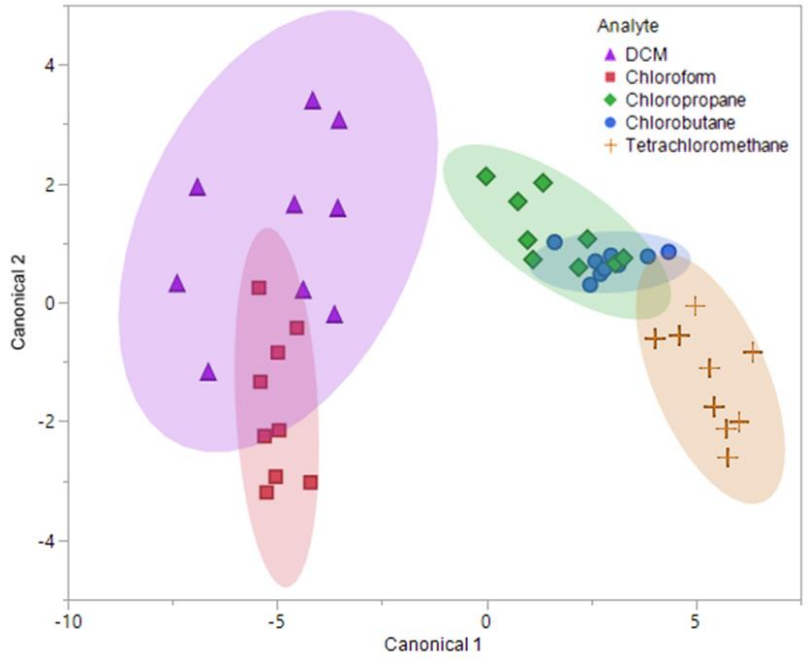

Figure B10. Canonical plot for discrimination of five chlorinated VOCs with respect to a four sensor VSA. Plot considers 45 total measurements consisting of three replicate measurements at three different flow ratios for each VOC (9 measurements per sample) using [P_{66614}][BS]-PDMS.

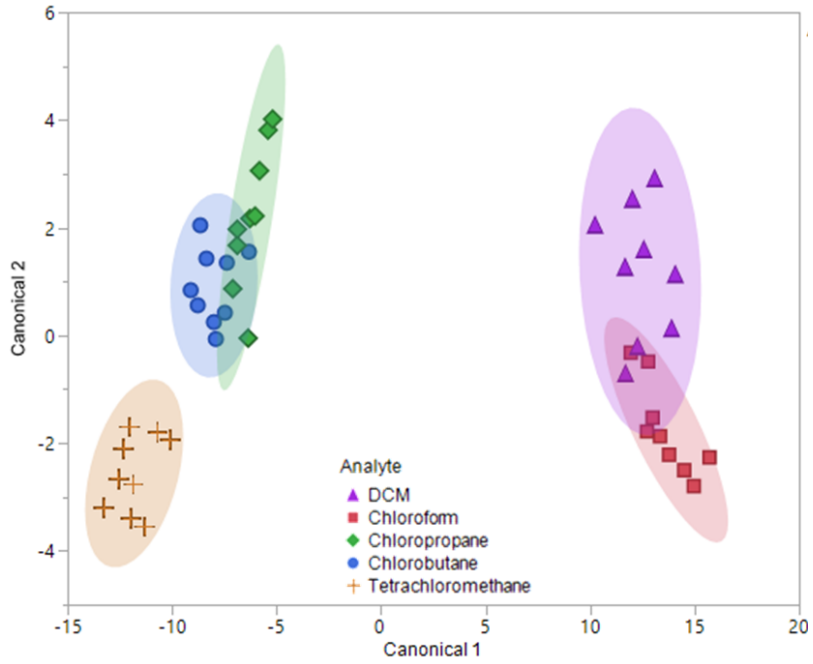

Figure B11. Canonical plot for discrimination of five chlorinated VOCs with respect to a six sensor VSA. Plot considers 45 total measurements consisting of three replicate measurements at three different flow ratios for each VOC (9 measurements per sample) using [P_{66614}][OBS]-PDMS.

APPENDIX C. SUPPORTING INFORMATION FOR CHAPTER 4

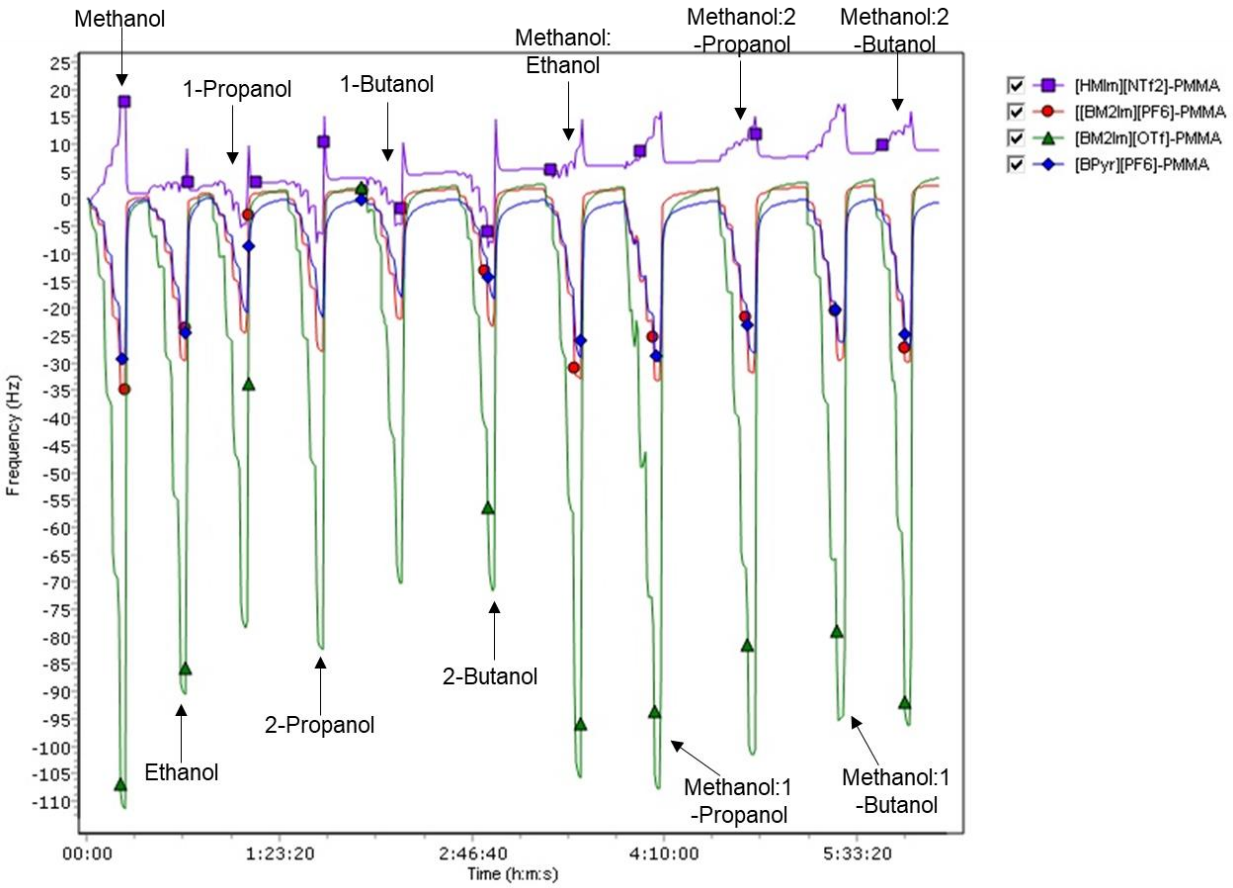

Figure C1. Sensorgram for first replicate measurement. Arrows indicate alcohol sample being measured at multiple flow ratios in 3-minute increments.

LIST OF REFERENCES

1. QCM-D Measurements. https://www.biolinscientific.com/measurements/qcm-d.

2. Volatile Organic Compounds' Impact on Indoor Air Quality. https://www.epa.gov/indoor-air-quality-iaq/volatile-organic-compounds-impact-indoor-air-quality (accessed February).

3. Indoor Air Quality (IAQ) - Technical Overview of Volatile Organic Compounds. https://www.epa.gov/indoor-air-quality-iaq/technical-overview-volatile-organic-compounds#8.

4. Ambient (outdoor) air quality and health. https://www.who.int/news-room/fact-sheets/detail/ambient-(outdoor)-air-quality-and-health.

5. Report on the Environment - Indoor Air Quality. https://www.epa.gov/report-environment/indoor-air-quality#note1.

6. Abdi, H.; Williams, L. J., Principal component analysis. *Wiley interdisciplinary reviews: computational statistics* **2010,** *2* (4), 433-459.

7. Abraham, J. K.; Philip, B.; Witchurch, A.; Varadan, V. K.; Reddy, C. C., A compact wireless gas sensor using a carbon nanotube/PMMA thin film chemiresistor. *Smart Materials and Structures* **2004,** *13* (5), 1045.

8. Adgate, J. L.; Church, T. R.; Ryan, A. D.; Ramachandran, G.; Fredrickson, A. L.; Stock, T. H.; Morandi, M. T.; Sexton, K., Outdoor, indoor, and personal exposure to VOCs in children. *Environmental health perspectives* **2004,** *112* (14), 1386-1392.

9. Agosta, W. C., *Chemical communication: the language of pheromones*. Henry Holt and Company: 1992.

10. Al Ghafly, H.; Siraj, N.; Das, S.; Regmi, B. P.; Magut, P. K. S.; Galpothdeniya, W. I. S.; Murray, K. K.; Warner, I. M., GUMBOS matrices of variable hydrophobicity for matrix-assisted laser desorption/ionization mass spectrometry. *Rapid Communications in Mass Spectrometry* **2014,** *28* (21), 2307-2314.

11. Albert, K. J.; Lewis, N. S.; Schauer, C. L.; Sotzing, G. A.; Stitzel, S. E.; Vaid, T. P.; Walt, D. R., Cross-reactive chemical sensor arrays. *Chemical reviews* **2000,** *100* (7), 2595-2626.

12. Asht, S.; Dass, R., Pattern recognition techniques: A review. *International Journal of Computer Science and Telecommunications* **2012,** *3* (8), 25-29.

13. Ayad, M. M.; Torad, N. L., Alcohol vapours sensor based on thin polyaniline salt film and quartz crystal microbalance. *Talanta* **2009,** *78* (4), 1280-1285.

14. Baldwin, E. A.; Bai, J.; Plotto, A.; Dea, S., Electronic noses and tongues: Applications for the food and pharmaceutical industries. *Sensors* **2011,** *11* (5), 4744-4766.

15. Baldwin, I. T.; Kessler, A.; Halitschke, R., Volatile signaling in plant–plant–herbivore interactions: what is real? *Current opinion in plant biology* **2002,** *5* (4), 351-354.

16. Barié, N.; Bücking, M.; Rapp, M., A novel electronic nose based on miniaturized SAW sensor arrays coupled with SPME enhanced headspace-analysis and its use for rapid determination of volatile organic compounds in food quality monitoring. *Sensors and Actuators B: Chemical* **2006,** *114* (1), 482-488.

17. Bhattarai, N.; Chen, M.; Pérez, R. L.; Ravula, S.; Chhotaray, P.; Hamdan, S.; McDonough, K.; Tiwari, S.; Warner, I. M., Enhanced chemotherapeutic toxicity of cyclodextrin templated size-tunable rhodamine 6G nanoGUMBOS. *Journal of Materials Chemistry B* **2018,** *6* (34), 5451-5459.

18. Bhattarai, N.; Mathis, J. M.; Chen, M.; Pérez, R. L.; Siraj, N.; Magut, P. K. S.; McDonough, K.; Sahasrabudhe, G.; Warner, I. M., Endocytic Selective Toxicity of Rhodamine 6G nanoGUMBOS in Breast Cancer Cells. *Molecular Pharmaceutics* **2018,** *15* (9), 3837-3845.

19. Blackledge, R. D., *Forensic Analysis on the Cutting Edge: New Methods for Trace Evidence Analysis*. Wiley: 2007.

20. Blande, J. D.; Holopainen, J. K.; Li, T., Air pollution impedes plant-to-plant communication by volatiles. *Ecology letters* **2010,** *13* (9), 1172-1181.

21. Bodenhöfer, K.; Hierlemann, A.; Noetzel, G.; Weimar, U.; Göpel, W., Performances of Mass-Sensitive Devices for Gas Sensing: Thickness Shear Mode and Surface Acoustic Wave Transducers. *Analytical Chemistry* **1996,** *68* (13), 2210-2218.

22. Bougharouat, A.; Bellel, A.; Sahli, S.; Ségui, Y.; Raynaud, P., Plasma polymerization of TEOS for QCM-based VOC vapor sensing. *The European Physical Journal - Applied Physics* **2011,** *56* (2), 24017.

23. Brennecke, J. F.; Maginn, E. J., Ionic liquids: Innovative fluids for chemical processing. *AIChE Journal* **2001,** *47* (11), 2384-2389.

24. Brunner, C.; Szymczak, W.; Höllriegl, V.; Mörtl, S.; Oelmez, H.; Bergner, A.; Huber, R.; Hoeschen, C.; Oeh, U., Discrimination of cancerous and non-cancerous cell lines by headspace-analysis with PTR-MS. *Analytical and bioanalytical chemistry* **2010,** *397* (6), 2315-2324.

25. Bunte, G.; Hürttlen, J.; Pontius, H.; Hartlieb, K.; Krause, H., Gas phase detection of explosives such as 2,4,6-trinitrotoluene by molecularly imprinted polymers. *Analytica Chimica Acta* **2007,** *591* (1), 49-56.

26. Burrell, A. K.; Del Sesto, R. E.; Baker, S. N.; McCleskey, T. M.; Baker, G. A., The large scale synthesis of pure imidazolium and pyrrolidinium ionic liquids. *Green Chemistry* **2007,** *9* (5), 449-454.

27. Bwambok, D. K.; El-Zahab, B.; Challa, S. K.; Li, M.; Chandler, L.; Baker, G. A.; Warner, I. M., Near-Infrared Fluorescent NanoGUMBOS for Biomedical Imaging. *ACS Nano* **2009,** *3* (12), 3854-3860.

28. Capan, I.; Tarımcı, Ç.; Capan, R., Fabrication of Langmuir–Blodgett thin films of porphyrins and investigation on their gas sensing properties. *Sensors and Actuators B: Chemical* **2010,** *144* (1), 126-130.

29. Capone, S.; Epifani, M.; Quaranta, F.; Siciliano, P.; Taurino, A.; Vasanelli, L., Monitoring of rancidity of milk by means of an electronic nose and a dynamic PCA analysis. *Sensors and Actuators B: Chemical* **2001,** *78* (1-3), 174-179.

30. Chao, C. Y.; Chan, G. Y., Quantification of indoor VOCs in twenty mechanically ventilated buildings in Hong Kong. *Atmospheric Environment* **2001,** *35* (34), 5895-5913.

31. Chen, M.; Bhattarai, N.; Cong, M.; Pérez, R. L.; McDonough, K. C.; Warner, I. M., Mitochondria targeting IR780-based nanoGUMBOS for enhanced selective toxicity towards cancer cells. *RSC Advances* **2018,** *8* (55), 31700-31709.

32. Chen, X.; Cao, M.; Li, Y.; Hu, W.; Wang, P.; Ying, K.; Pan, H., A study of an electronic nose for detection of lung cancer based on a virtual SAW gas sensors array and imaging recognition method. *Meas Sci Technol* **2005,** *16* (8), 1535.

33. Cheng, N.; Zhang, L.; Joon Kim, J.; Andrew, T. L., Vapor phase organic chemistry to deposit conjugated polymer films on arbitrary substrates. *Journal of Materials Chemistry C* **2017,** *5* (23), 5787-5796.

34. Delgado-Rodríguez, M.; Ruiz-Montoya, M.; Giraldez, I.; López, R.; Madejón, E.; Díaz, M. J., Use of electronic nose and GC-MS in detection and monitoring some VOC. *Atmospheric Environment* **2012,** *51*, 278-285.

35. DeNolf, G. C.; Haack, L.; Holubka, J.; Straccia, A.; Blohowiak, K.; Broadbent, C.; Shull, K. R., High Frequency Rheometry of Viscoelastic Coatings with the Quartz Crystal Microbalance. *Langmuir* **2011,** *27* (16), 9873-9879.

36. Derwent, R. G., Sources, distributions, and fates of VOCs in the atmosphere. In *Volatile Organic Compounds in the Atmosphere*, Hester, R. E.; Harrison, R. M., Eds. The Royal Society of Chemistry: 1995; Vol. 4, pp 1-16.

37. Di Natale, C.; Macagnano, A.; Martinelli, E.; Paolesse, R.; D'Arcangelo, G.; Roscioni, C.; Finazzi-Agro, A.; D'Amico, A., Lung cancer identification by the analysis of breath by means of an array of non-selective gas sensors. *Biosensors and Bioelectronics* **2003,** *18* (10), 1209-1218.

38. Drafts, B., Acoustic wave technology sensors. *IEEE Transactions on microwave theory and techniques* **2001,** *49* (4), 795-802.

39. Earle Martyn, J.; Seddon Kenneth, R., Ionic liquids. Green solvents for the future. In *Pure and Applied Chemistry*, 2000; Vol. 72, p 1391.

40. Egashira, M.; Shimizu, Y., Odor sensing by semiconductor metal oxides. *Sensors and Actuators B: Chemical* **1993,** *13* (1-3), 443-446.

41. Elosua, C.; Matias, I. R.; Bariain, C.; Arregui, F. J., Volatile organic compound optical fiber sensors: A review. *Sensors* **2006,** *6* (11), 1440-1465.

42. Ewing, R. G.; Atkinson, D. A.; Clowers, B. H., Direct real-time detection of RDX vapors under ambient conditions. *Analytical chemistry* **2012,** *85* (1), 389-397.

43. Ewing, R. G.; Clowers, B. H.; Atkinson, D. A., Direct real-time detection of vapors from explosive compounds. *Analytical chemistry* **2013,** *85* (22), 10977-10983.

44. Faiola, C.; Erickson, M.; Fricaud, V.; Jobson, B.; VanReken, T., Quantification of biogenic volatile organic compounds with a flame ionization detector using the effective carbon number concept. *Atmospheric Measurement Techniques (Online)* **2012,** *5* (8).

45. Fan, X.; Du, B., Selective detection of trace p-xylene by polymer-coated QCM sensors. *Sensors and Actuators B: Chemical* **2012,** *166*, 753-760.

46. Fanget, S.; Hentz, S.; Puget, P.; Arcamone, J.; Matheron, M.; Colinet, E.; Andreucci, P.; Duraffourg, L.; Myers, E.; Roukes, M. L., Gas sensors based on gravimetric detection—A review. *Sensors and Actuators B: Chemical* **2011,** *160* (1), 804-821.

47. Fens, N.; Schee, M.; Brinkman, P.; Sterk, P., Exhaled breath analysis by electronic nose in airways disease. Established issues and key questions. *Clinical & Experimental Allergy* **2013,** *43* (7), 705-715.

48. Fu, Y.; Finklea, H. O., Quartz Crystal Microbalance Sensor for Organic Vapor Detection Based on Molecularly Imprinted Polymers. *Analytical Chemistry* **2003,** *75* (20), 5387-5393.

49. Galpothdeniya, W. I. S.; Fronczek, F. R.; Cong, M.; Bhattarai, N.; Siraj, N.; Warner, I. M., Tunable GUMBOS-based sensor array for label-free detection and discrimination of proteins. *Journal of Materials Chemistry B* **2016,** *4* (8), 1414-1422.

50. Galpothdeniya, W. I. S.; McCarter, K. S.; De Rooy, S. L.; Regmi, B. P.; Das, S.; Hasan, F.; Tagge, A.; Warner, I. M., Ionic liquid-based optoelectronic sensor arrays for chemical detection. *RSC Advances* **2014,** *4* (14), 7225-7234.

51. Gardner, J. W.; Bartlett, P. N., A brief history of electronic noses. *Sensors and Actuators B: Chemical* **1994,** *18* (1), 210-211.

52. Gardner, J. W.; Bartlett, P. N., Electronic noses. Principles and applications. IOP Publishing: 2000.

53. Guenther, A.; Hewitt, C. N.; Erickson, D.; Fall, R.; Geron, C.; Graedel, T.; Harley, P.; Klinger, L.; Lerdau, M.; McKay, W., A global model of natural volatile organic compound emissions. *Journal of Geophysical Research: Atmospheres* **1995,** *100* (D5), 8873-8892.

54. Hatfield, J.; Neaves, P.; Hicks, P.; Persaud, K.; Travers, P., Towards an integrated electronic nose using conducting polymer sensors. *Sensors and Actuators B: Chemical* **1994,** *18* (1-3), 221-228.

55. Heywang, W.; Lubitz, K.; Wersing, W., *Piezoelectricity: Evolution and Future of a Technology*. Springer Berlin Heidelberg: 2008.

56. Hierlemann, A.; Weimar, U.; Kraus, G.; Schweizer-Berberich, M.; Göpel, W., Polymer-based sensor arrays and multicomponent analysis for the detection of hazardous oragnic vapours in the environment. *Sensors and Actuators B: Chemical* **1995,** *26* (1-3), 126-134.

57. Holbrey, J. D.; Seddon, K. R., Ionic Liquids. *Clean Products and Processes* **1999,** *1* (4), 223-236.

58. Holloway, A. F.; Nabok, A.; Thompson, M.; Ray, A. K.; Wilkop, T., Impedance analysis of the thickness shear mode resonator for organic vapour sensing. *Sensors and Actuators B: Chemical* **2004,** *99* (2), 355-360.

59. Hu, Z.; Deibert, B. J.; Li, J., Luminescent metal–organic frameworks for chemical sensing and explosive detection. *Chemical Society Reviews* **2014,** *43* (16), 5815-5840.

60. Hu, Z.; Pramanik, S.; Tan, K.; Zheng, C.; Liu, W.; Zhang, X.; Chabal, Y. J.; Li, J., Selective, sensitive, and reversible detection of vapor-phase high explosives via two-dimensional mapping: A new strategy for MOF-based sensors. *Crystal Growth & Design* **2013,** *13* (10), 4204-4207.

61. Jackson, D. S.; Crockett, D. F.; Wolnik, K. A., The indirect detection of bleach (sodium hypochlorite) in beverages as evidence of product tampering. *Journal of forensic sciences* **2006,** *51* (4), 827-831.

62. Jaffe, H.; Berlincourt, D., Piezoelectric transducer materials. *Proceedings of the IEEE* **1965,** *53* (10), 1372-1386.

63. Janzen, M. C.; Ponder, J. B.; Bailey, D. P.; Ingison, C. K.; Suslick, K. S., Colorimetric Sensor Arrays for Volatile Organic Compounds. *Analytical Chemistry* **2006,** *78* (11), 3591-3600.

64. Jin, X.; Yu, L.; Garcia, D.; Ren, R. X.; Zeng, X., Ionic liquid high-temperature gas sensor array. *Analytical chemistry* **2006,** *78* (19), 6980-6989.

65. Johannsmann, D., Viscoelastic, mechanical, and dielectric measurements on complex samples with the quartz crystal microbalance. *Physical Chemistry Chemical Physics* **2008,** *10* (31), 4516-4534.

66. Johannsmann, D., *The Quartz Crystal Microbalance in Soft Matter Research*. Springer International Publishing Switzerland, 2015.

67. Johannsmann, D.; Reviakine, I.; Richter, R. P., Dissipation in films of adsorbed nanospheres studied by quartz crystal microbalance (QCM). *Analytical chemistry* **2009,** *81* (19), 8167-8176.

68. Jordan, A. N.; Das, S.; Siraj, N.; de Rooy, S. L.; Li, M.; El-Zahab, B.; Chandler, L.; Baker, G. A.; Warner, I. M., Anion-controlled morphologies and spectral features of cyanine-based nanoGUMBOS – an improved photosensitizer. *Nanoscale* **2012,** *4* (16), 5031-5038.

69. KALCHENKO, V. I.; KOSHETS, I. A.; MATSAS, E. P.; KOPYLOV, O. N.; SOLOVYOV, A.; KAZANTSEVA, Z. I.; SHIRSHOV, Y. M., Calixarene-based QCM sensors array and its response to volatile organic vapours *Materials Science* **2002,** *20* (3), 73-88.

70. Kampa, M.; Castanas, E., Human health effects of air pollution. *Environmental pollution* **2008,** *151* (2), 362-367.

71. Kanda, K.; Maekawa, T., Development of a WO 3 thick-film-based sensor for the detection of VOC. *Sensors and Actuators B: Chemical* **2005,** *108* (1), 97-101.

72. Kansal, A., Sources and reactivity of NMHCs and VOCs in the atmosphere: A review. *Journal of hazardous materials* **2009,** *166* (1), 17-26.

73. Kern, W., The evolution of silicon wafer cleaning technology. *J Electrochem Soc* **1990,** *137* (6), 1887-1892.

74. Kesselmeier, J.; Staudt, M., Biogenic volatile organic compounds (VOC): an overview on emission, physiology and ecology. *Journal of atmospheric chemistry* **1999,** *33* (1), 23-88.

75. Kessler, A.; Baldwin, I. T., Defensive function of herbivore-induced plant volatile emissions in nature. *Science* **2001,** *291* (5511), 2141-2144.

76. Kikuchi, M.; Tsuru, N.; Shiratori, S., Recognition of terpenes using molecular imprinted polymer coated quartz crystal microbalance in air phase. *Science and Technology of Advanced Materials* **2006,** *7* (2), 156-161.

77. Kolic, P. E.; Siraj, N.; Cong, M.; Regmi, B. P.; Luan, X.; Wang, Y.; Warner, I. M., Improving energy relay dyes for dye-sensitized solar cells by use of a group of uniform materials based on organic salts (GUMBOS). *RSC Advances* **2016,** *6* (97), 95273-95282.

78. Koshets, I. A.; Kazantseva, Z. I.; Shirshov, Y. M.; Cherenok, S. A.; Kalchenko, V. I., Calixarene films as sensitive coatings for QCM-based gas sensors. *Sensors and Actuators B: Chemical* **2005,** *106* (1), 177-181.

79. Kouch, T. Know the Air You're Breathing: Volatile Organic Compounds. http://www.critical-environment.com/blog/know-the-air-you%E2%80%99re-breathing-volatile-organic-compound-2-of-4/ (accessed January 20).

80. Kulkarni, P. S.; Branco, L. C.; Crespo, J. G.; Nunes, M. C.; Raymundo, A.; Afonso, C. A. M., Comparison of Physicochemical Properties of New Ionic Liquids Based on Imidazolium, Quaternary Ammonium, and Guanidinium Cations. *Chemistry – A European Journal* **2007,** *13* (30), 8478-8488.

81. Kurosawa, S.; Kamo, N.; Matsui, D.; Kobatake, Y., Gas sorption to plasma-polymerized copper phthalocyanine film formed on a piezoelectric crystal. *Analytical Chemistry* **1990,** *62* (4), 353-359.

82. Liang, C.; Yuan, C.-Y.; Warmack, R. J.; Barnes, C. E.; Dai, S., Ionic Liquids: A New Class of Sensing Materials for Detection of Organic Vapors Based on the Use of a Quartz Crystal Microbalance. *Analytical Chemistry* **2002,** *74* (9), 2172-2176.

83. Liao, H.-C.; Hsu, C.-P.; Wu, M.-C.; Lu, C.-F.; Su, W.-F., Conjugated Polymer/Nanoparticles Nanocomposites for High Efficient and Real-Time Volatile Organic Compounds Sensors. *Analytical chemistry* **2013,** *85* (19), 9305-9311.

84. Lin, H.; Suslick, K. S., A colorimetric sensor array for detection of triacetone triperoxide vapor. *Journal of the American Chemical Society* **2010,** *132* (44), 15519-15521.

85. Liu, Y.-L.; Tseng, M.-C.; Chu, Y.-H., Sensing ionic liquids for chemoselective detection of acyclic and cyclic ketone gases. *Chemical Communications* **2013,** *49* (25), 2560-2562.

86. Lonergan, M. C.; Severin, E. J.; Doleman, B. J.; Beaber, S. A.; Grubbs, R. H.; Lewis, N. S., Array-based vapor sensing using chemically sensitive, carbon black−polymer resistors. *Chemistry of Materials* **1996,** *8* (9), 2298-2312.

87. Machado, R. F.; Laskowski, D.; Deffenderfer, O.; Burch, T.; Zheng, S.; Mazzone, P. J.; Mekhail, T.; Jennings, C.; Stoller, J. K.; Pyle, J., Detection of lung cancer by sensor array analyses of exhaled breath. *American journal of respiratory and critical care medicine* **2005,** *171* (11), 1286-1291.

88. Magnusdottir, K.; Kristinsson, J.; Jóhannesson, B., Adulterated alcoholic beverages. *Laeknabladid* **2010,** *96* (10), 626-628.

89. Magut, P. K. S.; Das, S.; Fernand, V. E.; Losso, J.; McDonough, K.; Naylor, B. M.; Aggarwal, S.; Warner, I. M., Tunable Cytotoxicity of Rhodamine 6G via Anion Variations. *Journal of the American Chemical Society* **2013,** *135* (42), 15873-15879.

90. Matsuguchi, M.; Uno, T., Molecular imprinting strategy for solvent molecules and its application for QCM-based VOC vapor sensing. *Sensors and Actuators B: Chemical* **2006,** *113* (1), 94-99.

91. Matsumoto, N.; Elder, M.; Ogihara, A., Japan's policy to reduce emissions of volatile organic compounds: factors that facilitate industry participation in voluntary actions. *Journal of Cleaner Production* **2015,** *108*, 931-943.

92. Mazzone, P. J.; Hammel, J.; Dweik, R.; Na, J.; Czich, C.; Laskowski, D.; Mekhail, T., Diagnosis of lung cancer by the analysis of exhaled breath with a colorimetric sensor array. *Thorax* **2007,** *62* (7), 565-568.

93. McConnell, V. D.; Schwab, R. M., The impact of environmental regulation on industry location. *Land Economics* **1990,** *66* (1), 67.

94. McHale, G.; Lücklum, R.; Newton, M. I.; Cowen, J. A., Influence of viscoelasticity and interfacial slip on acoustic wave sensors. *Journal of Applied Physics* **2000,** *88* (12), 7304-7312.

95. Montmeat, P.; Madonia, S.; Pasquinet, E.; Hairault, L.; Gros, C. P.; Barbe, J.; Guilard, R., Metalloporphyrins as sensing material for quartz-crystal microbalance nitroaromatics sensors. *IEEE Sensors Journal* **2005,** *5* (4), 610-615.

96. Morrison, J. Human nose can detect 1 trillion odours. https://www.nature.com/news/human-nose-can-detect-1-trillion-odours-1.14904.

97. Nyquist, J. E.; Wilson, D. L.; Norman, L. A.; Gammage, R. B., Decreased sensitivity of photoionization detector total organic vapor detectors in the presence of methane. *American Industrial Hygiene Association Journal* **1990,** *51* (6), 326-330.

98. O'Connell, M.; Valdora, G.; Peltzer, G.; Negri, R. M., A practical approach for fish freshness determinations using a portable electronic nose. *Sensors and Actuators B: chemical* **2001,** *80* (2), 149-154.

99. Palaniappan, A.; Li, X.; Tay, F. E.; Li, J.; Su, X., Cyclodextrin functionalized mesoporous silica films on quartz crystal microbalance for enhanced gas sensing. *Sensors and Actuators B: Chemical* **2006,** *119* (1), 220-226.

100. Ponrathnam, T.; Cho, J.; Kurup, P.; Nagarajan, R.; Kumar, J., Investigation of QCM sensors with azobenzene functionalized coatings for the detection of nitroaromatics. *J Macromol Sci A* **2011,** *48* (12), 1031-1037.

101. Potyrailo, R. A.; Surman, C.; Nagraj, N.; Burns, A., Materials and Transducers Toward Selective Wireless Gas Sensing. *Chemical Reviews* **2011,** *111* (11), 7315-7354.

102. Queralto, N.; Berliner, A. N.; Goldsmith, B.; Martino, R.; Rhodes, P.; Lim, S. H., Detecting cancer by breath volatile organic compound analysis: a review of array-based sensors. *Journal of breath research* **2014,** *8* (2), 027112.

103. Ramnial, T.; Ino, D. D.; Clyburne, J. A., Phosphonium ionic liquids as reaction media for strong bases. *Chemical Communications* **2005,** (3), 325-327.

104. Regmi, B. P.; Galpothdeniya, W. I. S.; Siraj, N.; Webb, M. H.; Speller, N. C.; Warner, I. M., Phthalocyanine-and porphyrin-based GUMBOS for rapid and sensitive detection of organic vapors. *Sensors and Actuators B: Chemical* **2015,** *209*, 172-179.

105. Regmi, B. P.; Monk, J.; El-Zahab, B.; Das, S.; Hung, F. R.; Hayes, D. J.; Warner, I. M., A novel composite film for detection and molecular weight determination of organic vapors. *J Mater Chem* **2012,** *22* (27), 13732-13741.

106. Regmi, B. P.; Speller, N. C.; Anderson, M. J.; Brutus, J. O.; Merid, Y.; Das, S.; El-Zahab, B.; Hayes, D. J.; Murray, K. K.; Warner, I. M., Molecular weight sensing properties of ionic liquid-polymer composite films: theory and experiment. *Journal of Materials Chemistry C* **2014,** *2* (24), 4867-4878.

107. Rehman, A.; Hamilton, A.; Chung, A.; Baker, G. A.; Wang, Z.; Zeng, X., Differential solute gas response in ionic-liquid-based QCM arrays: elucidating design factors responsible for discriminative explosive gas sensing. *Analytical chemistry* **2011,** *83* (20), 7823-7833.

108. Rodahl, M.; Höök, F.; Krozer, A.; Brzezinski, P.; Kasemo, B., Quartz crystal microbalance setup for frequency and Q-factor measurements in gaseous and liquid environments. *Review of Scientific Instruments* **1995,** *66* (7), 3924-3930.

109. Rodahl, M.; Kasemo, B., A simple setup to simultaneously measure the resonant frequency and the absolute dissipation factor of a quartz crystal microbalance. *Review of Scientific Instruments* **1996,** *67* (9), 3238-3241.

110. Rothenbacher, T.; Schwack, W., Rapid and nondestructive analysis of phthalic acid esters in toys made of poly (vinyl chloride) by direct analysis in real time

single-quadrupole mass spectrometry. *Rapid Communications in Mass Spectrometry: An International Journal Devoted to the Rapid Dissemination of Up-to-the-Minute Research in Mass Spectrometry* **2009,** *23* (17), 2829-2835.

111. Sankaran, S.; Mishra, A.; Ehsani, R.; Davis, C., A review of advanced techniques for detecting plant diseases. *Computers and Electronics in Agriculture* **2010,** *72* (1), 1-13.

112. Sauerbrey, G., Use of quartz vibration for weighing thin films on a microbalance. *Z. phys* **1959,** *155*, 206-212.

113. Schäfer, T.; Di Francesco, F.; Fuoco, R., Ionic liquids as selective depositions on quartz crystal microbalances for artificial olfactory systems—a feasibility study. *Microchemical Journal* **2007,** *85* (1), 52-56.

114. Schaller, E.; Bosset, J. O.; Escher, F., 'Electronic Noses' and Their Application to Food. *LWT - Food Science and Technology* **1998,** *31* (4), 305-316.

115. Schiebaum, K.-D.; Zhou, R.; Knecht, S.; Dieing, R.; Hanack, M.; Göpel, W., The interaction of transition metal phthalocyanines with organic molecules: a quartz-microbalance study. *Sensors and Actuators B: Chemical* **1995,** *24* (1-3), 69-71.

116. Schnorr, J. M.; van der Zwaag, D.; Walish, J. J.; Weizmann, Y.; Swager, T. M., Sensory Arrays of Covalently Functionalized Single-Walled Carbon Nanotubes for Explosive Detection. *Advanced Functional Materials* **2013,** *23* (42), 5285-5291.

117. Shorey, H. H., *Animal communication by pheromones*. Academic Press: 2013.

118. Shurmer, H.; Gardner, J.; Chan, H., The application of discrimination technique to alcohols and tobaccos using tin-oxide sensors. *Sensors and Actuators* **1989,** *18* (3-4), 361-371.

119. Simon, H.; Reff, A.; Wells, B.; Xing, J.; Frank, N., Ozone trends across the United States over a period of decreasing NOx and VOC emissions. *Environmental science & technology* **2014,** *49* (1), 186-195.

120. Siraj, N.; Hasan, F.; Das, S.; Kiruri, L. W.; Steege Gall, K. E.; Baker, G. A.; Warner, I. M., Carbazole-derived group of uniform materials based on organic salts: solid state fluorescent analogues of ionic liquids for potential applications in organic-based blue light-emitting diodes. *The Journal of Physical Chemistry C* **2014,** *118* (5), 2312-2320.

121. Siraj, N.; Kolic, P. E.; Regmi, B. P.; Warner, I. M., Strategy for Tuning the Photophysical Properties of Photosensitizers for Use in Photodynamic Therapy. *Chemistry – A European Journal* **2015,** *21* (41), 14440-14446.

122. Sisco, E.; Dake, J., Detection of Low Molecular Weight Adulterants in Beverages by Direct Analysis in Real Time Mass Spectrometry. *Anal Methods* **2016,** *8* (14), 2971-2978.

123. Speller, N. C.; Siraj, N.; McCarter, K. S.; Vaughan, S.; Warner, I. M., QCM VIRTUAL SENSOR ARRAY: VAPOR IDENTIFICATION AND MOLECULAR WEIGHT APPROXIMATION. *Sensors and Actuators B: Chemical* **2017**.

124. Speller, N. C.; Siraj, N.; Regmi, B. P.; Marzoughi, H.; Neal, C.; Warner, I. M., Rational Design of QCM-D Virtual Sensor Arrays Based on Film Thickness, Viscoelasticity, and Harmonics for Vapor Discrimination. *Analytical Chemistry* **2015,** *87* (10), 5156-5166.

125. Speller, N. C.; Siraj, N.; Vaughan, S.; Speller, L. N.; Warner, I. M., Assessment of QCM array schemes for mixture identification: citrus scented odors. *RSC Advances* **2016,** *6* (98), 95378-95386.

126. Speller, N. C.; Siraj, N.; Vaughan, S.; Speller, L. N.; Warner, I. M., QCM virtual multisensor array for fuel discrimination and detection of gasoline adulteration. *Fuel* **2017,** *199*, 38-46.

127. Staples, E. J.; Viswanathan, S., Ultrahigh-speed chromatography and virtual chemical sensors for detecting explosives and chemical warfare agents. *IEEE Sensors Journal* **2005,** *5* (4), 622-631.

128. Stetter, J. R.; Jurs, P. C.; Rose, S. L., Detection of Hazardous Gases and Vapors: Pattern

Recognition Analysis of Data from an Electrochemical Sensor

Array. *Analytical Chemistry* **1986,** *58*, 860-866.

129. Strashilov, V. L.; Alexieva, G. E.; Velichkov, V. N.; Mateva, R. P.; Avramov, I. D., Polymer-Coated Quartz Microbalance Sensors for Volatile Organic Compound Gases. *Sensor Letters* **2009,** *7* (2), 203-211.

130. Su, P.-G.; Sun, Y.-L.; Lin, C.-C., A low humidity sensor made of quartz crystal microbalance coated with multi-walled carbon nanotubes/Nafion composite material films. *Sensors and Actuators B: Chemical* **2006,** *115* (1), 338-343.

131. Suslick, B. A.; Feng, L.; Suslick, K. S., Discrimination of complex mixtures by a colorimetric sensor array: coffee aromas. *Analytical chemistry* **2010,** *82* (5), 2067-2073.

132. Toniolo, R.; Pizzariello, A.; Dossi, N.; Lorenzon, S.; Abollino, O.; Bontempelli, G., Room Temperature Ionic Liquids As Useful Overlayers for Estimating Food Quality from Their Odor Analysis by Quartz Crystal Microbalance Measurements. *Analytical Chemistry* **2013,** *85* (15), 7241-7247.

133. Tseng, M.-C.; Chu, Y.-H., Chemoselective gas sensing ionic liquids. *Chemical Communications* **2010,** *46* (17), 2983-2985.

134. Umali, A. P.; Anslyn, E. V., A general approach to differential sensing using synthetic molecular receptors. *Current opinion in chemical biology* **2010,** *14* (6), 685-692.

135. Vaughan, S. R.; Speller, N. C.; Chhotaray, P.; McCarter, K. S.; Siraj, N.; Pérez, R. L.; Li, Y.; Warner, I. M., Class specific discrimination of volatile organic compounds using a quartz crystal microbalance based multisensor array. *Talanta* **2018,** *188*, 423-428.

136. Voinova, M. V.; Rodahl, M.; Jonson, M.; Kasemo, B., Viscoelastic Acoustic Response of Layered Polymer Films at Fluid-Solid Interfaces: Continuum Mechanics Approach. *Physica Scripta* **1999,** *59* (5), 391-396.

137. Wang, F.; Gu, H.; Swager, T. M., Carbon nanotube/polythiophene chemiresistive sensors for chemical warfare agents. *Journal of the American Chemical Society* **2008,** *130* (16), 5392-5393.

138. Wang, X.; Ding, B.; Sun, M.; Yu, J.; Sun, G., Nanofibrous polyethyleneimine membranes as sensitive coatings for quartz crystal microbalance-based formaldehyde sensors. *Sensors and Actuators B: Chemical* **2010,** *144* (1), 11-17.

139. Warner, I. M.; El-Zahab, B.; Siraj, N., Perspectives on moving ionic liquid chemistry into the solid phase. *Analytical chemistry* **2014,** *86* (15), 7184-7191.

140. Weinhold, B., The future of fracking: new rules target air emissions for cleaner natural gas production. National Institute of Environmental Health Sciences: 2012.

141. Weller, A., Human pheromones: Communication through body odour. *Nature* **1998,** *392* (6672), 126.

142. Wenzel, S. W.; White, R. M., Flexural plate-wave gravimetric chemical sensor. *Sensors and Actuators A: Physical* **1990,** *22* (1), 700-703.

143. Westhoff, M.; Litterst, P.; Freitag, L.; Urfer, W.; Bader, S.; Baumbach, J. I., Ion mobility spectrometry for the detection of volatile organic compounds in exhaled breath of patients with lung cancer: results of a pilot study. *Thorax* **2009,** *64* (9), 744-748.

144. Wilson, A.; Baietto, M., Applications and Advances in Electronic-Nose Technologies. *Sensors* **2009,** *9* (7), 5099.

145. Wyatt, T. D., *Pheromones and animal behaviour: communication by smell and taste*. Cambridge university press: 2003.

146. Xu, X.; Li, C.; Pei, K.; Zhao, K.; Zhao, Z. K.; Li, H., Ionic liquids used as QCM coating materials for the detection of alcohols. *Sensors and Actuators B: Chemical* **2008,** *134* (1), 258-265.

147. Yamazoe, N.; Shimanoe, K., New perspectives of gas sensor technology. *Sensors and Actuators B: Chemical* **2009,** *138* (1), 100-107.

148. Yarita, T.; Nakajima, R.; Otsuka, S.; Ihara, T.; Takatsu, A.; Shibukawa, M., Determination of ethanol in alcoholic beverages by high-performance liquid chromatography–flame ionization detection using pure water as mobile phase. *Journal of Chromatography A* **2002,** *976* (1-2), 387-391.

149. Yinon, J., Peer Reviewed: Detection of Explosives by Electronic Noses. *Analytical Chemistry* **2003,** *75* (5), 98 A-105 A.

150. Yoo, Y. K.; Chae, M.-S.; Kang, J. Y.; Kim, T. S.; Hwang, K. S.; Lee, J. H., Multifunctionalized cantilever systems for electronic nose applications. *Analytical chemistry* **2012,** *84* (19), 8240-8245.

151. Yoon, J.; Chae, S. K.; Kim, J.-M., Colorimetric sensors for volatile organic compounds (VOCs) based on conjugated polymer-embedded electrospun fibers. *Journal of the American Chemical Society* **2007,** *129* (11), 3038-3039.

152. Yu, L.; Garcia, D.; Ren, R.; Zeng, X., Ionic liquid high temperature gas sensors. *Chemical Communications* **2005,** (17), 2277-2279.

153. Zhou, R.; Josse, F.; Göpel, W.; Öztürk, Z.; Bekaroğlu, Ö., Phthalocyanines as sensitive materials for chemical sensors. *Applied Organometallic Chemistry* **1996,** *10* (8), 557-577.

154. Zhu, W.; Li, W.; Yang, H.; Jiang, Y.; Wang, C.; Chen, Y.; Li, G., A Rapid and Efficient Way to Dynamic Creation of Cross-Reactive Sensor Arrays Based on Ionic Liquids. *Chemistry – A European Journal* **2013,** *19* (35), 11603-11612.

VITA

Stephanie Vaughan is a native of Denver, Colorado. She attended Xavier University of Louisiana in New Orleans, Louisiana where she obtained her Bachelor of Science degree in chemistry in May 2013. In August 2014, she joined the Chemistry Department at Louisiana State University and A&M College (LSU) in Baton Rouge, Louisiana to begin her graduate studies. Under the guidance of Professor Isiah Warner, her research focused on the development of reusable QCM-based sensor arrays for detection and discrimination of VOCs. While at LSU she received two fellowships, NSF LS-LAMP Bridge to the Doctorate Fellowship and LSU Initiative for Maximizing Student Development (IMSD) Graduate Scholar, and published four peer-reviewed manuscripts. Stephanie anticipates graduating with the degree of Doctor of Philosophy in Analytical Chemistry from Louisiana State University in December 2019.